# MODELING AGE-RELATED MOTOR LEARNING DEFICITS WITH FUNCTIONAL NEUROIMAGING CONNECTIVITY ANALYSES

By

GEORGE ANDREW JAMES

A DISSERTATION PRESENTED TO THE GRADUATE SCHOOL
OF THE UNIVERSITY OF FLORIDA IN PARTIAL FULFILLMENT
OF THE REQUIREMENTS FOR THE DEGREE OF
DOCTOR OF PHILOSOPHY

UNIVERSITY OF FLORIDA

2005

Dedicated to my family:  Mom, Dad, Neil, Grandmom, and Grandpop.
Thank you for your constant encouragement and unconditional devotion.

ACKNOWLEDGMENTS

First and foremost, I thank Dr. Yijun Liu for being my mentor through this journey. In a world of cell cultures and micropipettes, the prospect of finding a mentor interested in cognition and brain function began to look doubtful. Then I met Yijun, who introduced me to the awe-inspiring technique of functional magnetic resonance imaging. Yijun's guidance is best described by the prosaic idiom "Where there is a will, there is a way". Yijun has taught me that determination is essential for success, and his tutelage has fostered a sense of self-reliance that I will always cherish.

Secondly, I thank Dr. Christiana Leonard for her insightful advice throughout the doctoral process. Tiana's profound suggestions were essential for shaping not only this dissertation but also my merit as a scientist. From the first journal article I reviewed at her lab meetings, Tiana has encouraged me to think critically about scientific methodology and data interpretation. Thanks to Tiana's guidance, I feel well prepared for the scientific career that soon commences.

I also thank Drs. Keith White and Kenneth Heilman for serving on my doctoral committee. My statistical analyses would have floundered if not for Keith's keen recommendations, which included the Kolmogorov-Smirnov two-sample test. Ken's clinical perspective was highly valuable for guiding the research hypotheses. Together, Keith and Ken ensured that my dissertation remained grounded in both psychological theory and clinical relevance, respectively. Most importantly, Keith, Ken, and the rest of

my committee were always receptive to my ideas and eager to offer feedback; I am grateful for this more than anything else.

I additionally thank Dr. Gary Stevens, who introduced control charts to me as a means of analyzing reaction time variability. Finally, I thank the Evelyn F. McKnight Brain Research Grant for supporting this research. The grant's generous funding made this work possible.

TABLE OF CONTENTS

page

LIST OF TABLES

LIST OF FIGURES

Abstract of Dissertation Presented to the Graduate School
of the University of Florida in Partial Fulfillment of the
Requirements for the Degree of Doctor of Philosophy

MODELING AGE-RELATED MOTOR LEARNING DEFICITS WITH FUNCTIONAL NEUROIMAGING CONNECTIVITY ANALYSES

By

George Andrew James

December 2005

Chair: Yijun Liu
Major Department: Neuroscience

Functional connectivity analyses are recent advances in functional magnetic resonance imaging (fMRI) methodology that model the neural circuitry underlying cognitive performance. One technique, within-condition interregional covariance analysis (WICA), assesses the covariance of distinct brain regions across time to model cortical and subcortical networks mediating a given task. For this dissertation, WICA was used to model the neural network regulating sequential finger movements in humans. Additionally, WICA evaluated changes to this network during effortful (explicit) and effortless (implicit) learning of a serial reaction time task (SRTT) motor sequence. Finally, these functional connectivity models for motor performance were compared across age groups to test competing theories for age-related cognitive decline.

Fifty undergraduate participants were recruited for a behavioral pilot study that compared the effectiveness of three motor learning paradigms. Control charts were adapted for statistical analyses of behavioral responses that revealed relatively consistent rates of implicit learning across individuals despite considerable intersubject variability

for explicit motor learning rates. These findings suggest that implicit motor learning is an invariant process subject to supplementation by explicit strategy.

Eighteen young adults (<35 years old) and nine senior adults (60-75 years old) underwent fMRI scanning while implicitly and explicitly learning a motor sequence. Novel behavior-driven connectivity approaches were contrasted against traditional general linear model approaches to define regions of interest (ROI) mediating motor performance and learning. Both approaches gave analogous results. Connectivity models were then developed for each learning condition (random, implicit, and explicit) and age group (young and senior).

The functional connectivity models of brain activity did not differ between learning conditions for either age group. These null findings may stem from modeling insensitivities to dynamic processes. However, senior adult brains demonstrated significant decreases in functional connectivity compared to young adults during performance of random trials. Increased noise in senior brains was refuted as a possible explanation for the decreasing interregional correlations with age. Furthermore, the decreases in functional connectivity were not constrained to any single brain region, thus supporting aging models that propose distributed cognitive decline. These novel connectivity methods stand to supplement existing psychological models of behavior with physiological models of underlying neural circuitry.

# CHAPTER 1
# INTRODUCTION

Multiple psychological theories attempt to explain age-related impairments in cognitive performance, but no single theory has irrefutable support from biological evidence. This dissertation sought such evidence using functional magnetic resonance imaging (fMRI) to model the neural underpinnings of implicit and explicit motor learning, two cognitive processes respectively demonstrating stability and decline with aging. Young adult college students were first recruited for a behavioral study characterizing the dynamics of unconscious (implicit) and conscious (explicit) motor learning (chapter 2). The pilot study's findings were then used to develop new analytical approaches for connectivity modeling of subsequent neuroimaging investigation (chapter 3). Additional novel methodologies were developed for defining regions of brain activity during motor learning (chapter 4). Functional connectivity models were then developed for and contrasted across age and learning conditions to assess age-related neural origins for age-related motor learning deficits (chapter 5). The remainder of this chapter describes the aims of this dissertation and addresses scientific evidence relevant to learning decline with age.

## Specific Aims

While some cognitive processes (*e.g.*, memory) are generally susceptible to age-related decline, others (*e.g.*, language) are relatively spared (Birren and Schaie, 2001). Motor learning also demonstrates a dissociation: implicit learning remains intact despite age-related impairment of explicit learning (Howard and Howard, 1989). This observed

behavioral dissociation may be associated with selective impairments in brain regions that mediate each form of learning. However, previous neuroimaging attempts to model implicit and explicit motor learning have been hindered by methodological constraints. Learning has been treated as a static process, with brain activity patterns characterized before and after learning but not during actual behavioral change. Connectivity analyses can assess learning dynamically (He *et al.*, 2003; Liu *et al.*, 1999) and thus provide a clearer picture of functional changes with aging. We seek to better characterize the dynamics of functional neural connectivity for implicit and explicit motor learning and their age-related changes by accomplishing the following two specific aims:

**Aim 1. Model and compare motor system connectivity during implicit and explicit motor learning.** Distinct neuroanatomical circuits have been implicated in mediating implicit and explicit motor learning (Honda, 1998; Grafton, 1995; Rauch, 1995). Specifically, increased frontal lobe activity has been observed for explicit learning while implicit learning demonstrates increased activity of the cerebellum and supplementary motor cortex. However, these studies disagree on the specific brain regions that mediate each form of learning. More recent work (Willingham *et al.*, 2001) has suggested an overlap in the circuits subserving these learning processes. Thus, motor learning may depend not on which brain regions are involved in learning but instead the interactions between these brain regions. A primary goal of this research is establishing whether the functional connectivity between motor system components changes during the course of learning. The first aim of this dissertation is therefore to characterize and compare connectivity models for implicit and explicit motor learning generated from functional neuroimaging of young adults performing a serial reaction time task (SRTT)).

**Aim 2. Test the hypothesis that implicit learning retains its functional dynamics with aging.** Implicit motor learning is more resilient to age-related cognitive decline than explicit motor learning (Howard and Howard, 2004, 1992, 1989). We theorize that brain regions demonstrating strong functional connectivity during explicit learning (as measured by activity covariance between brain regions) may selectively become less coherent with aging. The subsequent breakdown in interregional connectivity may explain age-related learning impairments. In contrast, brain regions strongly correlated during implicit learning may not demonstrate such incoherence.

Functional connectivity methods will be used to develop neural-network models for implicit and explicit motor learning among older adults. We expect our model for implicit motor learning to undergo minimal changes in functional dynamics with aging, as demonstrated by a comparison of modeled functional connectivity between younger and older adults. In contrast, we hypothesize that explicit motor learning to undergo drastic changes in functional connectivity with age, as would be consistent with previous reports of explicit motor learning impairment with age.

## Motor Learning

Human motor behavior is among the most thoroughly studied psychological systems. As with other cognitive processes (language, memory), experimenters have sought for decades to evaluate how motor learning strategies affect performance. Yet Nissen and Bullemer (1987) documented a form of learning that was strategy-independent, effortless, and automatic. Dubbed implicit learning, this phenomenon was subsequently documented in other cognitive domains such as grammar acquisition and time perception (Squire and Zola, 1996).

The serial reaction time task (SRTT) is a popular tool due to its versatility at measuring both automatic (implicit) and effortful (explicit) motor learning. The SRTT requires participants to match button press responses with target location. Rapidly consecutive (~1 Hz) SRTT trials allow a participant's baseline reaction time speed and accuracy to be established within a few minutes. Furthermore, the target's location can be random or follow a temporal sequence; performance improvements during sequence trials reflect explicit learning (if the participant is consciously trying learning the sequence) or implicit learning (if the participant is not aware of the sequence).

Age-related declines in the rate of explicit learning have been documented using the SRTT (Howard and Howard, 2004, 1992, 1989). These behavioral changes extend beyond increasingly conservative strategies that optimize accuracy and have been attributed to decreases in cognitive processing speeds (Birren and Schaie, 2001). Yet Howard and Howard (1997, 1992, 1989) have demonstrated the retention of implicit learning with age. Their findings suggest that the neural network(s) mediating implicit motor learning are spared the age-related functional changes that diminish explicit learning.

## Neuroimaging

Motor behavior has been the focus of numerous neuroimaging investigations (Cabeza and Nyberg, 2000). Only the visual system has been more extensively characterized. Brain regions implicated in manual control and/or motor learning include the primary motor cortex (BA 4), lateral premotor cortex (BA 6), medial premotor cortex (also known as the supplementary motor area or SMA, BA 6), supramarginal gyrus (BA 40), dorsolateral prefrontal cortex (BA 46), striatum and the cerebellum. Specific contributions of these regions to motor learning are detailed below.

**Primary Motor Cortex (M1)**

**Anatomy.** Located anterior to the central sulcus, the primary motor cortex (M1) is distinct from the rest of the frontal lobe by its high density of large pyramidal cells in layer V and low density of layer IV granular cells (Brodmann 1909). The primary motor cortex receives extensive afferents from numerous regions including the somatosensory cortex (BA 3,1,2), somatic association areas (BA 5, 7b), and the premotor cortex (BA 6). M1 has several major efferent projections including the corticospinal, corticopontine, and corticobulbar tracts. Retrograde transneural viral transport studies (Strick and Hoover, 1999) indicate that M1 also receives feedback from the cerebellum and basal ganglia, although these efferents are indirectly relayed through the ventral lateral thalamic nucleus.

**Functionality.** The primary motor cortex controls movements of the limbs and face. Electrical stimulation of the cortex has revealed an organizational mapping of M1 to distinct body regions. Known as the motor homunculus, the cortical surface area of each represented body region is proportional to that region's degree of fine motor control (Penfield, 1938). Neuroimaging evidence has supplemented our understanding of the motor homunculus with the detection of the hand knob, a region of the motor cortex that is specifically active during contralateral hand movements (Yousry *et al.*, 1997). The hand knob is a neuroanatomical landmark appearing with a distinct epsilon- or omega-shape in axial slices through the brain.

The primary motor cortex has been shown to mediate both gross and fine motor behaviors. Severing the corticospinal tract (*i.e.*, by damaging the brainstem's pyramid) impairs independent finger movements in nonhuman primates (Tower, 1940; Lawrence and Kuypers, 1968). Primates with such lesions are forced to rely upon "power grips"

involving the whole hand when manipulating food or tools. In contrast, non-operated primates are capable of making "precision grips" that involve just the thumb and forefinger (Napier, 1961). Similar deficits have been observed in human patients suffering from hemiplegia following strokes; however, cortical damage from strokes is rarely limited to just the primary motor cortex (Twitchell, 1951).

**Premotor Cortex**

Located anterior to the primary motor cortex, the premotor cortex is frequently subdivided into three regions: the lateral premotor cortex, the medial premotor cortex (also known as the supplementary motor area or SMA), and the supplementary eye fields. Despite the similar cytoarchitecture of these three regions, they have distinct connections and roles in motor function. Like the frontal eye fields, the supplementary eye fields guide eye movements and will not be discussed further. While the lateral and medial premotor cortices share many anatomical projections, they are traditionally distinguished by their differing roles in mediating behavior.

**Anatomy.** The lateral premotor cortex influences movement through projections to the primary motor cortex (Muakkassa and Strick, 1979) and through the pyramidal tracts to the spinal cord (Martino and Strick, 1987; Hutchins et al., 1988; Dum and Strick, 1991). The lateral premotor cortex has a topographical organization similar to that found in the motor homunculus; for example, projections from the lateral premotor cortex to the MI hand region are dorsal to those projecting to the MI face region. While more anterior regions of the premotor cortex do not have direct projections to the primary motor cortex, their dense interconnectivity with posterior aspects of premotor cortex allows for an indirect connection.

The lateral and medial premotor cortices differ in their cortical inputs. The medial premotor cortex receives input from the medial parietal lobe (BA 5; Dum and Strick, 1991), the dorsal premotor cortex receives input from the dorsal parietal lobe (BA 5; Petrides and Pandya, 1984), and the lateral premotor cortex receives input from the lateral parietal lobe (BA 7b; Petrides and Pandya, 1984). Both lateral and medial premotor cortices receive afferent connections from dorsal prefrontal cortex (Barbas and Pandya, 1987.) Likewise, both regions project to the spinal cord via the pyramidal tract and the basal ganglia via the internal capsule.

**Functionality.** The premotor cortex plays a role in selecting motor responses. Deiber *et al.* (1991) conducted a PET study to determine changes in brain activity relating to selective movements. When subjects made a) random joystick movements in multiple directions, b) sequenced joystick movements according to a previously learned pattern, or c) directional joystick movements based upon auditory cues, they had greater premotor cortex (but not motor cortex) activation than when making repetitive joystick movements in only one direction. The lack of increased primary motor activity led Deiber to conclude that the premotor cortex played a primary role in selecting from possible movements.

The lateral premotor cortex is vital for learning cued responses. Monkeys with lateral premotor cortex lesions made considerably more errors than control counterparts when conditioned to manipulate a lever by either pulling or twisting depending upon a color cue (Passingham, 1988) or choosing between grasping a handle and touching a button based upon an object cue (Petrides, 1982). Since monkeys with these lesions were not impaired on choosing objects based upon color cues (Halsband and Passingham,

1985) or choosing button presses depending upon object cues (Petrides, 1987), these monkeys must be able to recognize cues and make motor responses normally. Thus, a lateral premotor cortex lesion must impair selection of the proper cued response.

In contrast to monkeys with lateral premotor cortex lesions, monkeys with SMA lesions have no deficit in selecting an appropriate motor response (*i.e.*, either pulling or pushing a joystick) depending upon a color cue but are less likely to learn behaviors lacking an overt cue (Passingham, 1987). Passingham (1987) conditioned monkeys to raise their arms by placing an invisible infrared beam overhead and rewarding the monkeys whenever either arm was raised to break the unseen beam. Monkeys with lateral premotor cortex lesions learned to raise their arm(s) nearly as well as control monkeys, while monkeys with SMA lesions made fewer arm-lifting responses than control monkeys (Passingham, 1987, 1989). Lacking overt cues, the monkeys with SMA lesions failed to learn that their uncued ("self-initiated") responses led to reward. The resulting double-dissociation suggests that the lateral premotor cortex mediates selection of externally cued motor response whereas the SMA mediates internally cued motor responses. Specifically, SMA is predicted to play a critical role in implicit motor learning, where response cues may not be overtly recognized.

Monkeys with SMA lesions are also impaired at tasks requiring sequential movements. Passingham (1987) conducted an experiment where access to a food well was blocked by a T-shaped obstruction. In order to access the food well, the monkey first was required to slide the obstruction up, then twist the obstruction clockwise, and finally raise the obstruction from the well surface. None of the three monkeys with SMA lesions could learn the sequence in one thousand trials, while monkeys with lateral premotor

cortex lesions mastered the task on average in fifty trials. Nakamura, Sakai, and Hikosaka have also demonstrated that sequential movements are impaired by inhibition of the SMA with muscimol injection (1999) in addition to identifying SMA neurons that are responsive during the learning of sequential procedure (1998).

Many of these findings for the SMA are eloquently reviewed by Tanji (1996). While some evidence suggests that the SMA may aid in mediating simple or externally cued motor tasks, a preponderance of studies indicate that the SMA is primarily involved in complex and self-mediated motor tasks. The SMA also mediates non-complex movements that might be difficult to execute; for example, movements of the little finger elicit greater SMA activation but equivalent MI activation than movements of the index finger (Erdler *et al.*, 2001). Tanji further illustrated the SMA's role in motor preparation and executing motor sequences with PET and lesion studies but warned against the fallacy of assuming that the SMA is the only area involved in such tasks. The relevance of this double dissociation between lateral premotor cortex and SMA function will become evident in the discussion of novel versus overlearned sequential finger movements below.

**Supramarginal Gyrus (BA 40)**

**Anatomy.** The supramarginal gyrus is bordered anteriorly by the primary sensory cortex (BA 3,1,2) and postcentral sulcus, posteriorly by the angular gyrus (BA 39), and superiorly by the superior parietal lobule (BA 7) (Zilles *et al.*, 2003). The supramarginal gyrus is distinguished from surrounding parietal cortex by its small cell bodies (especially in layers III and V), a relatively low density of cell bodies (especially in layers V and VI), and a prominent columnar cell arrangement.

**Functionality.** A metaanalysis of neuroimaging studies implicates the supramarginal gyrus in "somatosensory information sampling, letter copying, precisely tuned grip, reaching, discrimination of hand orientation, simultaneous performance of two signal-response tasks, mental rotation, spatial orientation, and the switching of response" (Seitz and Binkofski, 2003). Lesions to the supramarginal gyrus result in a variety of cognitive impairments. Common impairments include ideomotor apraxia (disruption of common yet complex tasks, such as using a toothbrush), conduction aphasia (repetitious speech or disrupted writing), astereognosis (perceptual impairments, usually for the hands), finger agnosia (discriminating among another's fingers or one's own), and right-left disorientation (Strub and Black, 1977; Brown, 1972; Geschwind, 1965). Supramarginal gyrus activity tends to be more bilateral than activity for other cortical regions, and left hemisphere legions may result in deficits on both sides of the body.

While the hand knob is a cortical representation mediating manual movements, the supramarginal gyrus is crucial for spatial representations of the hand. However, additional parietal regions may supplement the supramarginal gyrus in performing these functions, in much the same way as hand movements are supplemented by movements of the wrist and limb. Regardless of the exclusivity of these functions, they share a commonality of spatial awareness, particularly for hand orientation.

## Prefrontal Cortex

**Anatomy.** The prefrontal cortex encompasses most the frontal lobe except for the motor and premotor areas (BAs 4 and 6). The anterior cingulate (BA 24, 32) is arguably anatomically distinct from the prefrontal cortex, but is included here given their similar functional roles. The prefrontal cortex is further divided into the dorsolateral (BA 9, 45,

46) and orbitofrontal (BA 10, 11, 12) cortices. The dorsolateral prefrontal cortex receives afferents from parietal lobe (BA 7), cingulate and orbitofrontal cortex, while projecting efferents to the frontal eye fields (BA 8) and reciprocal orbitofrontal efferents (Morecraft *et al*., 1992; Goldman-Rakic *et al.*, 1984).

**Functionality.** As illustrated by the case of Phineas Gage, prefrontal cortex lesions can result in drastic behavior changes affecting mood, planning, and personality (Damasio *et al.*, 1994). These varying traits can be roughly subdivided by region. The orbitofrontal cortex mediates reward-seeking behaviors, especially those of emotional saliency. Neuroimaging studies frequently correlate orbitofrontal activity with rewarding stimuli such as food (Small *et al.*, 2001; O'Doherty *et al.*, 2000; Tataranni *et al.*, 1999) and music (Blood and Zatorre, 2001). The orbitofrontal cortex is also a key component in addiction models, with PET studies correlating orbitofrontal metabolism with self-reports of drug craving in participants addicted to cocaine (Volkow and Fowler, 2000). This latter finding establishes orbitofrontal activity as anticipatory and not reactionary, thus suggesting a role in the search for rewarding stimuli.

While the orbitofrontal cortex is associated with rewarding behaviors, the dorsolateral prefrontal cortex is involved in more logical functions such as planning and working memory. Functional neuroimaging (Buchsbaum *et al.*, 2005) and lesion (Amos, 2000; Sullivan *et al.*, 1993) studies have strongly linked the dorsolateral prefrontal cortex to performance on the Wisconsin Card Sorting task, a task that requires the identification of rule sets, their maintenance in working memory, recognition of transitions from one rule set to another, and adaptation of performance to new rule sets. Measures of cognitive inhibition and working memory (*i.e.*, the go/no-go and n-back

tasks, respectively) have also been associated with dorsolateral prefrontal activity (Owen *et al.,* 2005; Swainson *et al.,* 2003).

The anterior cingulate operates in conjunction with the dorsolateral and orbitofrontal cortices as a "relevance detector"(Miller and Cohen, 2001), monitoring the environment for emotionally or cognitively relevant stimuli. Specifically, the anterior cingulate is responsive to the commission of errors (Carter *et al.,* 2001). This region's role in detecting errors likely guides subsequent behaviors for improving accuracy.

**Basal Ganglia**

**Anatomy.** The basal ganglia are a collection of subcortical structures including the caudate nucleus and putamen, globus pallidus, and substantia nigra (Harrington and Halaad, 1998). The caudate nucleus and putamen are also called the striatum. These nuclei are linked through an extensive network of excitatory and inhibitory connections. The description "basal ganglia" has become outdated as its specific components are studied with increasing detail. However, the complex interdependence of these nuclei is beyond the scope of functional neuroimaging analyses; fMRI temporal resolution is simply too poor to capture the intricate millisecond timings amongst basal ganglia regions. As such, this review will consider the basal ganglia as a holistic collective.

The basal ganglia have extensive reciprocal anatomical connections with the thalamus and cortex. At least five distinct thalamocortical circuits originate from the basal ganglia and project to more anterior frontal regions including the SMA, the frontal eye fields (for controlling eye movement; not previously discussed), the orbitofrontal and dorsolateral prefrontal cortices, and the anterior cingulate (Alexander and Crutcher, 1990; Graybiel, 1990).

**Functionality.** The basal ganglia's inclusion in numerous neuroanatomical circuits suggests a supervisory role for integrating and selecting motor responses. Although the basal ganglia has no direct connection to the spinal cord, genetic disorders such as Parkinson's disease (PD) implicate the basal ganglia in mediating motor control through its influence on the cortex. For these disorders, neuronal loss (specifically in the substantia nigra) causes bradykinesis (slow movements), akinesia (difficulty initiating movements), tremors, and rigidity.

The basal ganglia also mediate performance of sequential movements. Harrington and Haaland (1991) compared performance of PD patients and healthy controls while performing pairs of sequential finger movements. Sequence pairs were either congruent (sharing a similar structure) or incongruent. Examples of a congruent pair are "IIM" and "RRM" (where I, M, and R are the index, middle, and ring fingers, respectively), while an incongruent pair would be "IIM" and "RMM".

If the basal ganglia mediate *programming* of sequences, then the reaction time gain for congruent trials would be reduced for PD patients relative to controls. This would reflect an inability to conceptualize the underlying similarity of sequence structure. In contrast, if the basal ganglia mediate *switching* between learned sequence structures, then PD patients would take longer to initiate the second sequence of the incongruent pairs than the congruent pairs; *i.e.,* the sequences are known ("programmed"), but the difficulty lies in switching between them. Reaction time data support the programming hypothesis; PD patients show less benefit from congruent sequences but do not take longer to initiate incongruent sequences.

In addition, the basal ganglia play a crucial role in the perception of time. PD patients demonstrate no deficits at making finger taps paced to a metronome or continuing at that frequency after the metronome has stopped. However, they demonstrate difficulties in gauging short time intervals (300-600 ms) between consecutive tones. These timing deficits could substantially impair learning of novel motor skills. The inferred role of the basal ganglia for orchestrating sequential movements makes it a suitable region for functional neuroimaging analyses of motor learning.

**Cerebellum**

**Anatomy.** The cerebellum can be subdivided into four regions: the vermis, intermediate zone, hemispheres, and flocculus. All four regions of the cerebellum are implicated in motor control. The vermis projects to the spinal cord via the vestibular nucleus and reticular formations; the intermediate zone and hemispheres project to the motor and premotor cortices via the thalamus, and the flocculus sends climbing fibers directly to the vestibular nuclei (Hikosaka, 1998). The dentate nucleus also has efferent projections to the basal ganglia (Hoshi *et al.*, 2005). The cerebellum receives afferents from most cortical areas and the thalamus, priming the cerebellum as a major regulator for motor behavior via feedback mechanisms.

**Functionality.** As in the motor cortex, somatotopic maps of the hand (and even the foot) have been found within the cerebellum (Rijntjes *et al.*, 1999). The cerebellar homunculi differ from the motor cortex in three ways. First, the cerebellar homunculi lack distinct anatomical landmarks such as the hand knob (Yousry, 1997). Secondly, each homunculus is mirrored across a plane (z=-35mm in Talairach space) such that distinct hand homunculi exist in both the vermis and cerebellar hemisphere. Finally,

while the previously discussed regions display contralateral control of the body (with the exceptions of the supramarginal gyrus and SMA, which demonstrate bilateral control), the cerebellum regulates ipsilateral body movements (Small *et al.*, 2002).

While human patients with cerebellar lesions display a variety of gross gait and coordination impairment (Hallet and Massquoi, 1993), the cerebellum is also involved in fine motor control of the fingers (Liu *et al.*, 2000). Transcranial magnetic stimulation of the cerebellum disrupts finger tapping accuracy (Theoret, Haque and Pascual-Leone, 2001). Additionally, neuroimaging evidence implicates the cerebellum in synthesizing independent finger movements into one complex movement (Ramnani *et al.*, 2001), suggesting a role in orchestrating sequential movements–a role consistent with the gait deficits accompanying cerebellar lesions.

Like the basal ganglia, the cerebellum orchestrates the timing of movements. Individuals with cerebellar lesions were impaired at timing motor responses to auditory cues, maintaining this pace in the absence of cues, and estimating time intervals (Ivry and Keele, 1989). These findings propose complimentary roles of the basal ganglia and cerebellum for mediating timing sequences. Additionally, a common mechanism appears to exist for both producing and perceiving time. As previously mentioned, the timing of motor responses is a key component for motor skill acquisition.

## Neuroimaging of Motor Learning

Numerous neuroimaging studies have attempted to further define the role of the motor areas above in mediating motor learning. These studies can roughly be divided into three groups: those investigating neuroanatomical mediation of a simple motor task, those investigating new versus overlearned motor behaviors, and those comparing explicitly to implicitly learned motor behaviors. Each study type is reviewed in turn.

**Simple Motor Tasks**

Gordon *et al.* (1998) conducted a functional MRI study investigating brain activity associated with typing movements. Participants were scanned while using a keyboard stripped of its ferromagnetic components (but unable to record behavioral data) to perform four tasks: repetitive keystrokes of one key with one right finger (task A), typing a sequence with one right finger (B), typing a sequence with fingers from both hands (C), and typing sentences with fingers from both hands (D).

Functional brain activity [as measured by increases in blood oxygen level dependence (BOLD) response during tasks relative to a resting baseline] increased in the primary motor cortex for tasks requiring movement of the contralateral hand(s). Tasks involving sequential movements (B, C, and D) resulted in significant increases in SMA BOLD activity (contralateral for B, bilateral for C and D) but only marginal increases in lateral premotor cortex activity (bilateral). These findings are in accordance with non-human primate research establishing SMA involvement in sequential movements (Passingham, 1987). The somatosensory (BA 3,1,2; not previously discussed due to its involvement in sensation and not motor performance) and parietal (BA 7) cortices demonstrated activation during task B (contralateral) and tasks C and D (bilateral), implying their respective involvement in tactile and spatial awareness. The basal ganglia demonstrated significant yet slight increases in functional activity for sequential tasks, suggesting a mediation of motor responses. The cerebellum was not examined.

Toni et al (1998) used fMRI to evaluate the time course of brain activity involved in overlearning a sequential motor behavior. Participants performed 44 repetitions of an 8 unit long sequence SRTT. As the sequence was learned (*i.e.*, before the accuracy error rate reached an asymptote of zero errors per trial), peak activity was observed in the

contralateral M1, SMA and lateral premotor cortex, dorsolateral prefrontal cortex, caudate nucleus, cerebellar vermis and hemispheres, and ipsilateral parietal lobe including the supramarginal gyrus. With the exception of the ipsilateral and not contralateral parietal activation, these data are in agreement with the anatomical literature discussed above. Only the contralateral supplementary motor area had enhanced activation during the late stages of the experiment, after the sequence had been overlearned. The lateral to medial shift in premotor activity suggests cue-independence indicating sequence mastery.

**Late versus Early Learning**

Toni's neuroimaging study complements behavioral evidence for different stages of motor learning (1998). Laforce and Doyon (2002) documented a potential double dissociation between the striatum and cerebellum on learning novel procedures. Subjects performed a mirror-tracing task wherein subjects traced geometric shapes while only able to see their hand, paper, and pencil through a mirror. Parkinson's disease patients made significantly fewer errors and were significantly faster at tracing previously practiced shapes than tracing novel shapes. In contrasts, patients with cerebellar lesions performed novel tasks more quickly (albeit nonsignificantly) than practiced ones. Other studies also support a dissociated role between the striatum and cerebellum in motor learning (Schugens *et al.*, 1998; Poldrack and Gabrieli, 2001).

Miyachi *et al.* (2002) conducted neuronal studies to further investigate the role of the basal ganglia in executing novel versus practiced sequences. Monkeys were trained on a sequential button-press task known as the "2x5" motor task. The task required an apparatus with twenty-five unlit buttons. Two buttons were lit per trial; the monkey had to press the buttons in the correct order to move on to the next trial. The monkey was

rewarded after completion of five such trials (termed a hyperset); failure to complete a trial in the correct order ended the hyperset and initiated another hyperset.

Basal ganglia neuronal recordings distinguished between novel and overlearned hypersets. Novel hypersets led to greater activity in striatum neurons anterior to the anterior commisure, whereas striatum neurons posterior to the anterior cingulate yielded greater response during the execution of overlearned sequences. One caveat to this study is that most the association and sensorimotor striatum contained a number of neurons responsive to both motor tasks. However, the interpretation of Miyachi *et al.* is supported by their earlier work (1997) showing that the GABA agonist muscimol disrupted novel hyperset learning when injected into the association striatum while disrupting the performance of overlearned sequences when injected into the sensorimotor striatum.

Müller *et al.* (2002) conducted a functional MRI study comparing brain activity in early and late stage of sequences learning. They found left caudate nucleus activity during early stages of learning an eight-unit long sequence and left SMA activity during late learning. Müller also found activation of the right middle frontal gyrus and bilateral parietal lobes during early learning but occipito-temporal cortex and parahippocampal activation during late learning. Both Müller and Toni's studies indicate dynamic changes in brain activity during motor learning.

In addition to supporting the roles of previously cited neuroanatomical structures in mediating motor behavior, these studies distinguish these regions' involvement in early and late learning stages. However, these findings are qualitative and do not address the

interdependence of brain regions during learning. Chapter 3 describes approaches for modeling the interactions between brain regions during the course of learning.

**Implicit versus Explicit Motor Learning**

Implicit motor learning is defined as the acquisition of a motor skill without conscious awareness. Critics have argued that implicit and explicit motor learning may not be dissociable processes but instead may represent a continuum of performance–*i.e.*, implicit learning may represent base learning mechanisms that are then modified by explicit awareness and strategies. The strongest evidence for the dissociation of implicit and explicit learning is provided by parallel learning studies (Mayr, 1996; Frensch and Miner, 1995) in which participants simultaneously learned one sequence explicitly (*e.g.*, a repeating pattern of geometric shapes) while learning another sequence implicitly (*e.g.*, stimulus location on a viewing screen). These studies illustrate an independence between learning approaches; however, the qualities learned (*i.e.*, shape and location) are arguably not comparable.

To resolve this issue, a neuroimaging study was conducted examining parallel learning of motor sequences (Willingham *et al.*, 2001). Twenty-two participants performed a serial reaction time task by making key press responses to a circle stimulus shifting among four locations. Participants were informed that stimulus location was random when the circle was black. A red circle indicated a pattern that the participants were explicitly instructed to learn. Unknown to the participants, two sequences were hidden among the "random" black circle trials; one was the same sequence presented in the explicit condition (explicit-covert), and the other was a novel sequence (implicit).

Participants reported that they noticed neither the explicit-covert nor the implicit sequence. The clever use of stimulus color was sufficient to mask sequence awareness.

Reaction time measures were significantly shorter for explicit-overt than explicit-covert sequences, explicit-covert than implicit, and implicit than random. Thus, SRTT performance benefits from both practice and awareness. The argument cannot be made that awareness alone differentiates explicit from implicit learning since performance on the explicit-covert sequence was intermediate to performance on the explicit-overt and implicit sequences.

The neuroimaging analyses indicated a surprising overlap of brain activity patterns across the three conditions. The comparison of each condition against random trials indicated an enhanced BOLD response in the ipsilateral putamen and contralateral dorsolateral prefrontal cortex (BA 10 and 46). The authors conclude that similar activity networks mediated each form of learning. If the same neural regions show activation across task, then perhaps the pattern of *communication* between regions can explain the behavioral improvements in performance.

The overlapping activity maps contrast with previous neuroimaging work that described different brain regions associated with implicit and explicit motor learning. While these studies (Honda *et al.*, 1998, Hazeltine *et al.*, 1997, Grafton *et al.*, 1995, Rauch *et al.*, 1995) agree that the prefrontal cortex tends to be more active during explicit than implicit learning, no consensus could be reached upon preferential involvement of the premotor cortices, basal ganglia, supramarginal gyrus or cerebellum. The elegant, within-subject design of the Willingham study controls individual differences in performance and brain circuitry that might have confounded these earlier interpretations. Additionally, improvements in MRI methodology and technology may explain some of these differences. Regardless, Willingham's findings seem most plausible given the

growing field of functional connectivity analyses (see Chapter 3) and accompanying impetus to model the brain as an entire network rather than independent, discrete regions.

## Aging

Older adults retain the ability to learn motor skills implicitly despite deficits in explicit motor learning (see below; Howard and Howard, 1997, 1992, 1989). We now discuss age-related changes in neuroanatomy and behavior involving motor function.

### Age-related Changes in Neuroanatomy

The brain undergoes a myriad of anatomical changes with aging. Many of these changes are constrained to specific anatomical regions and follow a similar progression among most aging individuals, while others are more global in scope. While some neuroanatomical changes are associated with age-related pathologies (*i.e.*, β-amyloid deposits and Alzheimer's disease), the discussion will be limited to those changes taking place during the normal course of aging that affect fine motor control and are not linked to specific pathologies.

**Global**. Post-mortem and neuroimaging studies have demonstrated age-related decreases in both brain weight and volume. At 30 years of age, the brain of the average male weighs around 1350 to 1450 grams; this weight decreases by 7% to 8% after 55 years of age (Creasey and Rapoport, 1985; Terry, DeTeresa, and Hansen, 1987). Brain volumes decrease by 2 to 3% for each decade after 50 years of age (Esri *et al*, 1997), with decreases occurring for both gray and white matter (Andersen *et al*., 1983; Resnick *et al*., 2000).

**White matter.** Many theories of age-related cognitive decline are rooted in the observed decline in white matter volume with aging. Changes in white matter can be difficult to characterize even with gross histological examination; fortunately, T2-

weighted MRI is capable of performing *in vivo* analysis of white matter density. While the greatest degree of rarefaction (density decrease) occurs for periventricular white matter, rarefaction is also common among subcortical and deep white matter (Pantoni and Garcia, 1995; Ketonen, 1998).

T2-weighted white matter signal changes can arise from a broad range of sources including demyelination, infarcts, edema, gliosis, hydrocephalus, or small lesions following infection or stroke (Chimowitz, Awad, and Furlan, 1989). Hypertension and cerebrovascular disease are risk factors associated with white matter signal abnormalities (Aizenstein *et al*., 2002; Awad *et al*., 1986; Cajade-Law *et al*., 1993). However, such signal abnormalities are also common among high-functioning elderly individuals and are thus poor predictors for cognitive impairment.

**Frontal.** Although gray matter atrophy occurs throughout the aging brain, the frontal and temporal lobes undergo disproportionately greater atrophy than the parietal and occipital lobes (Esri *et al*., 1997; Mann, 1994; Coffey *et al*., 1992; Gado *et al*., 1982). The cortical atrophy was initially believed to be caused by a decrease in neuronal population, but additional evidence suggests atrophy to result from a decrease in neurons' dendritic branches (Anderson and Rutledge, 1996; Raz *et al.*, 1997).

**Glia.** Glial changes have also been associated with aging. Increased proliferation of astrocytes and astrocytic processes occurs with aging throughout the brain but especially at subependymal sites such as caudate nucleus, subpial sites, and cerebellar deep nuclei (Schochet, 1998). The cytoplasms of these astrocytes can develop into corpora amylacea, basophilic spheroidal structures of 5 to 20 μm in diameter. These corpora amylacea arise in virtually all individuals over 40 years of age and have an

increased incidence with aging. Despite their proximity to nuclei of the basal ganglia and cerebellum, the presence of corpora amylacea has been associated to no known disease or cognitive or motor dysfunction (Schochet, 1998).

**Basal ganglia**. Zhang (2001) used pharmacological MRI to investigate age-related changes in dopaminergic stimulation of the basal ganglia in rhesus monkeys. Apomorphine, a mixed D1/D2 dopamine receptor agonist, causes reduced substantia nigra activation and increased globus pallidus activation in young monkeys. Older animals showed significantly less change in activity in these areas compared to young monkeys, suggesting that changes in basal ganglia neuropharmacology may be partially responsible for observed changes in motor function with aging.

MR imaging has shown iron deposition to increase with age, particularly around the basal ganglia. A significant correlation exists between iron accumulation and aging for the putamen, caudate, and substanita niagra but not for the globus pallidus (Bartzokis et al., 1997; Martin et al.,1998). Iron deposition can lead to free radical oxidation (Samson and Nelson, 2000), which may account for basal ganglia dysfunction. Free radicals may also account for the severe atrophy and degradation occurring in the caudate nucleus with age (Jernigan et al., 1991).

**Cerebellum**. Cerebellar volume decreases with age, with the difference most robust among the cerebellar hemispheres and vermis (Jernigan *et al*., 2001; Ge *et al.*, 2002). The anterior cerebellar hemispheres selectively undergo the greatest atrophy, with a 30% loss of volume and 40% loss of both Purkinje and granule cells (Anderson *et al.*, 2003). However, the total rate of cerebellar volume change is comparable to that of the

whole brain, occurring at about 2% per year after the fifth decade (Raz *et al*., 2001; Tang *et al.*, 2001).

**Age-related Changes in Motor Function**

The age-related changes in human neuroanatomy are expected to have functional consequences. For example, older adults demonstrate a weakened handgrip, weakened maximum pinch force, and a lesser ability to maintain a steady maximum pinch force and precision pinch posture–all of which could relate to muscular or peripheral motor neurons. But more cognitive tasks, such as the peg relocation tasks (where a subject must take a peg and consecutively place it in each hole of a pegboard) and tactile stimulus discrimination tasks, also demonstrate impairment increases with age (Ranganathan *et al.*, 2001).

Mattay (2002) conducted a fMRI study comparing performance on a cued button-pressing task between high-functioning older (> 50 years old) and younger (< 35 years old) adults. Mattay found that the response times of older adults (794 +/- 280 ms) were significantly longer ($p < 0.001$) than those of younger adults (547 +/- 97 ms). Older adults demonstrated greater activation of the contralateral SMA, contralateral lateral premotor area, contralateral sensorimotor cortex, and ipsilateral cerebellum. Older adults also had activation of the ipsilateral sensorimotor cortex, contralateral cerebellum, and bilateral putamen that was not evident in younger subjects. These data suggest not only an impairment of find motor control with age but that a compensatory mechanism may be in place whereby the cognitive workload is shared bilaterally in elderly brains. Granted, an alternative and less optimistic hypothesis is that the aging cerebrovasculature becomes less efficient at directing blood and oxygen to where it is needed most.

While Mattay has demonstrated that older adults are slower to make responses than younger adults, Howard and Howard (1997, 1992, 1989) have documented that older adults show equivalent improvement in response times relative to younger adults when performing implicitly learned motor sequences. Furthermore, this improvement in response time (RT gain) is much less in older adults than younger adults with explicitly learned motor sequences. These findings suggest that implicit motor learning does not experience the same degree of impairment with aging as does explicit motor learning. We propose that the retention of implicit motor learning with age stems from a relatively intact functional connectivity between the neural regions mediating implicit motor learning.

Functional neuroimaging studies have also found that the area of cortical activation decreases with age. A near infrared spectroscopy (NIRS) and fMRI study of the left motor cortex found that elderly subjects had decreased change in cortical oxygenation and a smaller area of cortical activation relative to younger subjects when performing a simple finger-tapping task with their right hands (Mehagnoul-Schipper *et al.*, 2002). But a confound for this and other neuroimaging studies of aging (Hesselmann *et al.*, 2001; Ross *et al.*, 1997) is the assumption that the hemodynamic response (and thus, baseline BOLD-fMRI signal intensities) is comparable between age populations. While characteristics of the hemodynamic response is essentially identical between older and younger adults, older subjects have a greater response variability and thus a higher signal-to-noise ratio (Buckner *et al.*, 2000; Huettel *et al.*, 2001). The increased voxel-wise noise in older adults is responsible for the apparent decrease in area of cortical

activation. In subsequent chapters, we will assess the potential influence of age-related voxel noise upon our connectivity modeling approaches.

# CHAPTER 2
# BEHAVIORAL PILOT STUDY

Neuroimaging analysis of dynamic cognitive processes remains a methodological challenge. Technical constraints limited previous neuroimaging investigations to static analyses of brain activity before and after learning (Honda *et al.*, 1998; Grafton *et al.*, 1995; Deiber *et al.*, 1991). Despite the ground-breaking work of Ivan Toni (1998) to qualitatively characterize the neural patterns that mediate learning, the optimal approach for quantifying these patterns remains contested.

A key complication to characterizing motor learning is within- and across-participant variability in behavioral responses. Improved methods for detecting the onset of learning (either within or across individuals) would lead to greater temporal resolution for data analysis, thus refining neuroimaging analyses for dynamic processes. A SRTT pilot study was run to collect behavioral data for subsequent development of temporal analyses. In addition to providing behavioral timecourses of explicit motor learning, the pilot study also allowed us to assess participants' performance and awareness of implicitly learned sequence.

Two SRTT paradigms were contrasted for optimal use in assessing implicit motor learning with functional neuroimaging. Implicit learning was measured for tasks without (hidden consecutive; HC) and with (hidden interleaved; HI) random trials inserted between sequence repetitions. Fifty undergraduates participated in the HI task (n=15), the HC task (n=13), and an explicit [informed consecutive (IC)] SRT task (n=22).

Control charts are tools potentially useful for studying the dynamics of implicit and explicit motor learning. These statistical tools were developed to detect perturbations in stable, normally distributed industrial processes (Shewhart, 1931). However, control charts are equally applicable to learning, where the "perturbation" is a learning-associated change in performance. In addition to displaying the magnitude of learning gains, control charts graphically depict the onset of learning and the attainment of asymptotic ceilings and floors in performance.

Control charts analyses of mean reaction time were conducted to both validate this tool in the context of previous literature regarding performance gains and to examine differences in the timecourses of implicit and explicit learning. Group reaction time standard deviations were also analyzed with control charts to study individual differences in learning-related performance.

## Methods

### Participants

Twenty-two undergraduate students (twelve female) participated in the informed consecutive (IC) experiment, thirteen undergraduates (seven female) participated in the hidden consecutive (HC) experiment, and fifteen undergraduates (seven female) participated in the hidden interleaved (HI) experiment. All participants were students satisfying introductory psychology course requirements and were recruited in accordance with University of Florida Institutional Review Board policy. All but two participants were strongly right-handed as measured by a modified Edinburgh Handedness Inventory (Oldfield, 1971); one left-handed participant was in the IC experiment and chose to perform the tasks with her left hand using horizontally flipped stimuli, while the other was in the HI experiment and chose to use her right hand.

**Apparatus**

Experiments were programmed in MS.NET Visual Basic (Microsoft, 2002) on a Dell PP01X Latitude C810 laptop computer (Dell, 2001).

**Procedure**

Motor learning was assessed through serial reaction time task (SRTT) (Nissen & Bullemer, 1987). Participants viewed a cartoon hand while their own hand rested atop the laptop computer's four home-row keys (index=j, middle=k, ring=l, and pinky=; for right-handed participants; index=a, middle=s, ring=d, and pinky=f for the left-handed participant). A red X obscured one of the four cartoon fingers (excluding thumb) at the start of each trial. Participants were instructed to make a key press response with the finger corresponding to the obscured finger as quickly and accurately as possible. The key press marked the end of each trial, causing the red X to disappear. The computer program recorded trial duration (*i.e.*, participant reaction tim e) and which key was pressed for each trial. Trials were of unlimited duration (ending with the key press) and had an inter-trial interval randomly varying between 600-1000 ms.

**Informed Consecutive (IC).** For the IC paradigm, participants went through 5 blocks of 288 trials each. Blocks 1 and 5 were the Random condition; Blocks 2, 3, and 4 were the Sequence condition. Trials in the Sequence blocks followed a 12-element sequence (2-3-4-1-3-2-1-2-4-3-1-4, where 1=index finger, 2=middle finger, 3=ring finger, and 4=pinky finger) that repeated 24 times consecutively. In contrast, trials of the Random blocks were pseudorandom [*i.e.*, random without runs (1-2-3-4), repeats (2-2), or trills (1-3-1-3)]. Participants were allowed indefinite rest periods between blocks but rarely took longer than fifty minutes to complete all five blocks. Prior to each Sequence block in the explicit condition, participants were informed that a sequence existed for that

block and given additional instructions to learn it. They were informed that all Sequence blocks used the same sequence but were given no other sequence details.

**Hidden Consecutive (HC).** The HC paradigm consisted of 12 blocks of 144 trials each. Blocks 1, 2, 3, 11, and 12 were Random blocks composed of the same pseudorandom order as the IC experiment. The remaining blocks (Sequence) consisted of twelve consecutive repetitions of the same sequence used in the explicit condition. Between blocks, participant awareness was gauged by asking participants if they had any questions. The HC paradigm had more numerous blocks of fewer trials than the IC paradigm so that more opportunities existed to gauge implicit learning between blocks. Participants were not instructed to learn the sequence or informed of its existence; any participants reporting a sequence were asked when they first noticed the sequence and instructed to learn the sequence for the remaining Sequence blocks.

**Hidden Interleaved (HI).** The HI paradigm consisted of 5 blocks of 294 trials each. All blocks started and ended with six pseudorandom trials. The remainder of each block consisted of a ten trial sequence (4-3-2-1-3-4-1-2-3-1) with six pseudorandom trials separating each occurrence of the sequence. The transitions between pseudorandom and sequence elements were modified to exclude trills, repeats, and runs; however, the sequence inadvertently contained a run (4-3-2-1), the ramifications of which are addressed in the discussion below. Sequence awareness was gauged as described for the HC paradigm.

## Results

### Informed Consecutive and Hidden Consecutive

Individual participant responses were averaged into “miniblocks” of 12 trials (*i.e.*, the sequence length). The IC and HC blocks were divided into 24 and 12 miniblocks

each, respectively. Mean group miniblock RT was calculated for each miniblock by averaging together individual miniblock RTs. Descriptive statistics were generated for each condition and block using these mean group miniblock RT values (Tables 2-1 and 2-2). For both experiments, the first group miniblock RT was excluded as an outlier.

One participant was excluded from the IC paradigm for not following instructions; the participant would not wait for cue before executing responses. For the remaining 21 participants, mean RT (411 ms) for trials in the Sequence condition (Blocks 2-4) was significantly less than mean Random RT (506 ms; $t(117)=18.0$; $p < .001$). Mean RT did not significantly differ between Blocks 1 and 5 ($p=.009$) but approached the significance threshold (alpha=0.05). Mean RT for each Sequence block was significantly less than mean RT for either Random block (all $p<.001$; all comparisons Bonferonni corrected). Analysis of variance with Bonferonni-corrected post-hoc comparisons shows RT to significantly ($p<.001$ each) and continuously decrease for each learning block.

Three participants in the HC paradigm noticed a sequence (during Blocks 4, 8, and 10). These three participants also had significantly faster responses (463 ms) during the first three random blocks than the remaining participants (545 ms, $p<.001$). Including these participants for the random blocks and excluding them for blocks in which they reported sequence awareness would introduce an attrition bias to group miniblock RT mean and variance, so these participants were excluded for all data analyses.

Control charts were constructed by plotting group miniblock RT means (*m*) against miniblock for both IC (Figure 2-1a) and HC (Figure 2-2a) paradigms. The first group of Random trials (Block 1 for explicit, Blocks 1-3 for implicit) were used to calculate baseline RT mean and standard deviation (*sd*). While the final Random

condition could be used to control for practice-related improvements in performance during the Random condition, Blocks 11 and 12 of the Hidden Consecutive experiment show considerably high variability that suggests confound from fatigue. Horizontal lines depicting baseline RT *m* +/- 3 *sd* were also plotted on the control charts. Since 99.7% of normally distributed RT observations should fall within 3 *sd* of the mean, observations beyond this upper and lower boundary will reflect perturbations in performance. Additional control charts were constructed to assess learning-related influences upon RT variability by plotting the *sd* of participants' miniblock RTs against miniblock (Figures 2-1b and 2-2b). For these control charts, the horizontal lines depict *m* +/- 3 *sd* for baseline standard deviations.

Table 2-1. Informed Consecutive Reaction Time Means and Standard Deviations

| Block | Mean (sd) RT (in ms) |
|---|---|
| 1 | 506 (158) |
| 2 | 435 (190) * |
| 3 | 385 (206) * |
| 4 | 352 (182) * |
| 5 | 485 (175) |

*Mean RT differs from all other blocks ($p < .001$)

Table 2-2. Hidden Consecutive Reaction Time Means and Standard Deviations

| Block | Mean (sd) RT (in ms) |
|---|---|
| 1 | 552 (171) |
| 2 | 543 (159) |
| 3 | 533 (169) |
| 4 | 508 (174) |
| 5 | 497 (171) * |
| 6 | 513 (192) |
| 7 | 493 (161) * |
| 8 | 489 (168) * |
| 9 | 480 (167) * |
| 10 | 485 (179) * |
| 11 | 492 (147) * |
| 12 | 507 (162) |

*Mean RT differs from Blocks 1, 2, and 3 ($p < .005$)

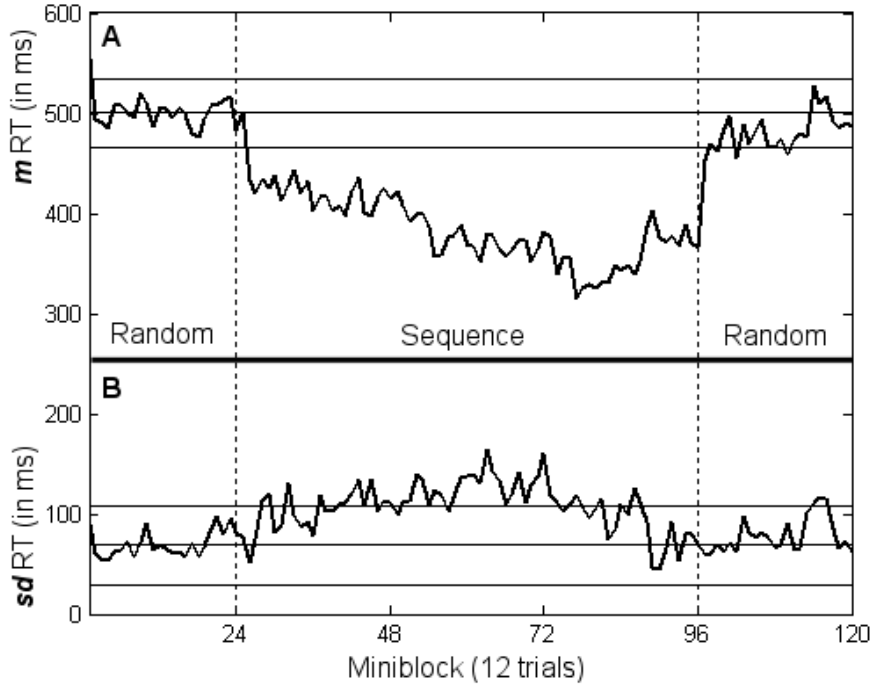


Figure 2-1. Control chart analyses of reaction time for Informed Consecutive. RT group means (A: top) and standard deviations (B: bottom) are plotted by miniblock.

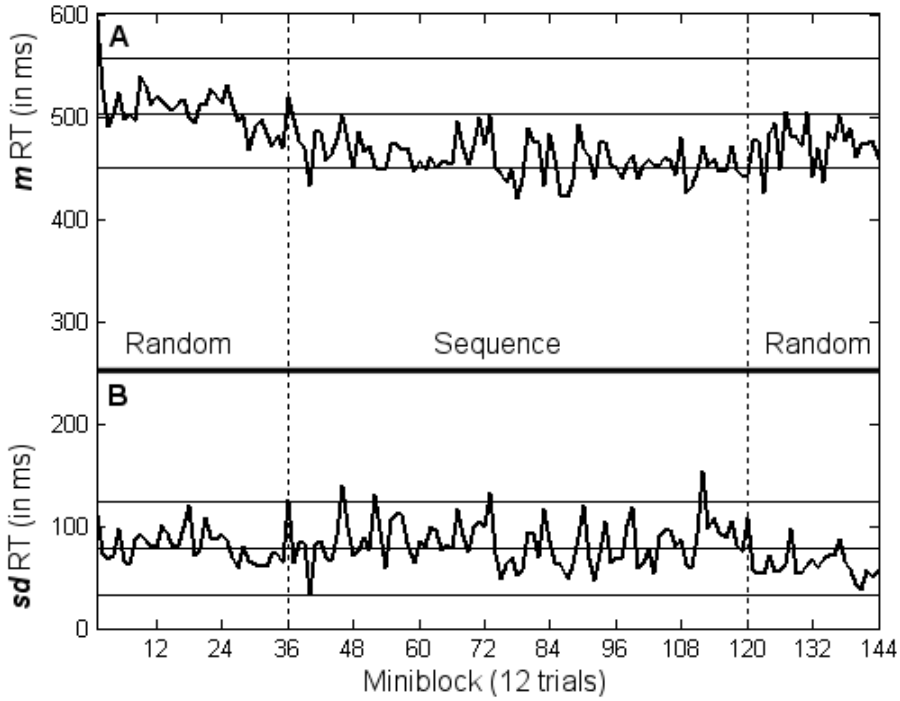


Figure 2-2. Control chart analyses of reaction time for Hidden Consecutive. RT group means (A: top) and standard deviations (B: bottom) are plotted by miniblock.

Table 2-3. Hidden Interleaved Reaction Time Means and Standard Deviations

| Block–Condition | Group Mean (σ) RT (in ms) |
|---|---|
| 1–Random | 516 (142) |
| 1–Sequence | 477 (118) * |
| 2–Random | 488 (121) |
| 2–Sequence | 471 (132) * |
| 3–Random | 491 (152) |
| 3–Sequence | 467 (126) * |
| 4–Random | 477 (116) |
| 4–Sequence | 462 (123) * |
| 5–Random | 488 (146) |
| 5–Sequence | 456 (150) * |

* Sequence trials significantly differ from Random trials of same block ($p<.001$, uncorrected)

**Hidden Interleaved**

One participant noticed a sequence during the fourth block of trials; his data for the fourth and remaining block were excluded from analysis. Group mean RT and $\sigma_{RT}$ were calculated as per the IC paradigm, except that miniblocks were six trials long for random trials and ten trials long for sequence trials. The first group miniblock of trials increased the first block's random trials' $\sigma_{RT}$ by 33 ms and was excluded as an influential outlier. Table 2-3 provides descriptive statistics for non-excluded group mean RT and mean $\sigma_{RT}$. RT was significantly less for sequence (471 ms) than random blocks (500 ms; $p < .001$). The interleaved nature of trials in the HI paradigm makes control chart representations of participant performance difficult to interpret. Thus, only descriptive statistics for this experiment are discussed.

## Discussion

Control charts are presented here as a tool for gauging when learning occurs. A normally distributed process can be statistically described as "in control" or "out of control" (Ye, 2003). A process is considered in control if its variance is only subject to chance (*i.e.*, is naturally occurring). In contrast, out of control processes exhibit some

external influence upon the process that elevates them beyond an expected range or otherwise perturbs the normal distribution of observations.

As with any statistical tool, multiple criteria of varying stringency are available for inferring the presence of a perturbation. Common criteria include the occurrence of single or multiple consecutive points outside the range or a non-normal distribution of multiple observations about the mean (Ye, 2003). Due to the expense associated with investigating perturbations, industrial control charts typically limit false positives by using a broad range (typically a "six sigma" deviation of +/- 6 *sd*). Given our relatively small number of trials, we chose a range of 3 *sd* to prevent false negatives. But to counter the increased occurrence of false positives, the following additional criteria were selected: a process was considered out of control if 1) two consecutive observations from the same block both appeared more than 3 group *sd* above or below *m*, or 2) a block had 75% or more of its observations occurring above or below *m*.

Using these criteria, the Informed Consecutive control chart demonstrates reliable RT decreases as early as the second miniblock of Block 2 (Figure 2-2a). RT remained consistently more than 3 *sd* below the mean for most of the experiment, reaching a floor of approximately 375 ms at the end of the Block 4 before returning to the baseline range in Block 5. The Hidden Consecutive control chart shows an initial decrease in RT in early Sequence blocks (Block 5), but RTs consistently reach a floor of approximately 460 ms only in later Sequence blocks (Blocks 8-10). These findings suggest that gains from implicit learning are delayed relative to those from explicit learning. Furthermore, while a significant difference was demonstrated for the Hidden Interleaved sequence, this difference is not as large as those observed for the Consecutive sequence paradigms.

Despite differences in paradigm design, these experiments reinforce what is already known about implicit and explicit learning. Values for explicit and implicit RT gains as reported in the literature vary with experimental design. Variables such as sequence length, number of trials, presence of distractor tasks, mean participant age, and conditional order (first-, second-, or higher-order) can considerably influence the learning effect of SRT tasks (Stadler & Frensch, 1998). However, average explicit and implicit RT gains for a first-order SRT task with young adult participants without distractions are around 100 ms and 50 ms, respectively (Stadler & Frensch, 1998), and are comparable to those reported here for the Informed and Hidden Consecutive paradigms (95 and 40 ms, respectively).

Aside from allowing the estimation of learning gains and their onsets, a novel contribution of control charts lies in their analysis of behavioral learning variability. For both of the IC paradigm's Random blocks, group miniblock *sd*s remain within the established baseline boundaries. But group miniblock *sd*s exceed this range for the sequence blocks, with the plot of group miniblock *sd*s following a quadratic trend that peaks during Block 3. Two distinct sources could contribute to the learning-related increase in variance. One possibility is within-participant variation in performance. Participants may be learning the sequence "piecemeal" by mastering some sequence elements faster than others. If this were true, RT should decrease for sequence elements that have been learned but remain unchanged for elements not yet learned. This in turn increases the variability of an individual's RTs for trials within the same sequence run (*i.e.*, miniblock). Another explanation is across-participant variation in performance. A participant may learn all elements of the sequence at the same rate, but with some

participants learning faster than others. If this were true, group RT variance would increase while the variance in individual RTs remained constant.

Individual participant data are provided in Appendix A. Only one of the 21 participants in the IC paradigm had a significant difference in individual *sd*s across random and sequence trials ($\alpha$ = .05, uncorrected). With 24 miniblocks of trials per block, it is possible to detect a 75% increase in *sd*s with 95% power at $\alpha$=.05 (two-tailed). Thus, the observed increase in RT variance cannot originate from within-participant sources; it must stem from individual differences in learning speeds. This also explains the quadratic trend for group miniblock *sd*s; individual differences in learning may initially create disparity, but across-participant variance eventually diminishes as all participants learn the sequence.

In sharp contrast to explicit learning, group miniblock *sd*s are largely constant throughout the HC sequence trials. None of the *sd*s in the implicit sequence's trials exceed the upper 3 *sd* boundary. While our selected control chart criteria do indicate elevated variability for Blocks 5, 6, and 10, only half of the blocks demonstrate mean RT decreases (Blocks 5, 8, 9 and 10). While explicit learning RT *m* and *sd* have a strongly negative correlation ($r$=-.85, p<.0001), implicit learning shows no such relationship ($r$=.01, p=.86, *ns*). This constancy of RT *sd*s for the implicit experiment suggests a crucial point not previously addressed in the motor learning literature: implicit learning may not be susceptible to the same individual differences observed in explicit learning.

Individual differences in learning speed are well established for explicitly learned motor skills (Ackerman and Cianciolo, 2000; Ackerman, Kyllonen, and Roberts, 1999) but not for implicit motor learning or other implicit learning tasks [*i.e.*, the artificial

grammar task (Reber, Walkenfeld, and Hernstadt, 1991; Reber, 1967)]. The presence of individual differences during explicit but not implicit learning suggests that learning differences arise largely from conscious sources such as strategy, attention, or effort. Thus, implicit learning may represent an invariant learning mechanism, while explicit learning is the modulation of this mechanism through controlled processes.

Implicit learning has been argued as essential for acquiring subtle environmental cues necessary for survival, and thus possibly conserved by evolution (Reber and Allen, 2000). Such conservation could explain the retention of implicit motor learning with age (Howard and Howard, 1989, 1992). Although implicit motor learning does show some age-related sensitivity to task complexity (Feeney, Howard, and Howard, 2002) and task interference (Frensch and Miner, 1995), its relative robustness to aging compared to explicit learning may reflect an underlying survival mechanism. However, further examination of differences between explicit and implicit learning requires that the lack of individual differences in implicit motor learning observed in the current study be replicated with larger sample sizes and possibly across populations.

This pilot study also suggests the Hidden Consecutive paradigm to be superior to the Hidden Interleaved paradigm for the functional neuroimaging study. Only one of HI's fifteen participants noticed the presence of a repeating sequence, which is somewhat surprising given the inadvertent inclusion of a run (4-3-2-1) within the sequence. But despite the greater proportion of HC participants noticing the repeating sequence (3/13 vs 1/15 for HI, the HC paradigm produced more robust RT gains. Additionally, the similarity between the IC and HC paradigms allows for more direct comparison of participant performance across conditions–which is particularly pertinent for the within-

subject neuroimaging design described below (Chapter 3). Although more participants noticed the HC sequence, this paradigm was selected for future neuroimaging investigations of implicit motor learning.

## Conclusions

The adaptation of control charts demonstrated here presents an intuitive tool for objective analysis of learning rates in behavioral datasets. The temporal information imbedded within control charts makes them ideal for analyzing dynamic performance changes. Accurate knowledge of when learning occurs is especially crucial physiological experiments that model dynamic changes in brain connectivity that accompany learning. Control charts help meet the continuing demand for novel data analysis techniques that improve our capabilities to characterize behavioral data (Kakade and Dayan, 2002; Smith *et al*., 2004). The intuitive nature of control charts and ease in constructing them further enhances their appeal for analyses of psychological data.

For this study, control charts were able detect consistent implicit learning rates across individuals. The lack of individual differences is surprising given the considerable individual differences observed for explicit learning rates. Despite years of implicit and explicit motor learning research, these differences in learning rates were only discernable with this novel adaptation of control charts. The consistency among implicit learning rates may reflect an underlying, automatic mechanism for acquiring and processing environmental cues that may subsequently be enhanced with explicit strategy. Additional work in non-motor modalities (*e.g.*, perceptual priming) may confirm this invariance of implicit learning rates and further elucidate its mediation by learning strategy.

# CHAPTER 3
# METHODOLOGY

## Participants

**Young Adults.** Eighteen [8 males; mean (sd) age = 25 (2.1) years] right-handed graduate students at the University of Florida participated in this experiment for monetary compensation. All participants were recruited in accordance with Institutional Review Board policy and provided their informed consent prior to participating. Handedness was assessed by a modified version of the Edinburgh Handedness Inventory (Oldfield, 1971). Participants were excluded if they had metal in their bodies, reported any psychiatric or neurological illness, arthritis of the hand or wrist, or any condition that would interfere with task performance or make participation uncomfortable.

**Senior Adults.** Nine [5 males; mean (sd) age = 67 (5.0) years] right-handed participants between 60 and 75 years old participated in this experiment for monetary compensation. Although only participants with masters' or doctoral degrees were originally sought in an attempt to equate the educational attainment between groups, this criterion was relaxed when no such participants could be recruited. The same inclusion and exclusion criteria applied to both senior and younger adults. All participants were recruited in accordance with Institutional Review Board policy and provided their informed consent prior to participating.

## Experimental Paradigm

The experimental protocol required two sessions of MRI scanning depicted in Figure 3-1. Since each session lasted approximately one hour, scanning occur over two days to prevent confounding influence from fatigue. Each scan is described in greater detail below.

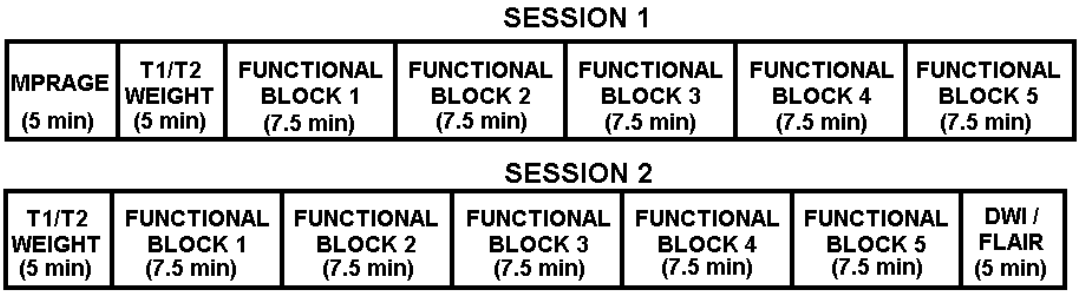


Figure 3-1. Magnetic Resonance Imaging Scans by Session.

**Pre-scan**. Prior to scanning, participants completed questionnaires assessing MRI safety (*i.e.*, the absence of metal within their bodies) and handedness. Participants lay supine within a 3T head-dedicated Allegra MRI scanner (Siemens AG). Participants wore a headset and microphone for communication with the experimenters (Resonance Technologies) and a button response glove for making manual responses to visual stimuli (MRI Devices). Foam pads were used to reduce participant head movement. A RF coil (MRI Devices) was snapped around the participant's head to record the MR signal.

**Localizer**. Every session began with a 15-second localizing scan (not depicted) to confirm that the head rested within the spherical center of the coil that produced the most stable signal.

**MPRAGE**. The MPRAGE pulse sequence–colloquially called a "3-D scan"–acquired high-resolution anatomic images with the following parameters:

matrix=512x512, TR=1500ms, TE=4.38ms, FOV=240mm, FA=8$^{o}$, 160 slices (1.4mm thick, no gaps)

**T1/T2 weighted**. T1- and T2- weighted images were acquired at the same slice thickness and orientation as the functional scans to allow for co-registration of the functional and MPRAGE images. The T1- and T2- images respectively attribute high intensity values to high-density (cortex) and low-density (cerebral-spinal fluid) matter. T1/T2-weighted images parameters: matrix=256x256, TR=5.24s, TE=13ms, FA=150$^{o}$, FOV=240mm, 36 slices (3.8mm thick, no gaps).

**Functional**. Echo-planar imaging (EPI) was used to assess brain activity, measured as slight temporal changes in the blood oxygen level dependence (BOLD) of cortical matter. Participants performed the serial reaction time (SRT) task as per the behavioral study (see Chapter 2). Each trial lasted 1.5 seconds, with an 800 ms response window and random delay in stimulus onset of 0-200 ms to prevent anticipation of stimulus onset. Thus, each image (3 seconds long) encompassed two complete trials. The first six young adult participants performed 288 (7 min, 20 sec) trials per functional scan without rest. A rest period was included in the remaining participants' scans to serve as a baseline for subsequent statistical comparisons across participants[1]. For the remaining eleven young adult and all senior adult participants, each scan consisted of 240 trials (6 min) followed by a rest period (1 min, 20 sec).

Each session was designed with five functional scans. Scans 1 and 5 consisted of random trials, while trials in scans 2-4 followed a 12-element long repeating sequence

[1] For the seventh young participant, the experimenters verbally cued the resting condition onset. This approach led to inconsistent onsets of resting conditions across scans, so the resting condition was automated for subsequent participants.

[sequence 1: 2-5-4-3-5-2-4-5-3-2-3-4; sequence 2: 4-5-2-3-5-4-3-4-2-5-3-2]. As in the behavioral study, the sequence was non-predictive and excluded runs, trills, and repeats. Sequences were counterbalanced across participants and sessions. Participants were not informed of the sequence for the first session. If participants noticed the sequence, they were asked to learn in. For the second session, participants were instructed to learn the sequence but were provided no sequence details. Scan 5 (Random) was omitted in 8 cases due to participant fatigue, technical difficulties, or time constraints.

Echo-planar imaging was performed with the following parameters: matrix=64x64, TR=3s, TE=25ms, FA=90$^{o}$, FOV=240mm, 36-40 slices of 3.8mm thickness (no gaps). Preprocessing was performed in BrainVoyager (Brain Innovations) with motion correction, linear detrending, and slice-scan time correction. Temporal smoothing was performed with a lowpass filter (0.08 Hz) in Matlab. No spatial smoothing was performed.

**FLAIR**. Fluid-attenuated inversion recovery (FLAIR) imaging was performed to assess potential white matter lesions[2]. FLAIR imaging scans lasted approximately five minutes and were performed with the following parameters: matrix=256x256, TR=6000ms, TE=80ms, FA=180$^{o}$, FOV=240mm, 36-40 slices of 3.8mm thickness (no gaps).

**DTI**. Diffusion tensor imaging (DTI)[2] assesses the multi-directional diffusion of water molecules within nerve fibers to trace white matter pathways. Water diffusion was measured in 12 directions in 2 minutes with the following parameters: matrix=128x128, TR=4500ms, TE=94ms, FOV=240, 30 slices of 3.8 mm thickness (no gaps).

[2] FLAIR and DTI scans were not performed on all participants due to time constraints, technical difficulties, or participant fatigue.

## Determining the Onset of Learning

A comparison of brain activity by learning state necessitates a means for assessing reliable changes in performance due to learning. Four approaches were used: a) analysis of RT data by control chart, b) analysis of RT data by *C*-statistic, c) participant responses when asked "How well do you know this sequence?", and d) visual inspection of RT data. Participant self-reports were only available for explicit learning sessions, since inquiring of the sequence during implicit learning would have prompted sequence awareness. Figure 3-2 depicts a sample control chart for one young adult participant's temporally smoothed (0.08 Hz low pass filter) RT data in the explicit session, while Table 3-1 provides accompanying *C*-statistics and percent accuracies for each block, participant self-reports for each session, and the block best demonstrating behavioral measures of learning as determined by the following criteria. Behavioral data for all participants are presented in a similar format in Appendix A.

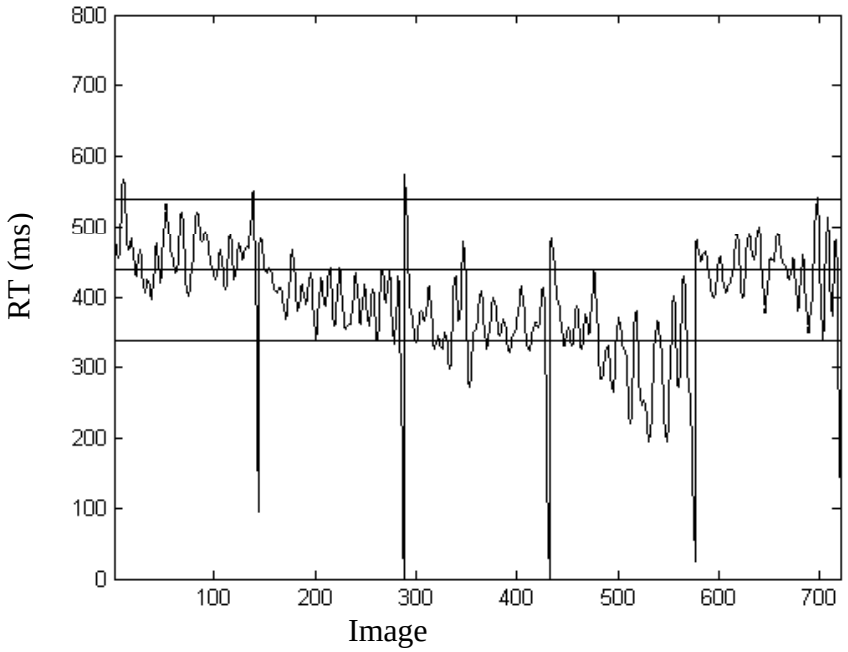


Figure 3-2. Sample Control Chart Depiction of Reaction Time.

Table 3-1. Sample Analysis of Behavioral Measures.

| Session | Explicit-Young Participant #1 | | | | |
|---|---|---|---|---|---|
| Block | 1 | 2 | 3 | 4 | 5 |
| Tryon's C | 1.05 | 1.35 | 1.10 | 3.86 | 0.00 |
| Accuracy | 96% | 99% | 96% | 96% | 94% |
| Participant Response<br><br>Sequence Learned | Participant not asked when sequence was learned<br><br>Block 4 | | | | |

**Control chart**. Control charts were created by plotting mean reaction time against image. Since participants performed two trials per image, the RT of these two trials was averaged. If one trial was a non-response, the other trial's RT was used. If both trials were non-responses, that image's RT was assigned a value of 0.

As previously described, a control chart is a statistical tool for detecting perturbations in static processes. Here, control charts are used to detect deviations from baseline SRTT performance due to learning. The same criteria are used as in the behavioral pilot study to detect RT deviations from baseline: a) two consecutive observations outside of the 3 sigma boundary, or b) one observation outside this range with at least 75% of the block's observations less than or exceeding the baseline mean.

**C-statistic**. The *C*-statistic, also known as Tryon's *C* (1982), is a statistical tool for analyzing changes of slope with time. It is an elegantly simple technique, able to be performed by hand and suitable for large samples or samples with as few as 8 observations. The *C*-statistic evaluates a block of trials to determine if the sum of squared differences between consecutive trials, divided by the *C*-statistic's standard error, exceeds a significant threshold. The *C*-statistic uses the same significance thresholds as the *t*-statistic, so a C-statistic exceeding 1.96 with greater than 30 trials is significant at alpha = .05 (two-tailed). A significant finding indicates a non-zero slope.

**Accuracy**. Percent accuracies are provided for each block's trials.

**Participant Self-Reports**. At the conclusion of each explicit sequence block, participants were asked "How well do you know the sequence?" Participants claiming to know the entire sequence were asked to report as much of the sequence as they could. At the conclusion of the implicit session, participants were asked, "Did you notice the sequence? If so, when?"

**Sequence Learned**. This table cell indicates which block was selected for subsequent neuroimaging analyses of learning. Criteria for selection included congruent findings for at least two of the three behavioral analyses (control chart, *C*-statistic, and self-report) described above. If these methods provided no consensus, the block indicated by the control chart was selected. Two senior participants (#7 and 8) reported difficulty pressing the response buttons. They consistently performed at less than 90% accuracy were not included in subsequent analyses.

## Connectivity Modeling

Connectivity analyses are increasingly popular tools for modeling functional neuroimaging data (He *et al.*, 2001). Functional connectivity models assess the temporal covariance across brain regions of interest (ROIs) to gauge the interdependence across ROIs during task performance. They are thus more valuable than the ROI "laundry lists" common in early neuroimaging literature, since they can illustrate the modulation of neural networks with task performance. Functional connectivity methods have been further refined for assessing temporally varying ROI correlations. (He *et al.*, 2003).

Two statistical methods have dominated functional connectivity analyses: structural equation modeling (SEM) and correlational models. Structural equation modeling seeks to establish causal relationship between ROIs. SEM can also describe the

interactions of external variables, such as age or time, upon the defined neural networks of brain activity. However, SEM has many underlying assumptions–most notably independence of observations–that pose statistical challenges for adaptation to neuroimaging datasets (Solodkin, 2004). Additionally, SEM requires an *a priori* model of functional connectivity, based either upon neuroanatomy or exploratory modeling of additional datasets. [Although exploratory adaptations of SEM exist, this technique is computationally infeasible for models with greater than 6 ROIs. (Zhuang *et al.*, 2005)].

Correlational models encompass a broad range of statistical approaches that share one common aim: to determine the correlation between two or more brain ROIs' activity time courses. These approaches are summarized in He *et al.* (2003) and discussed at length below. The advantage of correlational approaches is that they require no *a priori* models of brain function. Additionally, they may be used to generate visually intuitive maps of brain connectivity. However, the correlations are bivariate (between two ROIs' time courses) and cannot control for influences from other modeled variables. Finally, correlational models are relatively novel approaches for data analyses; unlike SEM, no consensus has been reached in the scientific community upon the ideal correlational approach, so these approaches have yet to be incorporated into any neuroimaging software package. But despite these drawbacks, the exploratory aim of this research to develop models for implicit and explicit motor learning makes correlational modeling the more feasible of the two approaches.

### Within-condition Interregional Covariance Analysis (WICA)

Within-condition interregional covariance analysis (WICA) is a correlational modeling technique with three independent steps that summarize or improve upon existing correlational methods (He, 2003).

**WICA Step 1: Seeding**. The simplest of WICA's three steps is the seeding approach. This method derives its name from the selection of voxels from a ROI cluster (the "seed"). Following seed selection, an average time course is calculated for voxels within the seed. The time course of every voxel in the brain is then correlated against the seed time course to produce a statistical map that represents the correlation (*i.e.*, strength of connectivity) between brain regions and the seed. While these seeding maps offer quick visual interpretation of brain regions functionally connected to the seed ROI, each map is specific to a single ROI. Furthermore, additional statistical steps are required to combine seeding maps across participants (see ROI selection, below).

**WICA Step 2: ROI-based approach**. The second of WICA's three steps evaluates functional connectivity across multiple ROIs. This approach analyzes brain connectivity during task performance and then compares connectivity networks across different tasks. The ROI-based approach requires that participants' functional brain data be normalized to a baseline. First, ROIs are defined for each participant. Next, the average activity (usually mean or median) is calculated for each participant's ROIs' time courses. These values are static, *i.e.*, a single value is calculated that represents the ROI's activity for the duration of the task. Then, ROI values are correlated within task condition across participants to determine the correlational strength of each ROI-ROI pairing within a task. Finally, the process is repeated for all tasks for subsequent comparison of correlational models.

The method proposed by He *et al.* (2003) has been refined as follows for applicability to data not normalized against a baseline. As before, ROIs are defined for each participant (see Chapter 4). Then, for each participant's block of functional data,

the Pearson's correlation is calculated for each pairing of ROI activity timecourses. Each block can then be assigned to a condition (*e.g.*, Random, Explicit Learning, or Implicit Learning), with ROI-ROI correlational pairs grouped per condition. For example, an experiment with 5 participants and 2 Explicit Learning blocks per participant would result in 10 independent correlations of primary motor activity and SMA activity (and 10 primary motor–lateral premotor correlations, and 10 lateral premotor–SMA correlations, etc.) per Explicit Learning condition. The observed correlations for a given ROI-ROI pair can then be compared across conditions with the Kolmogorov-Smirnov 2-sample test (K-S 2S), since this test makes no assumptions about an underlying distribution for the variables. If the KS-2S detects a significant difference across conditions, the median values of each condition's correlational pairs can describe the direction of this difference.

**WICA Step 3: Dynamic connectivity**. The third WICA step assesses changes in functional connectivity with time. WICA steps 2 and 3 are methodologically quite similar, as both correlate ROI activity values across participants. But whereas the second step condenses ROI activity time courses into average values and correlates these values, the third step correlates ROI activity values *for every image* across participants. Thus, dynamic changes in interregional correlations (*i.e.*, changes in correlational strength from image to image) can be assessed both within and across functional tasks. One requirement of this approach is that a definitive starting point must exist for all participants. And as per WICA step 2, this step requires predefined regions of interest. Our methodological approaches for defining these ROIs are detailed in the next chapter.

# CHAPTER 4
# ROI SELECTION

## Overview

Functional neuroimaging datasets paradoxically suffer from paucity (due to small sample sizes stemming from expense) while providing a plethora of data per participant. Despite recent refinements of statistical methodology (Zhuang *et al.*, 2005), current multivariate analyses cannot handle this overabundance of data. Analysis techniques thus necessarily partition the data into discrete subunits, *i.e.*, anatomical regions of interest, that are then selectively analyzed based upon *a priori* hypotheses. Neuroimaging connectivity analyses are crucially dependent upon how regions of interest are defined.

Solodkin *et al.* (2004) proposed the following approach for ROI selection. First they performed a general linear model random-effects analysis comparing brain activity during motor task performance versus rest. The observed clusters of task-related activity were labeled by anatomical location. A 7mm sphere was centered about the voxel at each cluster's center of gravity. The ROI included voxels within the sphere whose activities significantly differed during task from rest. The activity time courses of these significantly active voxels were then averaged together to produce the ROI time course.

Since our echo-planar images were collected as approximately 4mm wide cubic voxels, a 7mm sphere would include fewer than 20 voxels per ROI. In order to avoid the substantial resampling required for this approach, a sphere was not used to define the ROI. Instead, the voxel at the cluster's center of gravity and its six nearest neighboring voxels (those immediately superior, inferior, left, right, anterior and posterior) were used

to constitute each ROI. The ROI time course was calculated by averaging the activity time courses of these seven voxels.

**Random**

A random-effects general linear model (GLM) analysis (Friston *et al.*, 1995) was performed in BrainVoyager 2000 (Brain Innovation, Maastricht, Netherlands) to find brain regions whose activities significantly differed between motor performance and rest during blocks of Random trials. A separate GLM was performed in both young (n=59 blocks) and senior adult (n=36 blocks) participants. These analyses modeled brain regions that mediate SRTT performance in each age group, which may or may not also mediate learning. The young adult analysis was further limited to participants with rest periods since the GLM requires a resting baseline for comparison.

**Learning**

Explicit learning of a motor sequence may recruit brain regions in addition to those necessary for motor execution. A GLM was specified for each age group to define brain regions active during learning. These GLMs included the first block (if any) for each subject in which performance significantly improved compared to the Random blocks, as determined in Appendix B. Implicit learning could not be accurately modeled for young adults with this method, since only two young adult participants showed significant improvement in reaction times and had resting conditions during their sessions.

A drawback to all of these approaches is that learning-specific ROIs are co-mingled with those that mediate motor execution. We adapted seeding analyses to discern ROIs involved in motor learning. Specifically, behavioral measures of learning (*i.e.,* reaction times) were used as our seeding correlate. Statistical maps were produced that expressed the correlation between each ROI and RT. ROIs involved with learning were expected to

be negatively correlated with RT, since performance improvements equate into improvements in participants' speed. Unlike the ROI seed method, the behavior-driven seed approach is not limited to regions locked within a functional circuit. Furthermore, the map of learning-related brain regions generated by this approach could be contrasted to the random condition GLMs to assess the additional recruitment of brain regions.

## Methods

### Random

General linear models were constructed for analyzing brain regions mediating the execution of random SRT trials. Each GLM incorporated data from blocks of random trials (Blocks 1 and 5) of every session and subject, with a separate model constructed for each age group. A predictor was defined to compare activity during the first 120 trials against the final 24 trials of each block. The GLM–after accounting for shifts in baseline activity across blocks and the hemodynamic delay of BOLD response–assessed voxel-wise increases or decreases in brain activity during random SRT trials relative to rest. A random-effects analysis was used for both young and senior adults because this analysis is less susceptible than fixed-effects analysis to imbalance from outliers. However, a caveat for the senior adult analysis is that random effects analysis may not have sufficient detection power when used with fewer than 10 participants.

### Learning

Two functional connectivity seeding approaches were used to assess ROIs associated with learning: behavioral-seeding and ROI-seeding. These analyses were performed on the first block for which each participant demonstrated an improvement, as determined by analysis of reaction time data in Appendix B.

### RT-seeding

The seeding analyses were performed with BrainVoyager 2000 (Brain Innovation, Maastricht, Netherlands) using an approach similar to the GLM described for analyzing performance during random SRT trials. The GLM above simply divided the time course into task vs. rest. The behavioral seeding approach used reaction time measures (temporally smoothed with a 0.08 Hz lowpass filter) as a predictor for each block. Unlike the task GLM, the RT-seed was not restricted to blocks with resting periods, so all young adult participants could be included.

### ROI-seeding

The RT-seeding approach indicated several voxel clusters whose activities were negatively correlated with RT. One of the most significantly correlated clusters, located in the cerebellum, was used as a ROI-seed to establish regions with which it was functionally connected. A GLM was constructed as per the RT-seed approach, but using the time course of the cerebellum cluster's activity (*i.e.*, the cluster's central voxel and its six nearest neighboring voxels) as each block's predictor.

## Results

The glass brain is a graphical approach that depicts clusters of brain activity significantly associated with a task by collapsing three dimensions into three separate 2D projections. Figure 4-1 shows glass brain models of brain activity during performance of random trials for young and senior adults, respectively. Glass brain models for RT- and ROI-seeding analyses of young adult performance during explicit learning are shown in Figure 4-2. The data used to construct the glass brain models underwent Gaussian spatial smoothing (6 mm FWHM) to improve presentation quality. The young adult explicit

learning condition is modeled to illustrate this technique. Talairach coordinates in Table 4-1 indicate the most significant voxel in three of the group-condition combinations.

**Young Adults, Random GLM**. Performance of Random SRTT trials was accompanied by ipsilateral (left) activation of the primary motor cortex, lateral premotor cortex, anterior cingulate, and supramarginal gyrus. Activity is represented as a single cluster in Figure 4-1 because it was extensive throughout these cortical regions. Supplementary motor area activity was also ipsilateral and is depicted as a separate cluster due to its relative confinement to the SMA and lesser statistical significance.

Table 4-1. Foci of Functional Activity by ROI and Analysis Method (in mm Talairach).

| ROI | Young Adult Random | | | | Senior Adult Random | | | | Young Adult RT-Seed: Explicit | | | | Young Adult ROI-Seed: Explicit | | | |
|---|---|---|---|---|---|---|---|---|---|---|---|---|---|---|---|---|
| | x | y | z | max ***t*** | x | y | z | max ***t*** | x | y | z | max ***t*** | x | y | z | max ***t*** |
| Dorsolateral Prefrontal | -24 | 38 | 23 | 4.7 | -28 | 36 | 22 | 5.25 | - | - | - | | - | - | - | |
| Anterior Cingulate | -8 | 1 | 52 | 7.4 | -1 | 0 | 53 | 12.2 | -8 | 0 | 37 | -5.11 | -3 | -4 | 42 | 24.7 |
| Supplementary Motor Area | -4 | -7 | 58 | 13.4 | -10 | -11 | 60 | 9.2 | - | - | - | | - | - | - | |
| Putamen | -25 | -3 | 6 | 5.7 | -27 | -2 | 6 | 7.0 | - | - | - | | 23 | -8 | 6 | 26.4 |
| Lateral Premotor | -31 | -19 | 56 | 10.2 | -26 | -11 | 56 | 12.9 | - | - | - | | - | - | - | - |
| Caudate | -10 | 9 | 12 | 8.2 | -15 | -12 | 15 | 4.9 | - | - | - | | -10 | 3 | 4 | 27.1 |
| Primary Motor Area | -34 | -28 | 48 | 15.7 | -33 | -17 | 53 | 15.3 | -33 | -33 | 50 | -4.8 | - | - | - | |
| Supramarginal Gyrus | -26 | -43 | 38 | 9.1 | -26 | -47 | 50 | 15.7 | -29 | -47 | 48 | -5.7 | - | - | - | |
| Superior Temporal Sulcus | -51 | -21 | 17 | | - | - | - | - | - | - | - | | -54 | -43 | 14 | 25.7 |
| Calcarine Fissure | -25 | -86 | 5 | 7.0 | -22 | -74 | 1 | 3.1 | -3 | -81 | 2 | -6.0 | - | - | - | |
| Cerebellum | 26 | -44 | -27 | 14.7 | 31 | -47 | -21 | 6.7 | 27 | -44 | -26 | -8.2 | 27 | -44 | -26 | 25.1 |

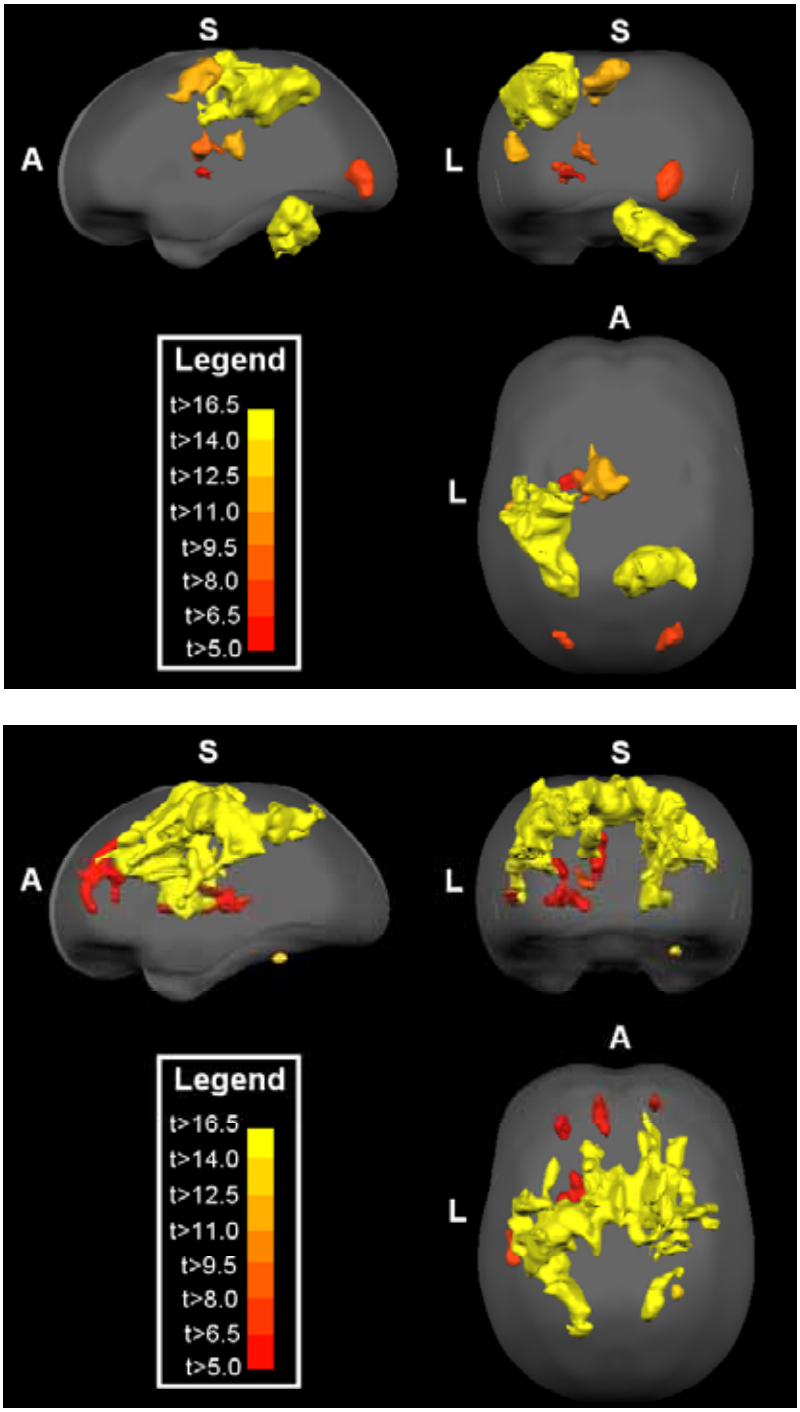


Figure 4-1. Glass brain representations of functional activity during Random trials. Activity clusters are depicted for young (top) and senior (bottom) adults. Abbreviations depict orientations: anterior (A), superior (S) and left (L). Both models were produced with random-effects GLM analyses indicating clusters of voxels with *t*-values > 5 at least 200mm$^3$ in size. Note: The volume threshold is selected arbitrarily to improve figure quality. The senior adult cerebellum cluster is included despite its size (197 mm$^3$).

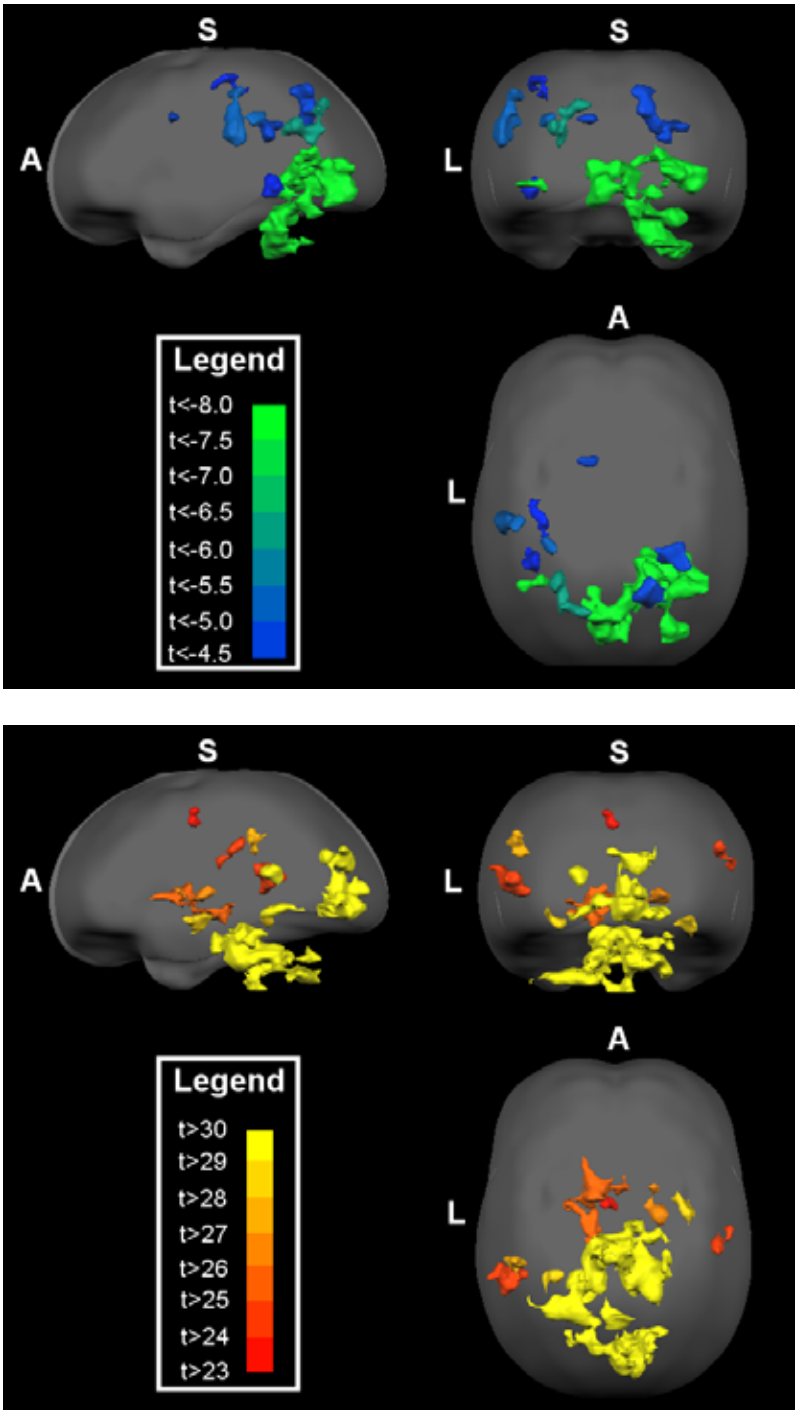


Figure 4-2. Glass brain representations of functional activity during Explicit trials. Activity clusters are depicted for young adults using reaction time (top) and cerebellum (bottom) as connectivity seeds. Abbreviations depict orientations: anterior (A), superior (S) and left (L). The RT-seed model depicts correlations with *t*-values < 4, while the cerebellar seed model depicts correlations with *t*-values > 23. Both models were produced with random-effects GLM analyses indicating clusters of voxels at least 200mm$^3$ in size.

The caudate, putamen, and superior temporal sulcus also demonstrated contralateral activity during young adults' performance of Random SRTT trials. These regions demonstrated moderate statistical significance (maximum t-value = 8.2 for caudate, 5.7 for putamen, 11.2 for temporal). Visual cortex activity was of comparable significance (max t-value = 7.0) but occurred bilaterally. Ipsilateral activity was only observed for the cerebellum (max t-value= 14.7) throughout layers III-VI.

**Senior Adults, Random GLM**. Similar to the young adults, senior adults performing Random SRTT trials demonstrated activation of the primary motor cortex, SMA, lateral premotor cortex, anterior cingulate, parietal lobe, supramarginal gyrus, caudate nucleus, putamen, and inferior frontal/superior temporal gyrus. Unlike young adults, regional activity was remarkably bilateral for senior adults. Activity was widespread throughout these regions, leading to its representation as a single cluster.

Activity was also observed in the ipsilateral cerebellum. Although young adults' cerebellar activity cluster encompassed a volume nearly two orders of magnitude larger than senior adults' cluster, the locations of each clusters' most significant voxel differed by less than 8 mm.

The dorsolateral prefrontal cortices of senior adults showed task-related activation that was not observed for young adults. This activity was located along the middle frontal sulcus (BA 9) and was not observed for young adults even at lower statistical thresholds. Surprisingly, senior adults did not demonstrate consistent activation of the visual cortex.

**Young Adults, Explicit, RT-seed**. Reaction time was negatively correlated with activity of the ipsilateral cerebellum, bilateral visual cortex, bilateral supramarginal

gyrus, bilateral anterior cingulate, and contralateral primary motor cortex during explicit learning of a motor sequence. These correlations were statistically weaker (|*t*-value| < 8 for RT-seed) than activity clusters associated with performance of Random SRTT trials (|*t*-value| < 16) for either young or senior adults. Yet activity foci for these ROI were largely consistent across Random and RT-seed analyses, with only the anterior cingulate foci differing by more than 8 mm.

The center of the anterior cingulate volume bordered the corpus callosum, raising the possibility that this regional activity may be artifactual due to head movement. Three additional activity clusters–two in the parietal lobe and one bordering the parahippocampal gyrus–has centers within white matter and were most probably artifact. These regions were accordingly not included in Table 4-1.

**Young Adults, Explicit, ROI-seed**. Activity throughout the entire brain demonstrated a strongly significant (|*t*-value|>10) positive correlation with the cerebellum seed cluster. Discrete clusters of activity could only be attained by elevating the *t*-value minimum threshold to 23. The most significant activities were observed in a single activity cluster extending throughout the bilateral cerebellum and occipital lobe.

Cerebellum activity was also significantly and positively correlated with the caudate (r=.61, *t*-value=27.1), putamen (r=.72, *t*-value=26.4), and anterior cingulate (r=.75, *t*-value=24.7). The superior temporal gyrus also demonstrated significant correlation (r=.76, *t*-value=25.7) with the cerebellum.

## Discussion

The brain regions associated with young adults' performance of Random SRTT trials can be categorized by association with motor behavior. The primary motor cortex is predominantly responsible for motor execution (Yousry, 1997). The premotor cortex

prepares response execution (Passingham, 1988; Passingham, 1987), while the basal ganglia prevents unintentional behaviors and provides performance feedback (Harrington and Haaland, 1991). Finally, the cerebellum assists in orchestrating motor responses (Ivry and Keele, 1989).

Additional regional activity may not necessarily be associated with motor behavior. For example, the calcarine fissure processes visual stimuli; activity in this region is likely independent of motor response execution. Similarly, the supramarginal gyrus monitors spatial hand position (Zilles *et al.*, 2003), and the anterior cingulate evaluates task performance for the commission of errors (Carter *et al.*, 2001).

Senior adults performing Random SRTT trials demonstrated markedly different patterns of brain activity than young adults. The most notable difference was increased symmetry in activity for all brain regions except the cerebellum. Brain activity during Random SRTT performance appears more bilateral for senior adults than for young adults. This observation is consistent with previous reports of age related increases in symmetry (Cabeza, 2002). The two most popular theories accounting for age-related increases in brain activation symmetry are functional compensation and dedifferentiation (Dolcos *et al.*, 2002). Functional compensation contends that age-related neural changes (*e.g.*, cortical atrophy) result in one hemisphere recruiting the other hemisphere to supplement performance in originally lateralized cognitive tasks. In contrast, dedifferentiation postulates that reductions in brain asymmetries may reflect a continuous streamlining of brain function with learning experiences. The theories are not mutually exclusive and neither has overwhelming empirical support, so the mechanism behind age-related reduction in functional hemispheric asymmetries requires more research.

Only the cerebellum did not demonstrate bilateral activity in senior adults; cerebellar activity was considerably smaller and less statistically significant for senior adults than young adults. The activity cluster appeared in the anterior ipsilateral hemisphere for both young and senior adults. As previously discussed, this region undergoes disproportionately more atrophy than other cerebellar regions (Andersen *et al.*, 2003). Thus, the reduced volume of activation in senior adults is not unexpected.

Senior adults also demonstrated bilateral activity of the prefrontal cortex. This activation suggests the utilization of cognitive resources most likely arising from compensation (*e.g.*, the task may place additional demand upon senior adults' attentional resources). However, the prefrontal activity may represent a cohort effect. Although participants' typing aptitudes were not measured, the younger adults presumably had more frequent interaction with computer keyboards and thus greater practice at executing independent finger movements. The response requirements of the SRTT may be more novel for senior adults and thus require recruitment of the prefrontal cortex. As such, the prefrontal activation in senior adults cannot be directly associated with functional compensation due to age.

Surprisingly, senior adults lacked a significant visual cortex response during Random SRTT trials. Bucker *et al.* (2000) demonstrated that the amplitude of the visual cortex BOLD response decreases with age despite a consistent response amplitude for the primary motor cortex. They also reported a weaker effect size for visual cortex activation of senior adults; their conclusions, in conjunction with the smaller senior adult sample size, may account for the sub-threshold visual cortex activity in this study. Bucker warns against study designs that assume comparable response amplitudes across populations.

The connectivity methods described in Chapter 3 utilize within-subject analyses that require no such assumptions.

Activity of the anterior cingulate, primary motor cortex, supramarginal gyrus, calcarine fissure, and cerebellum was significantly correlated with improvements in performance (RT) for young adults during explicit learning of a SRTT sequence. The activity foci for these regions were largely homologous to those observed for the Random SRTT trials. The exception is the anterior cingulate, whose activity focus shifted 15 mm inferior from Random to Explicit trials. The proximity of the anterior cingulate focus to the corpus callosum suggests movement artifact.

The shift in activity foci across analysis method (Random SRTT GLM vs. Explicit RT-seed) could be problematic for subsequent connectivity modeling. For example, the young adult GLM primary motor cortex voxel time course (x=-33, y=-17, z=53) may not be correlated with the RT-seed primary motor cortex voxel time course (x=-33, y=-33, z=50). To address this issue, the ROI time courses of clusters determined by each approach were correlated for the young subjects' explicit learning blocks, again using the blocks determined in Appendix B (n=15). The median intra-subject correlations were as follows: M1, $r$=.98, supramarginal gyrus, $r$=.96; anterior cingulate, $r$=.95; calcarine fissure, $r$=.91. These strong correlations suggest that the choice of ROI cluster coordinates will not dramatically affect the resulting connectivity analyses. The ROIs from the Random GLM were selected since the greater statistical power of this analysis (see below) ensured more consistent activity in this region across participants.

Despite the smaller sample size in the RT-seed comparison (n=15 vs. n=59 for Random), this random effects analysis should have sufficient power to detect activation

of the prefrontal cortex, premotor cortex, and basal ganglia. However, RT may be a poor predictor of BOLD changes due to its increased variability. The BOLD response rarely changed by more than 3%, but RT improved by up to 60% during explicit learning. The larger variability of RT measures leads to correlations with BOLD signal of both weaker magnitude and weaker statistical significance. This is evident in Figure 4-2, where no correlational *t*-value exceeded 8 in magnitude.

In contrast to the RT-seed, the cerebellum seed produced correlations of incredibly strong statistical significance. Whereas the disparity between RT and BOLD variances led to weak correlations, the similarity of interregional BOLD variances led to correlations of strong magnitude and statistical significance. The entire brain demonstrated strong correlation with the cerebellum; interpretable statistical maps could only be produced by raising the minimum *t*-value to 21.

At this threshold, the cerebellum seed's activity was strongly correlated with activity of the bilateral cerebellum, bilateral visual cortex, contralateral anterior cingulate, bilateral caudate and putamen, and contralateral superior temporal sulcus. The cerebellum's correlation with the superior temporal sulcus was unanticipated since the latter primarily mediates language and not motor performance. The afferent and efferent connections between all other regions and the cerebellum were previously discussed.

The strong bilateral correlation of cerebellum activity indicates that this analytical approach is poor for differentiating functional connectivity from effective (*e.g.*, anatomic) connectivity (Biswal *et al.*, 1995). The RT-seed analysis and the GLM analyses of Random SRTT trials for both age groups only indicated activation of the ipsilateral cerebellum. The strong correlation between cerebellar hemispheres is

probably task independent. Thus, the RT-seed approach for functional connectivity analysis, while suffering from low statistical power, is a better estimator of task-related functional connectivity than the ROI-seeding method.

In conclusion, the RT-seed method was superior to the ROI-seed method for defining task-relevant clusters of functional activity. However, the RT-seed approach suffers from poor statistical power due to the heightened variability of RT measures. For this dataset, the clusters defined for each ROI by the Random SRTT GLM were strongly correlated with those defined by the RT-seed method. The ROIs generated by the Random SRTT GLM were thus justified for use in subsequent connectivity analyses.

# CHAPTER 5
# CONNECTIVITY MODELS

The regions of interest defined in the previous chapter can be used in conjunction with the WICA ROI-based approach to develop functional connectivity models of implicit and explicit motor learning for each age group. These models will support or refute models for age-related cognitive decline such as the frontal aging hypothesis.

## Materials

ROI-based connectivity modeling was performed as described in Chapter 3. Analyses of random SRT task performance used Blocks 1 and 5 of each session (respective to age group), while the explicit and implicit learning analyses used the blocks showing behavioral evidence of learning. Data are presented in Appendix A. Unless otherwise noted, only one block was used per participant who showed evidence of learning

ROI-based connectivity modeling was performed with in-house programs written in Matlab (The MathWorks Inc.). Initially, all analyses were performed using the ROIs generated from the young and senior adult Random conditions (Table 4-1). Using these ROIs served two purposes. First, analyzing functional data during the random SRT trials allowed for establishing "baseline" models of brain regions that mediate motor execution. Second, since these ROIs differed (albeit slightly) from the learning-related ROIs, analyses of learning trials with these ROIs assessed the influence (if any) learning has upon motor executions.

Connectivity models were then developed for learning conditions using ROI coordinates from the RT-seed approach. Since these clusters were negatively correlated with reaction time (and thus implicated in learning), these models were expected to illustrate learning differences to which the random trial ROIs might be insensitive.

To recap the ROI-based connectivity modeling approach, the correlations between ROIs wereestablished for every block in each age (young, senior) and condition (random, explicit, implicit) group. The ROI-ROI correlations were then compared across age groups and conditions with the Kolmogorov-Smirnov two-sample test, since this test requires no assumptions about underlying variable distributions.

## Results

Figures 5-1 through 5-4 are RT control charts for each groups in the implicit (session 1) and explicit (session 2) learning sessions. For the implicit sessions, data from blocks during which participants reported sequence awareness are excluded. Horizontal lines represent mean (middle) RT for Block 5 plus (upper) and minus (lower) three standard deviations. The young adult control charts combine data for the first 120 images of each trial block for participants with and without rest periods; the last 24 images of each trial block were omitted for a young participants #1-7.

ANOVA analyses of RT data revealed significant age, session, block, age x session, age x block, session x block, and age x session x block interaction effects (all $p < .01$, Bonferonni corrected). The age x session x block interaction is readily apparent in the control charts. Young adults demonstrate greater RT gains in the explicit session (131 ms from Block 4 to Block 5) than senior adults (65 ms). Yet the reverse appears true for implicit learning; senior adults demonstrate a distinct learning effect during Block 4 of the implicit session (50 ms) that is not readily apparent for young adults (25

ms). Attrition may in part explain this finding, since more young adults (6/18) noticed the sequence than senior adults (1/9) and were subsequently excluded from Figure 5-1.

Control chart analyses indicate trends similar to those reported in the pilot behavioral study. For both age groups, explicit learning RT gains are greater than implicit learning RT gains (Table 5-1). RT gains are also evident earlier in both groups for explicit than implicit learning. For explicit learning, the control charts depict increasing RT standard deviations (σRT) corresponding to decreasing RT means for both groups. For implicit learning, young adults demonstrated marginal RT improvement. Although young adult baseline RT variance was greater for implicit than explicit learning, σRT did not exceed the three sigma baseline range. Likewise, senior adults demonstrated reliable implicit RT gains without significant change in σRT.

Table 5-1. Reaction Times by Session, Age, and Block.

| Session | Age | Block | Mean (sd) RT (in ms) | Accuracy | N |
|---|---|---|---|---|---|
| 1 | Young | 1 | 460 (101) | 97% | 4449 |
| | | 2 | 432 (119) | 97% | 4408 |
| | | 3 | 405 (121) | 96% | 4387 |
| | | 4 | 396 (123) | 97% | 4558 |
| | | 5 | 411 (97) | 96% | 3129 |
| | Senior | 1 | 528 (116) | 96% | 2051 |
| | | 2 | 487 (111) | 96% | 2101 |
| | | 3 | 485 (122) | 96% | 2060 |
| | | 4 | 463 (126) | 96% | 2027 |
| | | 5 | 513 (113) | 95% | 2068 |
| 2 | Young | 1 | 431 (97) | 97% | 4436 |
| | | 2 | 350 (119) | 96% | 4326 |
| | | 3 | 290 (127) | 96% | 4299 |
| | | 4 | 272 (122) | 96% | 4185 |
| | | 5 | 403 (96) | 96% | 3597 |
| | Senior | 1 | 515 (107) | 96% | 2040 |
| | | 2 | 474 (138) | 96% | 1996 |
| | | 3 | 458 (144) | 96% | 2001 |
| | | 4 | 433 (146) | 96% | 2033 |
| | | 5 | 498 (109) | 96% | 2051 |

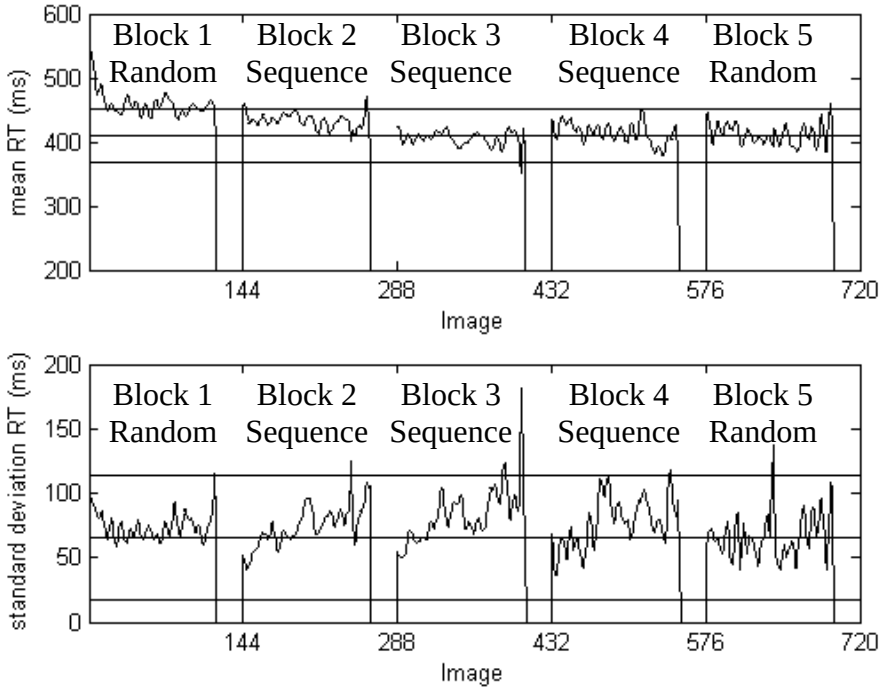


Figure 5-1. Young Adult Group Performance for Session 1 (Implicit). Top: mean group RT by image. Bottom: standard deviation of group RT by image.

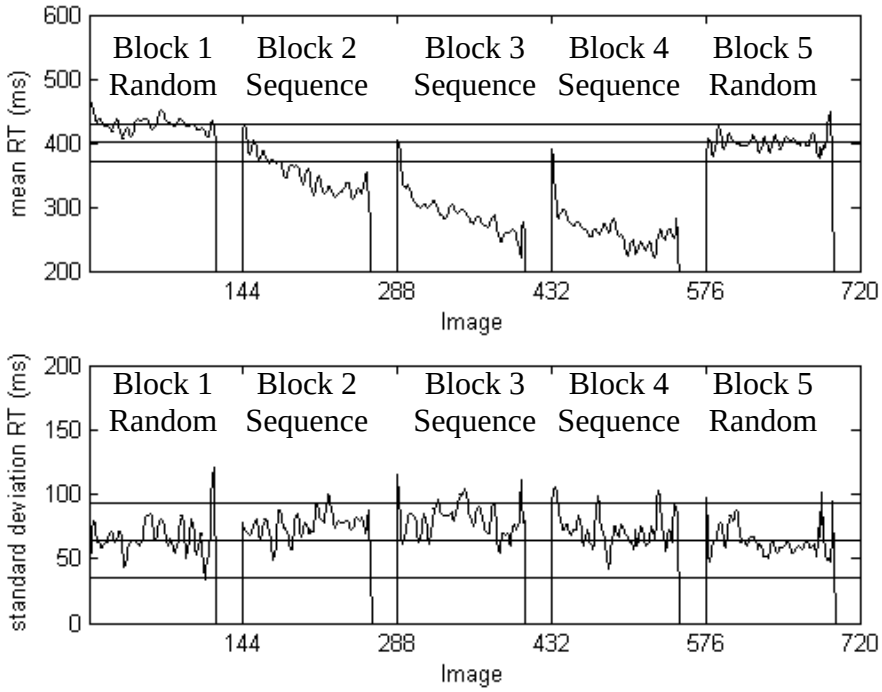


Figure 5-2. Young Adult Group Performance for Session 2 (Explicit). Top: mean group RT by image. Bottom: standard deviation of group RT by image.

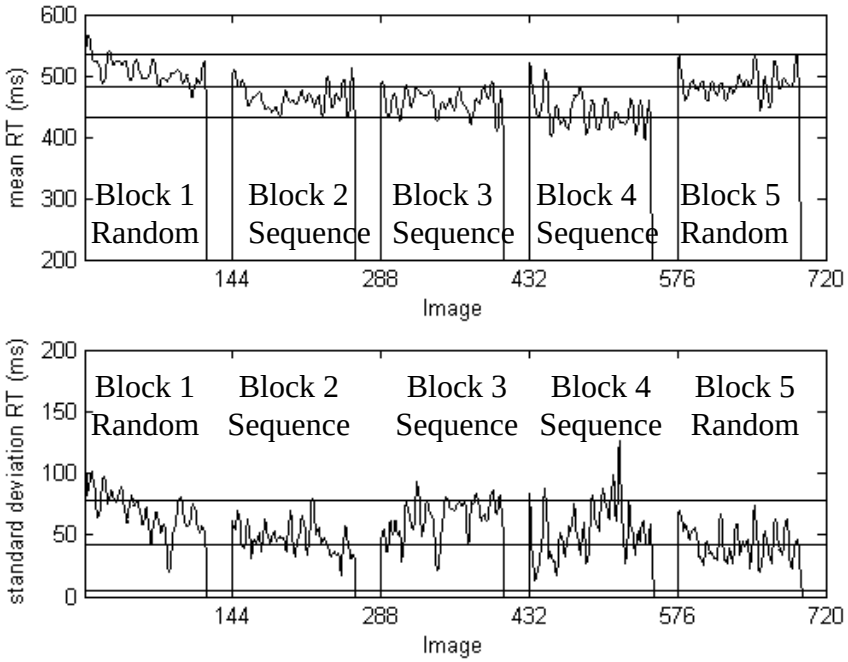


Figure 5-3. Senior Adult Group Performance for Session 1 (Implicit). Top: mean group RT by image. Bottom: standard deviation of group RT by image.

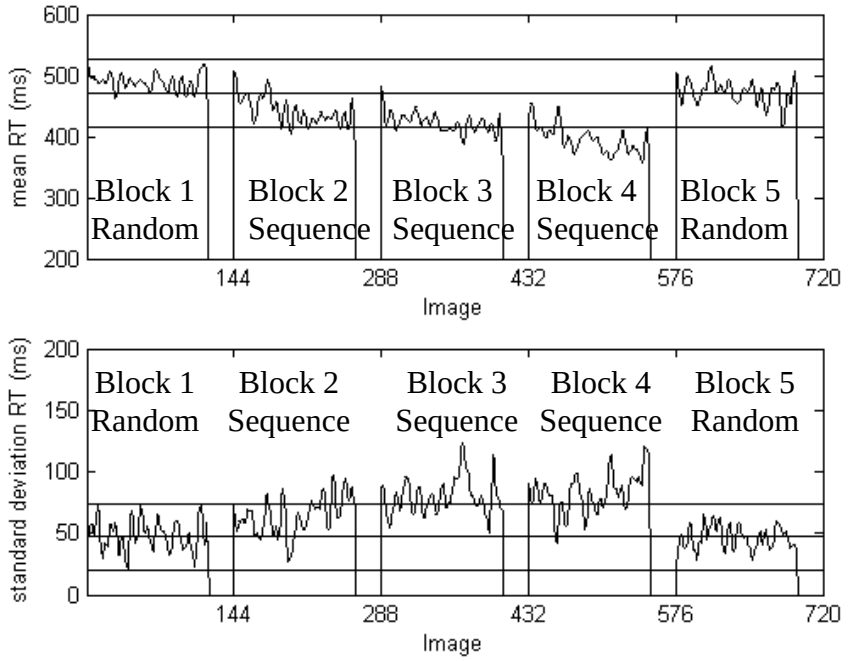


Figure 5-4. Senior Adult Group Performance for Session 2 (Explicit). Top: mean group RT by image. Bottom: standard deviation of group RT by image.

Table 5-2. Median ROI-ROI Correlations for Young adults: Random condition.

| | RT | M1 | LPM | CBELL | SMA | PUT | AC | FRONT | CAUD | V1 | PAR |
|---|---|---|---|---|---|---|---|---|---|---|---|
| RT | 1.00 | 0.11 | 0.09 | 0.08 | 0.11 | 0.13 | 0.09 | 0.09 | 0.08 | 0.10 | 0.12 |
| M1 | | 1.00 | 0.85 | 0.69 | 0.77 | 0.74 | 0.77 | 0.73 | 0.60 | 0.56 | 0.80 |
| LPM | | | 1.00 | 0.73 | 0.79 | 0.74 | 0.78 | 0.72 | 0.61 | 0.63 | 0.78 |
| CBELL | | | | 1.00 | 0.70 | 0.68 | 0.71 | 0.63 | 0.58 | 0.58 | 0.71 |
| SMA | | | | | 1.00 | 0.75 | 0.81 | 0.73 | 0.64 | 0.56 | 0.75 |
| PUT | | | | | | 1.00 | 0.75 | 0.76 | 0.76 | 0.59 | 0.78 |
| AC | | | | | | | 1.00 | 0.76 | 0.65 | 0.57 | 0.78 |
| FRONT | | | | | | | | 1.00 | 0.67 | 0.54 | 0.74 |
| CAUD | | | | | | | | | 1.00 | 0.50 | 0.62 |
| V1 | | | | | | | | | | 1.00 | 0.60 |
| PAR | | | | | | | | | | | 1.00 |

Table 5-3. Median ROI-ROI Correlations for Young adults: Explicit condition.

| | RT | M1 | LPM | CBELL | SMA | PUT | AC | FRONT | CAUD | V1 | PAR |
|---|---|---|---|---|---|---|---|---|---|---|---|
| RT | 1.00 | -0.20 | -0.01 | -0.16 | 0.08 | 0.01 | -0.03 | -0.02 | -0.03 | -0.09 | -0.07 |
| M1 | | 1.00 | 0.83 | 0.61 | 0.77 | 0.77 | 0.79 | 0.76 | 0.62 | 0.52 | 0.81 |
| LPM | | | 1.00 | 0.70 | 0.79 | 0.79 | 0.79 | 0.78 | 0.65 | 0.62 | 0.74 |
| CBELL | | | | 1.00 | 0.72 | 0.72 | 0.75 | 0.69 | 0.61 | 0.69 | 0.68 |
| SMA | | | | | 1.00 | 0.75 | 0.81 | 0.67 | 0.63 | 0.55 | 0.69 |
| PUT | | | | | | 1.00 | 0.76 | 0.74 | 0.73 | 0.62 | 0.72 |
| AC | | | | | | | 1.00 | 0.74 | 0.66 | 0.60 | 0.71 |
| FRONT | | | | | | | | 1.00 | 0.70 | 0.51 | 0.76 |
| CAUD | | | | | | | | | 1.00 | 0.53 | 0.55 |
| V1 | | | | | | | | | | 1.00 | 0.56 |
| PAR | | | | | | | | | | | 1.00 |

Table 5-4. Median ROI-ROI Correlations for Young adults: Implicit condition.

| | RT | M1 | LPM | CBELL | SMA | PUT | AC | FRONT | CAUD | V1 | PAR |
|---|---|---|---|---|---|---|---|---|---|---|---|
| RT | 1.00 | 0.03 | 0.12 | -0.03 | -0.01 | 0.15 | 0.14 | -0.06 | 0.11 | 0.02 | 0.00 |
| M1 | | 1.00 | 0.83 | 0.70 | 0.80 | 0.75 | 0.80 | 0.72 | 0.66 | 0.78 | 0.81 |
| LPM | | | 1.00 | 0.79 | 0.81 | 0.73 | 0.84 | 0.71 | 0.64 | 0.74 | 0.79 |
| CBELL | | | | 1.00 | 0.74 | 0.61 | 0.77 | 0.65 | 0.57 | 0.65 | 0.72 |
| SMA | | | | | 1.00 | 0.77 | 0.84 | 0.73 | 0.63 | 0.65 | 0.76 |
| PUT | | | | | | 1.00 | 0.76 | 0.69 | 0.73 | 0.59 | 0.67 |
| AC | | | | | | | 1.00 | 0.74 | 0.67 | 0.73 | 0.78 |
| FRONT | | | | | | | | 1.00 | 0.76 | 0.57 | 0.79 |
| CAUD | | | | | | | | | 1.00 | 0.47 | 0.59 |
| V1 | | | | | | | | | | 1.00 | 0.68 |
| PAR | | | | | | | | | | | 1.00 |

Table 5-5. Median ROI-ROI Correlations for Senior adults: Random condition.

| | RT | M1 | LPM | CBELL | SMA | PUT | AC | FRONT | CAUD | V1 | PAR |
|---|---|---|---|---|---|---|---|---|---|---|---|
| RT | 1.00 | 0.00 | 0.05 | 0.05 | 0.03 | 0.00 | 0.01 | 0.04 | -0.02 | 0.05 | 0.02 |
| M1 | | 1.00 | 0.66* | 0.53* | 0.69 | 0.57 | 0.55* | 0.47* | 0.49 | 0.40 | 0.57* |
| LPM | | | 1.00 | 0.64* | 0.81 | 0.68 | 0.63 | 0.61 | 0.60 | 0.49 | 0.70 |
| CBELL | | | | 1.00 | 0.69 | 0.49* | 0.57* | 0.58 | 0.50 | 0.50 | 0.60 |
| SMA | | | | | 1.00 | 0.64 | 0.61* | 0.60* | 0.54 | 0.52 | 0.59* |
| PUT | | | | | | 1.00 | 0.53* | 0.59* | 0.62 | 0.46 | 0.55* |
| AC | | | | | | | 1.00 | 0.48* | 0.40* | 0.39* | 0.64 |
| FRONT | | | | | | | | 1.00 | 0.50* | 0.51 | 0.48* |
| CAUD | | | | | | | | | 1.00 | 0.46 | 0.56 |
| V1 | | | | | | | | | | 1.00 | 0.51 |
| PAR | | | | | | | | | | | 1.00 |

*Correlation distribution significantly differs from Young Random [p<0.05 (Bon. corr.)]

Table 5-6. Median ROI-ROI Correlations for Senior adults: Explicit condition.

| | RT | M1 | LPM | CBELL | SMA | PUT | AC | FRONT | CAUD | V1 | PAR |
|---|---|---|---|---|---|---|---|---|---|---|---|
| RT | 1.00 | -0.21 | -0.17 | -0.08 | -0.13 | -0.27 | -0.17 | -0.08 | -0.05 | 0.00 | -0.20 |
| M1 | | 1.00 | 0.37 | 0.40 | 0.31 | 0.32* | 0.52* | 0.18* | 0.38 | 0.35 | 0.55 |
| LPM | | | 1.00 | 0.62 | 0.81 | 0.58 | 0.70 | 0.50 | 0.61 | 0.51 | 0.64 |
| CBELL | | | | 1.00 | 0.70 | 0.49 | 0.67 | 0.58 | 0.55 | 0.43 | 0.69 |
| SMA | | | | | 1.00 | 0.66 | 0.67 | 0.64 | 0.67 | 0.54 | 0.67 |
| PUT | | | | | | 1.00 | 0.46 | 0.53 | 0.65 | 0.46 | 0.53 |
| AC | | | | | | | 1.00 | 0.51 | 0.61 | 0.48 | 0.62 |
| FRONT | | | | | | | | 1.00 | 0.58* | 0.52 | 0.39 |
| CAUD | | | | | | | | | 1.00 | 0.57 | 0.66 |
| V1 | | | | | | | | | | 1.00 | 0.40 |
| PAR | | | | | | | | | | | 1.00 |

*Correlation distribution significantly differs from Young Explicit [p<0.05, Bon. corr.]

Table 5-7. Median ROI-ROI Correlations for Senior adults: Implicit condition.

| | RT | M1 | LPM | CBELL | SMA | PUT | AC | FRONT | CAUD | V1 | PAR |
|---|---|---|---|---|---|---|---|---|---|---|---|
| RT | 1.00 | 0.05 | -0.08 | -0.28 | 0.09 | 0.01 | -0.06 | -0.10 | -0.07 | 0.02 | 0.02 |
| M1 | | 1.00 | 0.63 | 0.35 | 0.70 | 0.55* | 0.62 | 0.38 | 0.67 | 0.36 | 0.66 |
| LPM | | | 1.00 | 0.62 | 0.80 | 0.62 | 0.70 | 0.54 | 0.72 | 0.36 | 0.57 |
| CBELL | | | | 1.00 | 0.69 | 0.48* | 0.74 | 0.30 | 0.66 | 0.56 | 0.62 |
| SMA | | | | | 1.00 | 0.71 | 0.76* | 0.56 | 0.68 | 0.70 | 0.71 |
| PUT | | | | | | 1.00 | 0.60 | 0.45 | 0.56 | 0.36 | 0.53 |
| AC | | | | | | | 1.00 | 0.59* | 0.63 | 0.52 | 0.68 |
| FRONT | | | | | | | | 1.00 | 0.51 | 0.19 | 0.37 |
| CAUD | | | | | | | | | 1.00 | 0.49 | 0.76 |
| V1 | | | | | | | | | | 1.00 | 0.56 |
| PAR | | | | | | | | | | | 1.00 |

* Correlation distribution significantly differs from Young Implicit [p<0.05, Bon. corr.]

Tables 5-2 to 5-7 depicts median ROI-ROI correlations for all age groups and conditions. These correlations were generated using cluster foci from the Random SRTT trial GLMs of each age group. The histograms in Appendix B depict the corresponding ROI-ROI correlation distributions. The following ROI-ROI pairs demonstrated significant reductions ($p<.01$, Bonferonni corrected) in functional connectivity with age: M1-LPM, M1-CBELL, M1-AC, M1-FRONT, M1-PAR, LPM-CBELL, CBELL-PUT, CBELL-AC, SMA-AC, SMA-FRONT, SMA-PAR, PUT-AC, PUT-FRONT, PUT-PAR, AC-FRONT, AC-CAUD, AC-V1, FRONT-CAUD, FRONT-PAR[2].

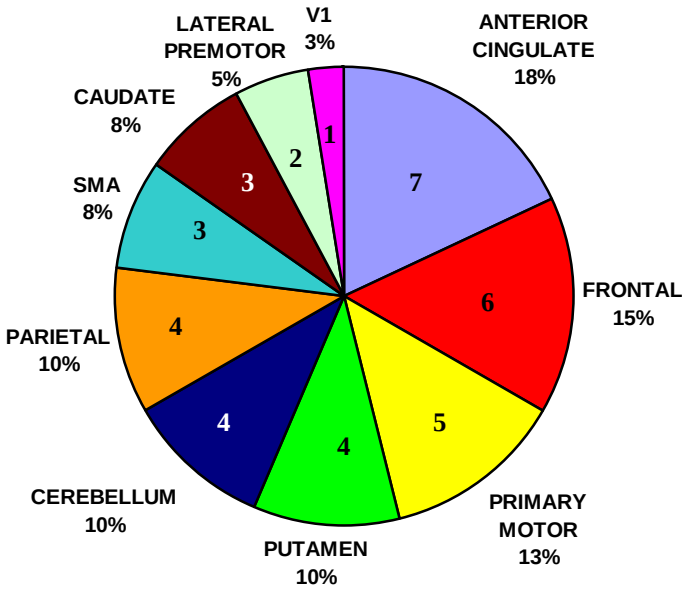


Figure 5-5. Pie Chart of ROIs Demonstrating Decreased Correlations with Age. Value in pie wedge indicates the number of times the ROI appears in each of the 19 unique ROI-ROI pairings.

The ROI-ROI pairings demonstrating decreased functional connectivity with age did not appear limited to any specific region (Tables 5-2 to 5-7). Only 6 of the 19 unique

[2] M1: primary motor area; LPM: lateral premotor area; CBELL: cerebellum; AC: anterior cingulate; FRONT: dorsolatera prefrontal; PAR: parietal; PUT: putamen; SMA: supplementary motor area; CAUD: caudate; V1: calcarine fissure

pairings (31%) involved the prefrontal cortex. For example, decreases in functional connectivity were also apparent for striatocerebellar connections (putamen-cerebellum).

The increase functional connectivity between two ROIs across age groups can be estimated by the difference between the squares of median *r*-values. For example, the median prefrontal-anterior cingulate correlation differed by 0.28 across age groups ($r$ = .76 for young, $r$ = .48 for senior). Thus, the prefrontal cortex on average could account for 34% more [$(.76)^2$-$(.48)^2$] of the anterior cingulate's variance for young than senior adults-the greatest age-related increase in explained variance. The nineteen unique ROI-ROI pairings had a mean (sd) increase in explained variance of 25% (6%).

One alternative explanation lies in reports of increased voxel noise with age (Huettel, 2001). A correlation is a standardized expression of the covariance between two variables divided by the total variance these variables explain. If functional data acquired from senior adult brains tend to be noisier than young adult brains, then activity in senior adults would be expected to be more variable, thus equating to an artificial reduction in functional connectivity.

We tested this hypothesis by calculating the variances of each ROI time series (for the Random condition blocks) and comparing each ROI's variance across age groups with the Kolmogorov-Smirnov two-sample test. Functional data were not more variable for senior adults than younger adults ($p < 0.05$, uncorrected). We can thus infer that the senior adults' brains in this sample were not significantly noisier than young adults' brains. However, this study was not designed to explicitly assess functional noise. More sophisticated experimental designs and analyses might have detected noise that our analyses missed. But since the same statistical used to detect ROI-ROI correlational

differences across age groups failed to detect age-related differences in ROI variances, it seems unlikely that increased noise is an explanation for the observed differences.

All three learning conditions demonstrated significant decreases in ROI-ROI correlations with age. Yet within age groups, ROI-ROI correlations did not differ across learning conditions, even at an uncorrected $\alpha = .05$. In light of these null findings, the tables and histograms depicting correlation medians and histograms (respectively) using RT-seed ROIs are not provided. The inclusion of all sequence blocks with significant improvements in RT (to their respective learning conditions) did not produce a discernible difference in correlations across learning conditions (also not shown). Additionally, no significant differences in correlation distributions were found across learning conditions when using the less conservative *t*-test in lieu of the Kolmogorov-Smirnov two-sample test. Approximately half of all correlational distributions were non-normal, as determined by the Lilliefors test, so using the less conservative *t*-test would be inappropriate.

## Discussion

Both young and senior adults demonstrated robust improvements in RT attributable to explicit learning of the motor sequence. The mean RT improvement for young adults (131 ms) was comparable to those reported in the behavioral pilot study (95 ms). Senior adult explicit learning RT gains (65 ms) were smaller than those of young adults, but were consistent with previous findings (Howard and Howard, 1997, 1992, 1989). Surprisingly, implicit learning gains for senior adults (50 ms) exceeded those for young adults (25 ms), despite previous reports of equivalent learning gains across ages.

A larger percentage (66%) of senior adults than young adults (33%) demonstrated behavioral evidence of learning without explicit sequence awareness. The group implicit learning gains are consequently diminished for young adults. The relatively small percentage of young adults demonstrating implicit learning is atypical and may reflect inopportune sampling. Although the young adult participants were graduate students and presumably of higher educational attainment than the senior adults, it is unclear why greater educational would result in poorer implicit learning.

For two groups of sizes n1 and n2, the Kolmogorov-Smirnov two-sample test should be sufficiently powerful to detect a difference when $(n1*n2)/(n1+n2) > 4$ (The MathWorks Inc.). Thus, even for the senior adult comparisons, the large number of random trial correlations (n=36) should ensure enough power to detect a difference across conditions. The lack of significant differences (correcting for multiple comparisons) between learning and random conditions is surprising and unexpected.

Individual differences in learning speed may contribute to these null findings. Each block lasted six minutes, but visual inspection of reaction times (Appendix B) suggests inter-subject behavioral variability during these learning blocks. Using young adult performance on explicit learning as an example, participant #1 shows modest RT improvement throughout Blocks 2-4, while participant #6 demonstrates dramatic improvement only during the final half of Block 3. One could argue that the interregional correlations–like behavioral measures of reaction time–significantly change during the course of a learning block. Thus, the proposed method may be suitable for assessing static processes (*e.g.,* performance and brain activity during random SRT trials) but may be insensitive to dynamic processes (*i.e.,* learning).

The dynamic connectivity method described in Chapter 3 may be feasible for measuring learning-associated changes in correlated brain activity. But this method will require precise definition of the onset of learning, which in turn requires additional refinement to the previously proposed RT analyses. Continuing improvements are being made to this methodology with hopes of determining learning-related changes in functional connectivity of the motor system.

Since we have eliminated artifactual sources for the differences in correlation distributions across age groups, the reduced correlations must reflect age-related decreases in functional connectivity. These methods could not discern differences in interregional correlations across learning conditions within age groups. Thus, the hypotheses proposed in the specific aims, such as increased correlations between the prefrontal cortex and other brain regions, could not be directly tested. However, the age-related differences across random trial conditions are consistent with global decreases in interregional connectivity.

According to the frontal aging hypothesis, only correlations involving the prefrontal cortex (and arguably anterior cingulate) should have decreased with age. However, the present evidence suggests that decreases in interregional correlations were not limited to the frontal cortex. Age-related decreases were observed for corticocerebellar (primary motor–cerebellum), corticostriatal (parietal–putamen) and striatocerebellar (putamen–cerebellum) correlational pairings. Even the lateral premotor and supplementary motor area, despite their proximity and occupation of the same Brodmann area, demonstrate decreased functional connectivity with age.

These findings are more consistent with global cognitive slowing than a functional disconnect with a specific anatomical region. Investigations of memory function have revealed age-related decreases in cognitive processing speeds that were not constrained to any single stage (encoding, retrieval) of memory function (Madden, 2001). An analogous macroscopic model of age-related cognitive decline is supported by these neuroimaging data, with functional incoherence limited to no single brain region

This study has several weaknesses. Unfortunately, correlation does not imply causality. Group differences independent of age (or indirectly linked to age) such as differences in vigilance cannot be excluded. Senior adults tend to adopt conservative strategies that sacrifice response speed for accuracy (Madden, 2001); excluding non-responses, mean Random SRTT trial accuracy measures did not differ across age groups despite a significant difference in mean RT (young, 429 ms; senior, 514 ms, $t$=59, $p<.001$), so cognitive strategy is unlikely to account for these findings. Pending methodological refinement, structural equation modeling could establish causal relationships between ROI activities and behavioral measures.

Neuroanatomical analyses of cortical shrinkage or disruption of white-matter pathways might provide a causal explanation for the observed functional connectivity decreases with age. For example, the coherence of a white matter pathway linking two ROIs might correlate with the functional connectivity between these regions. Ideally, the functional connectivity methods could be further refined to detect interregional correlational differences between implicit and explicit learning. Brain regions with functional connectivities differing across both age and condition comparisons could then

serve as starting points for subsequent neuroanatomical investigations. The FLAIR and DTI anatomical scans could be used for this purpose in subsequent analyses.

# CHAPTER 6
# CONCLUSIONS

## Improving Methodology

**Control charts**. This dissertation proposes multiple methodological refinements for current behavioral and functional neuroimaging research analyses. The most prominent refinement is the adaptation of control charts for analyzing reaction time data. Control charts are used here to detect trends in behavioral data that might otherwise be missed by traditional analysis of variance (ANOVA)–for example, the increased group variability for explicit learning gains compared to implicit learning. Control charts are an intuitive graphical tool for summarizing trends in psychological data.

Control charts were also used to determine the onset of learning gains. While control charts often gave findings that were consistent with other approaches (such as Tryon's *C* and participant self-report), these tools did not always produce congruous results. The discongruency may in part stem from the considerable variability in reaction time data, which shows considerable noise even after a stringent lowpass filter (0.08 Hz). Additional exploration of these techniques–for example, using Tryon's *C* on every run through the sequence to discern precisely when a participant's performance deviates from baseline–may result in an improved capacity for detecting the onset of learning.

Incidentally, control charts indicated invariant individual differences in implicit learning rates for both young and senior adults, an observation not previously addressed by the learning literature. In contrast, participants demonstrated substantial individual differences in rates of explicit motor learning. Implicit motor learning is proposed to be a

continual, unchanging mechanism for acquiring a motor skill subject to selective improvement by explicit strategy.

**Behavioral seeding analyses**. Functional connectivity seeding analyses using behavioral data (reaction time) were able to discern brain regions specifically involved with learning. Unfortunately, the RT data used by this method proved far noisier than the traditional ROI-seeding approach; again, increased noise is an inescapable consequence of the inherent variability of RT data. Despite the reduced statistical power of the RT-seed method, this approach remains an improvement over ROI-seeding methods, which were insufficient for discriminating task-based functional activity.

**ROI-based connectivity modeling**. This dissertation proposes a statistical refinement of traditional ROI-based approaches to connectivity modeling. The modeling approach presented here first correlates ROI activity time courses within individuals, thus retaining temporal information where other approaches condense information across time. Distributions of these correlations are then compared (either across learning conditions or age groups) by means of the Kolmogorov-Smirnov two-sample test. This statistical test is more appropriate than the *t*-tests employed by other groups (Solodkin 2004); since it makes no assumptions concerning the underlying sample distribution. As an added benefit, this approach requires no baseline (*i.e.*, resting) conditions, although such conditions may be useful for other analyses (*e.g.*, defining ROIs with GLM).

## Aim 1. Model and Compare Motor System Connectivity during Implicit and Explicit Motor Learning

The first specific aim of modeling differences in functional connectivity between explicit and implicit motor learning was not successfully achieved. No significant differences were found between young adult functional connectivity models generated for

random trial performance and either learning condition. These results did not change with the inclusion of multiple learning blocks per individual (as opposed to the first block demonstrating learning effects).

One possibility for these null findings is that changes in brain connectivity may be somewhat subtle and thus overshadowed by the much stronger connectivity mediating motor performance. The modeled brain regions selected were strongly correlated during random trial performance, with medians ranging from 0.50 (caudate-V1) to 0.85 (M1-lateral premotor). Given the strong baseline correlations, this method may simply lack the sensitivity to detect learning-related shifts in functional connectivity. Conceivably, multiple brief rest periods (~20 sec each) interspersed throughout the SRTT would allow sampling of resting connectivity throughout the experiment and thus improve the specificity of the correlations. Additionally, allowing participants to practice the SRTT prior to functional scanning could eliminate the practice effects accompanying the learning effects, thus improving the sensitivity of the behavioral analyses.

Another possibility is that the learning effects are too heterogeneous across participants. For example, the young adult implicit learning model only included 6 blocks of data (one block per participant demonstrating behavioral evidence of learning). Participants may begin learning at different points within that block or may be learning at different rates[3]. These individual differences could dilute the overall learning effect. A larger sample size would most likely improve the power of this technique to discern differences in modeled functional connectivity across learning conditions.

[3] The latter is a more probable explanation for explicit learning, given the previously discussed differences in RT variance across learning conditions

## Aim 2. Test the Hypothesis that Implicit Learning Retains its Functional Dynamics with Aging

No differences were found between functional connectivity models of learning and random performance for senior adults. However, numerous significant differences in functional connectivity were reported across age groups in all three learning conditions. One-third of the fifty-five unique ROI-ROI correlations significantly decreased in the senior adult functional connectivity model.

These decreases were not attributable to age-related increases in fMRI noise. ROI activity time courses were not significantly more variable for senior than young adults. Approximately one-third of the ROI-ROI correlations that decreased with age involved the anterior cingulate or dorsolateral prefrontal cortex (Figure 6-1). These regions were predicted to be more greatly involved with explicit than implicit motor learning and thus were predicted to show weaker correlations with age. However, numerous ROI-ROI connections not involving either the prefrontal cortex or anterior cingulate also demonstrated decreases with age, such as the SMA–parietal, primary motor–lateral premotor, and cerebellum-putamen correlations. Thus, despite the inability to discern differences in connectivity models across learning conditions, the frontal aging hypothesis can be eliminated as the source of age-related cognitive decline.

The senior adult model indicates global decreases in the functional connectivity that can be interpreted as biological evidence complimenting psychological models for general cognitive slowing. All of the modeled regions demonstrate some degree of decreased connectivity, although the visual cortex appears most spared. These analyses provide the framework for future functional or neuroanatomical investigations; for example, DTI tracings of white-matter pathways connecting regions that demonstrated

age-related decreased in functional connectivity. Likewise, the phenomenon of robust symmetrical activation observed for senior adults could be the focus of interhemispheric functional connectivity analyses to address functional compensation hypotheses. This dissertation adds support to the general cognitive slowing aging model while laying the groundwork for subsequent neuroimaging investigations of aging and cognition.

APPENDIX A
PILOT STUDY BEHAVIORAL DATA

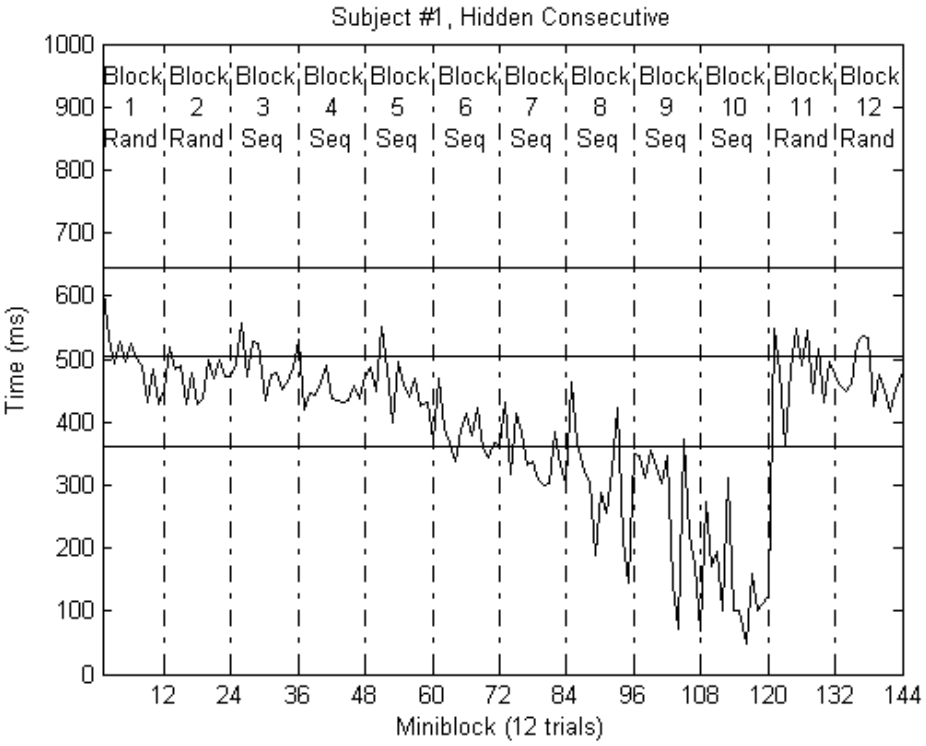


Figure A-1. Subject #1, Hidden Consecutive.

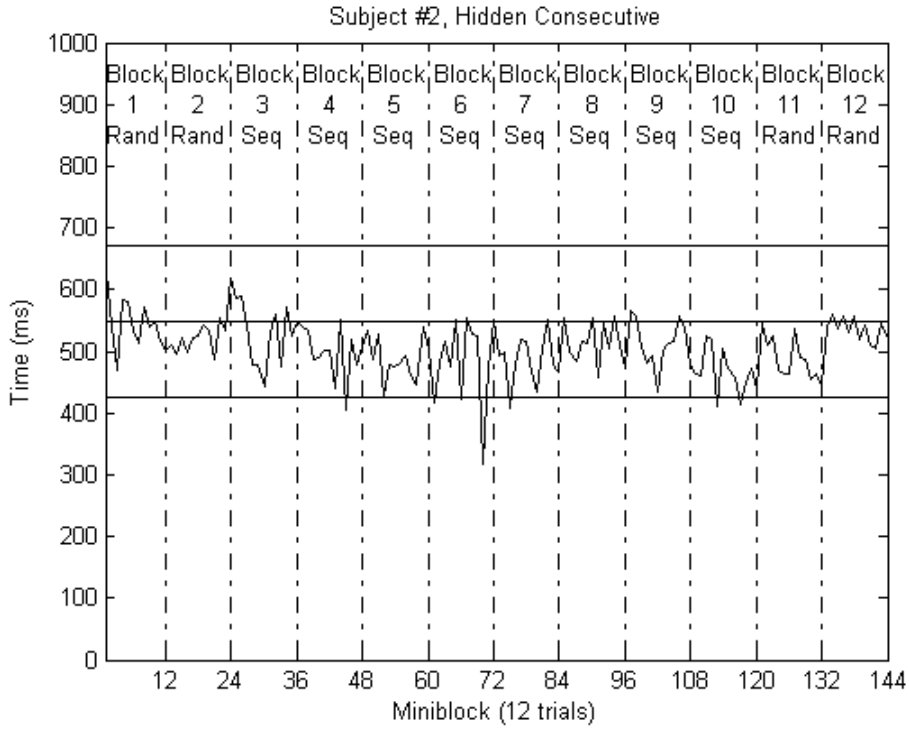


Figure A-2. Subject #2, Hidden Consecutive.

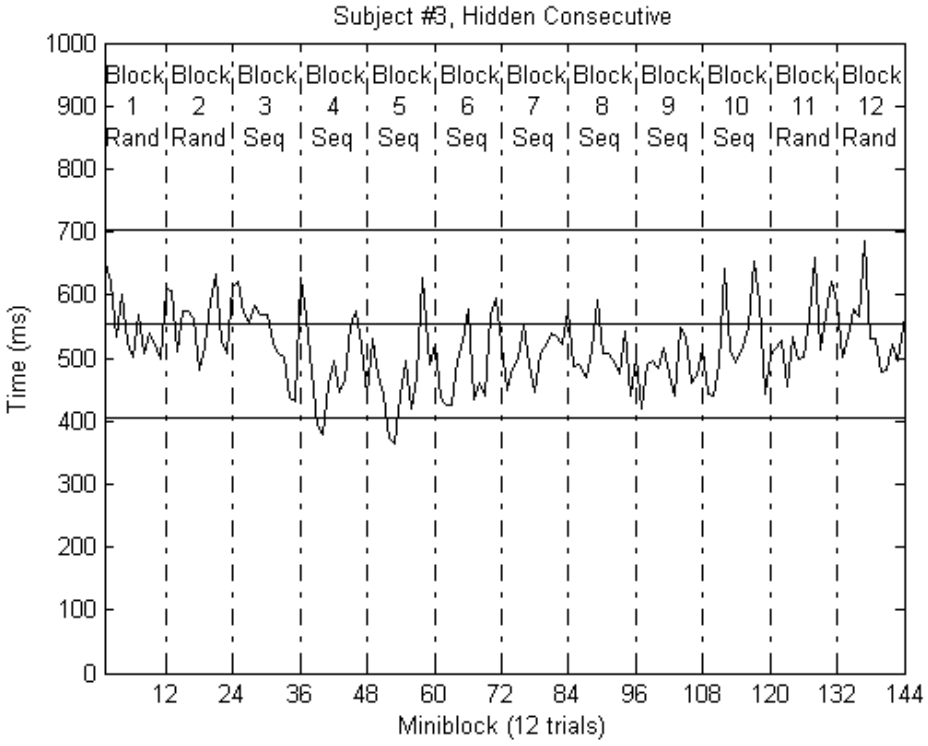


Figure A-3. Subject #3, Hidden Consecutive.

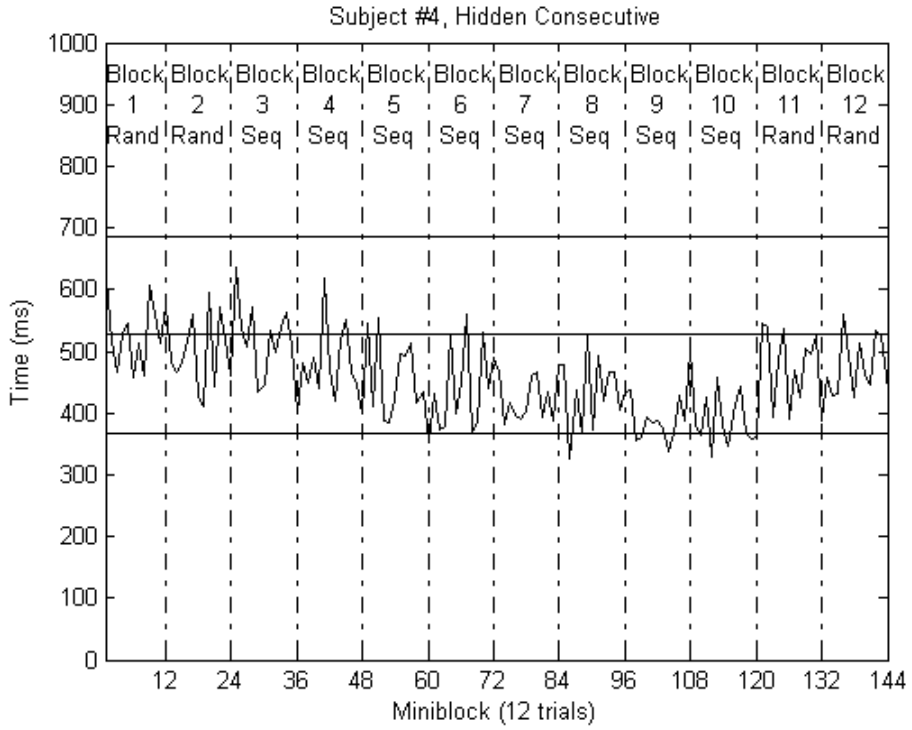


Figure A-4. Subject #4, Hidden Consecutive.

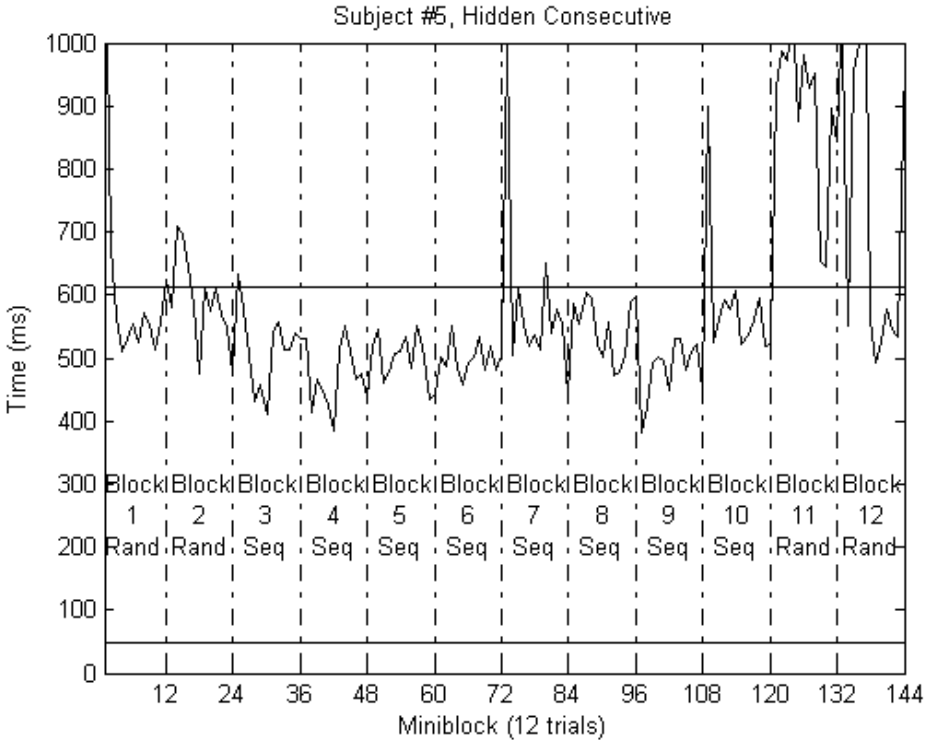


Figure A-5. Subject #5, Hidden Consecutive.

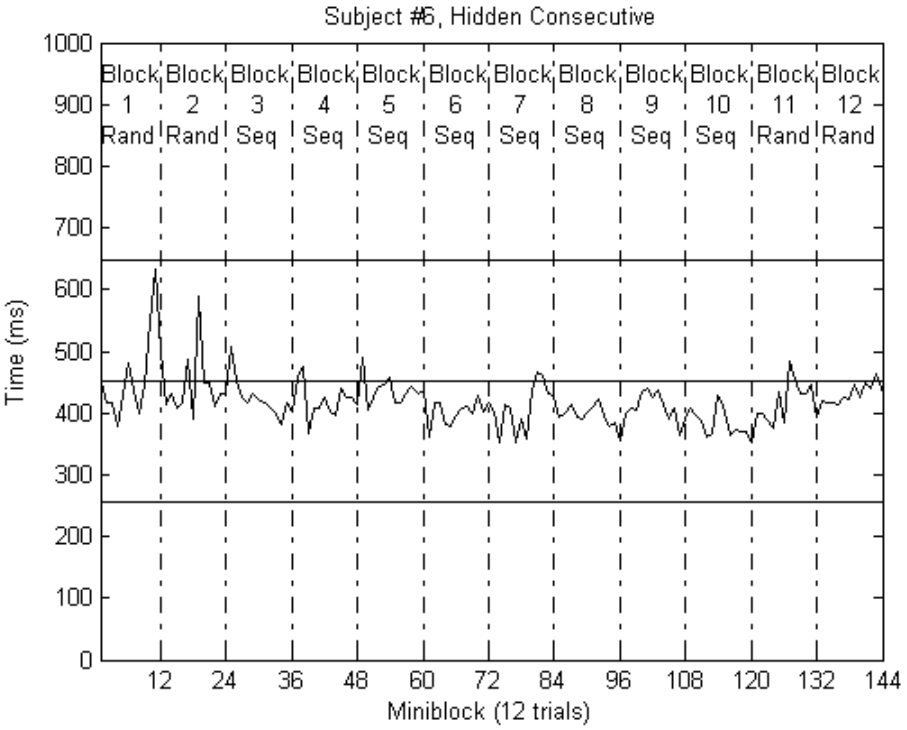


Figure A-6. Subject #6, Hidden Consecutive.

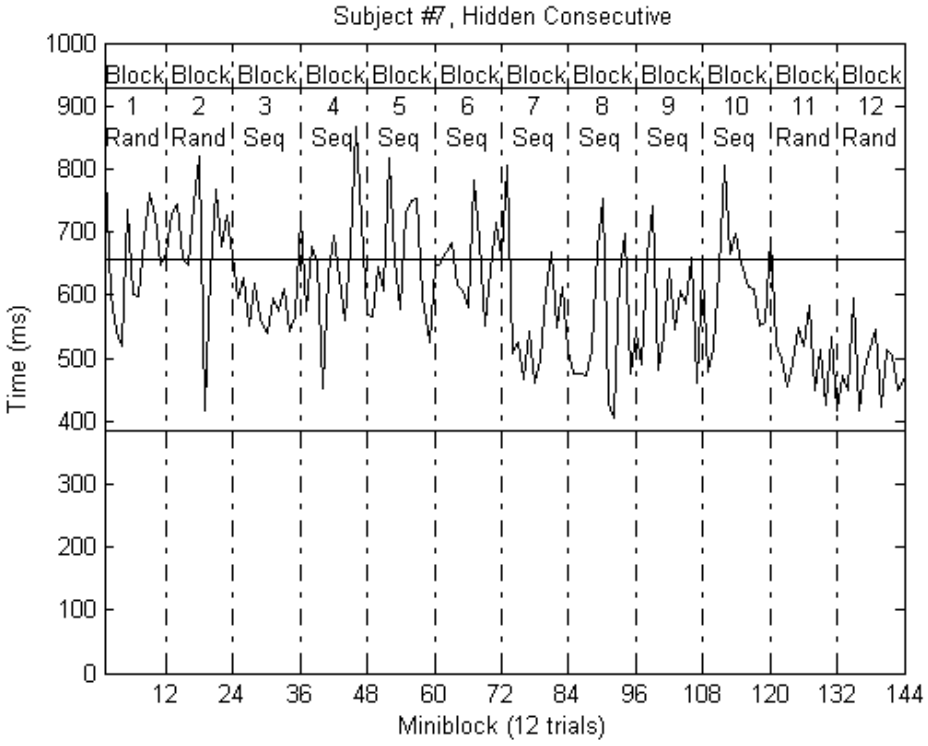


Figure A-7. Subject #7, Hidden Consecutive.

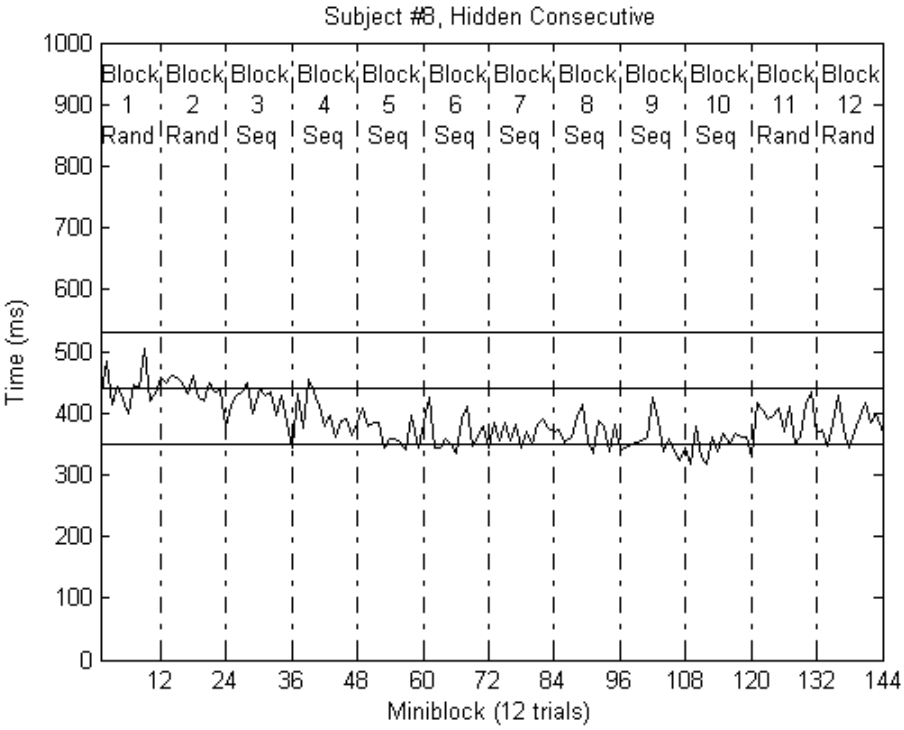


Figure A-8. Subject #8, Hidden Consecutive.

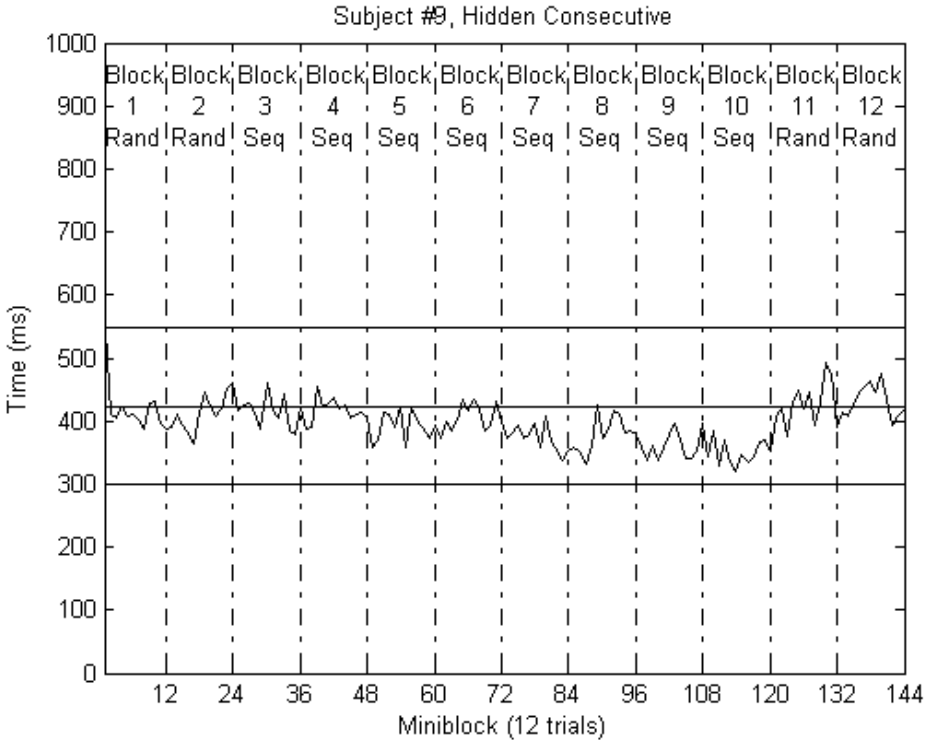


Figure A-9. Subject #9, Hidden Consecutive.

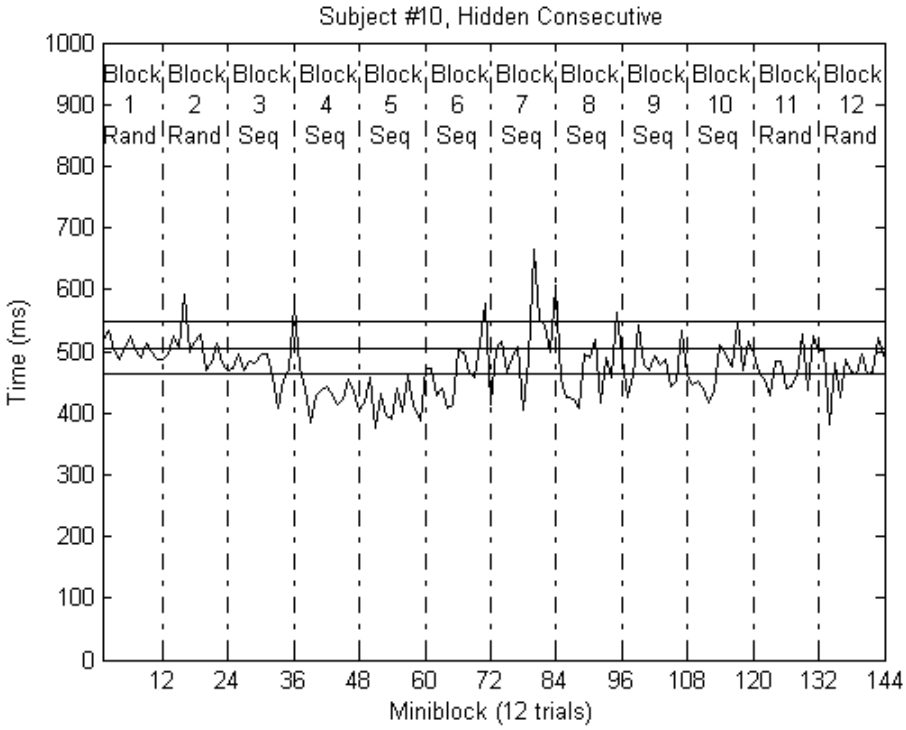


Figure A-10. Subject #10, Hidden Consecutive.

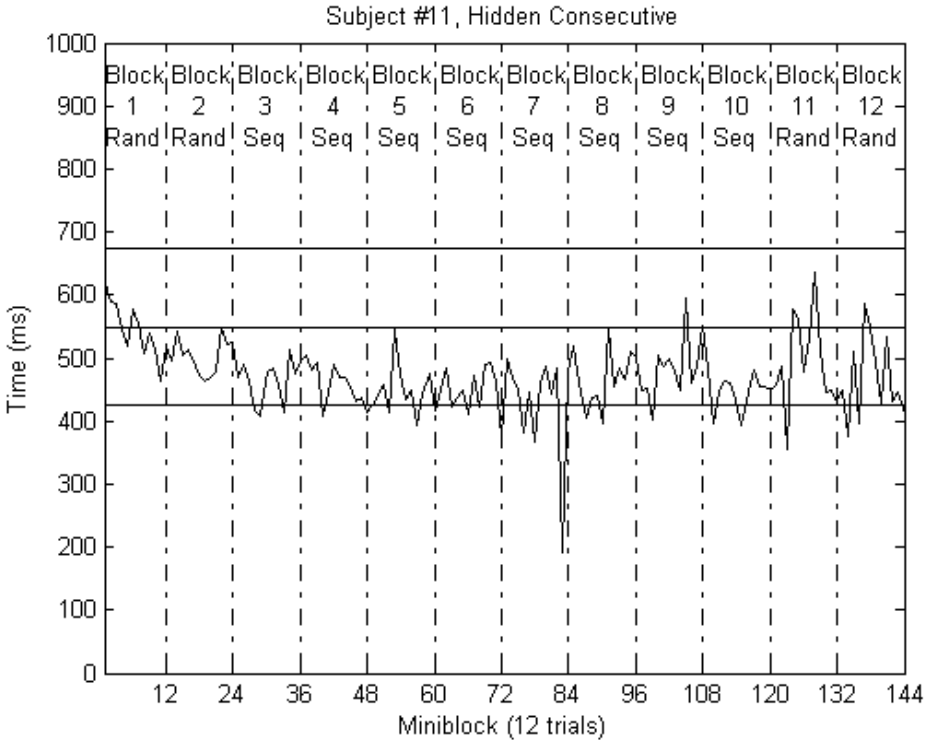


Figure A-11. Subject #11, Hidden Consecutive.

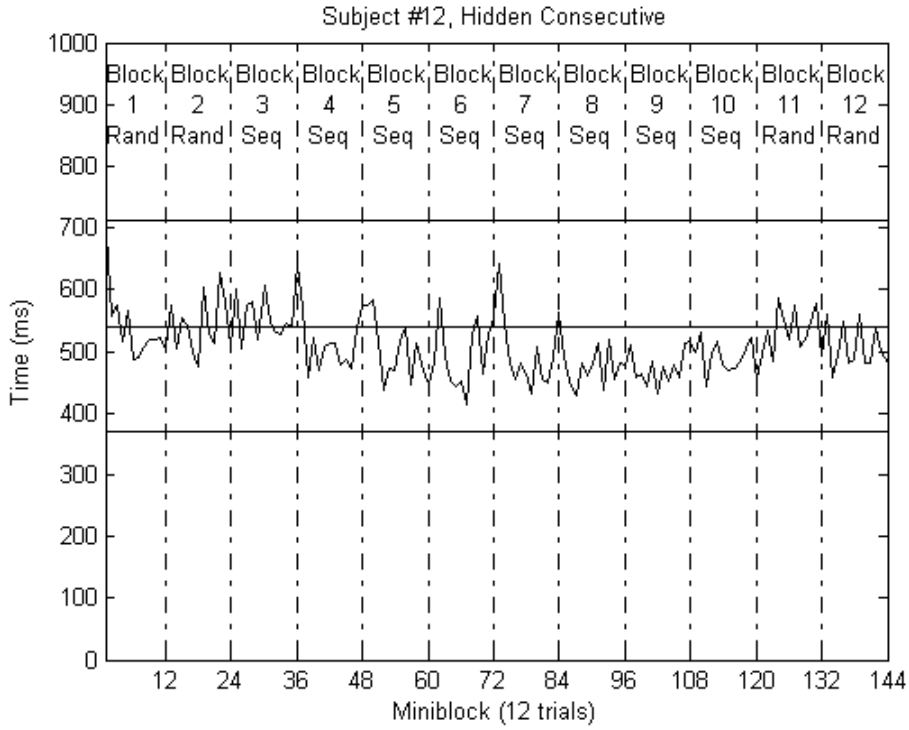


Figure A-12. Subject #12, Hidden Consecutive.

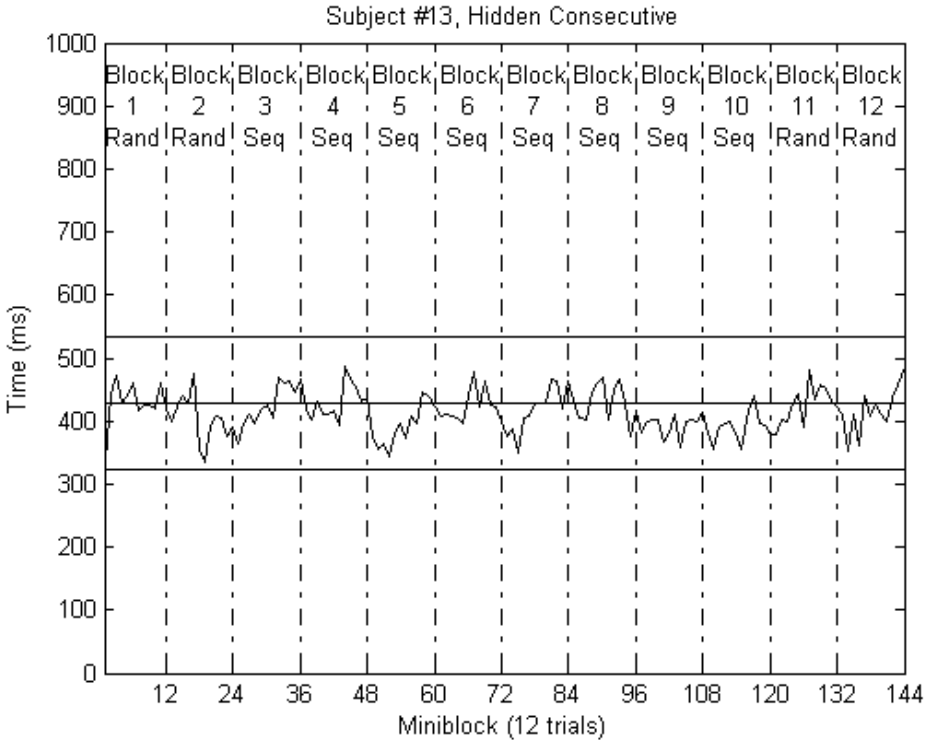


Figure A-13. Subject #13, Hidden Consecutive.

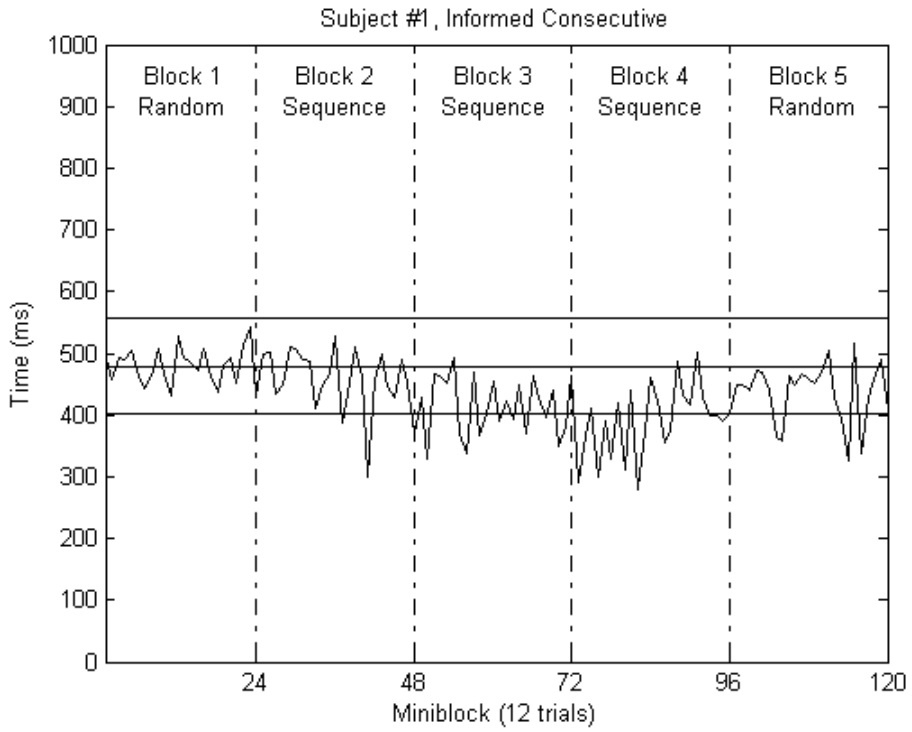


Figure A-14. Subject #1, Informed Consecutive.

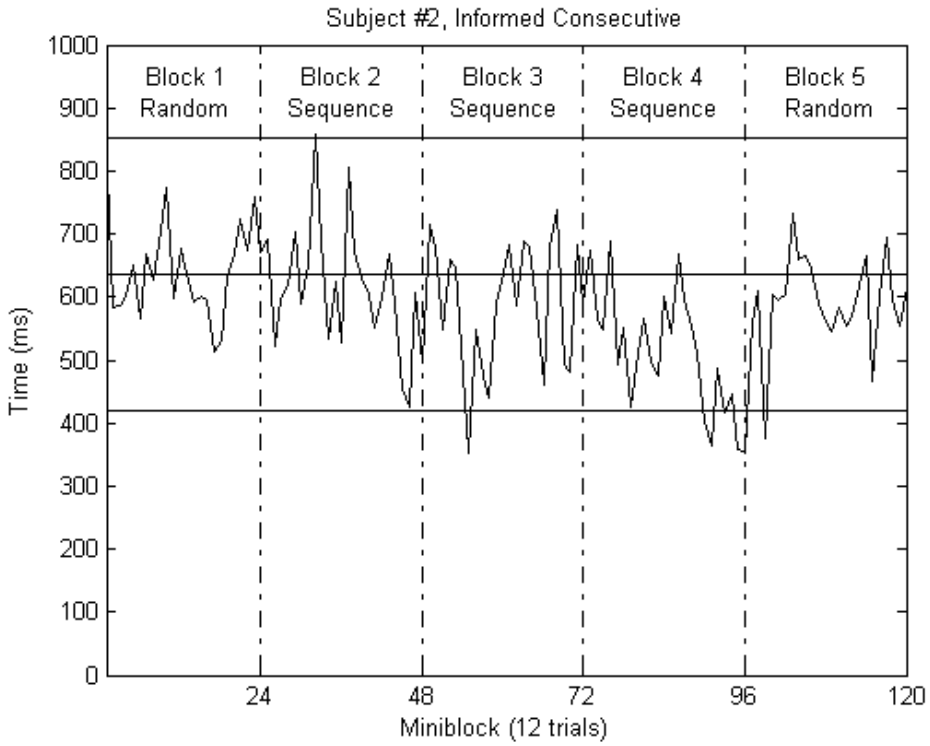


Figure A-15. Subject #2, Informed Consecutive.

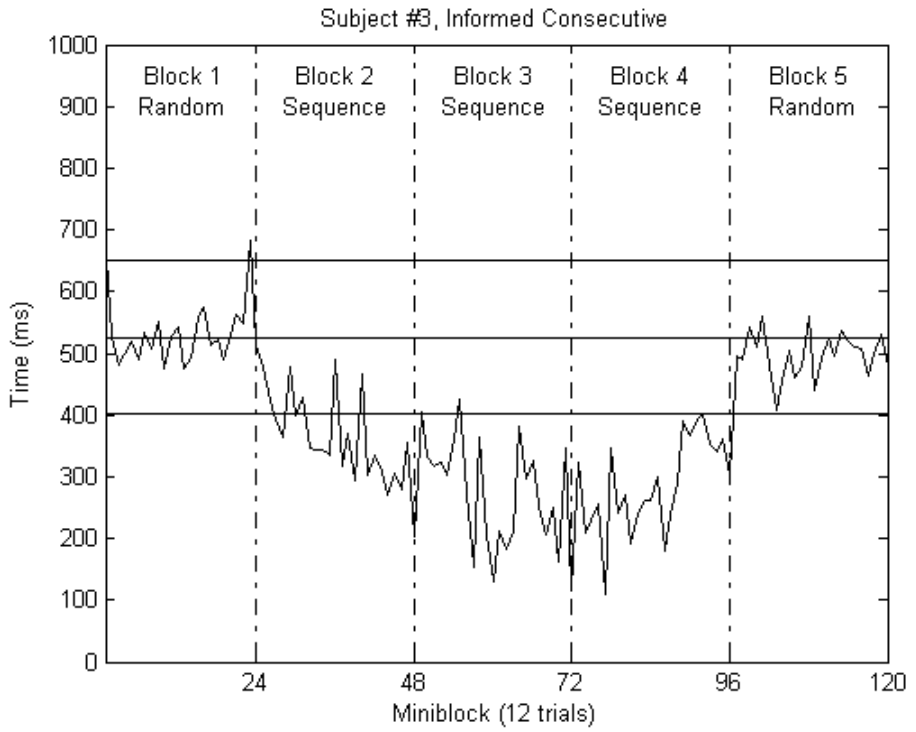


Figure A-16. Subject #3, Informed Consecutive.

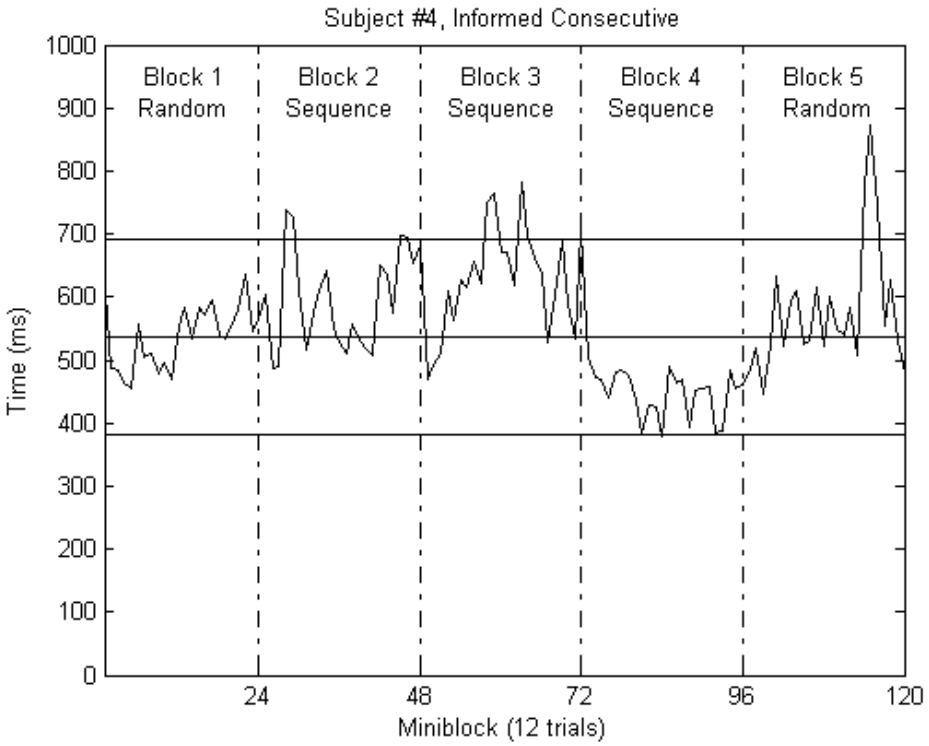


Figure A-17. Subject #4, Informed Consecutive.

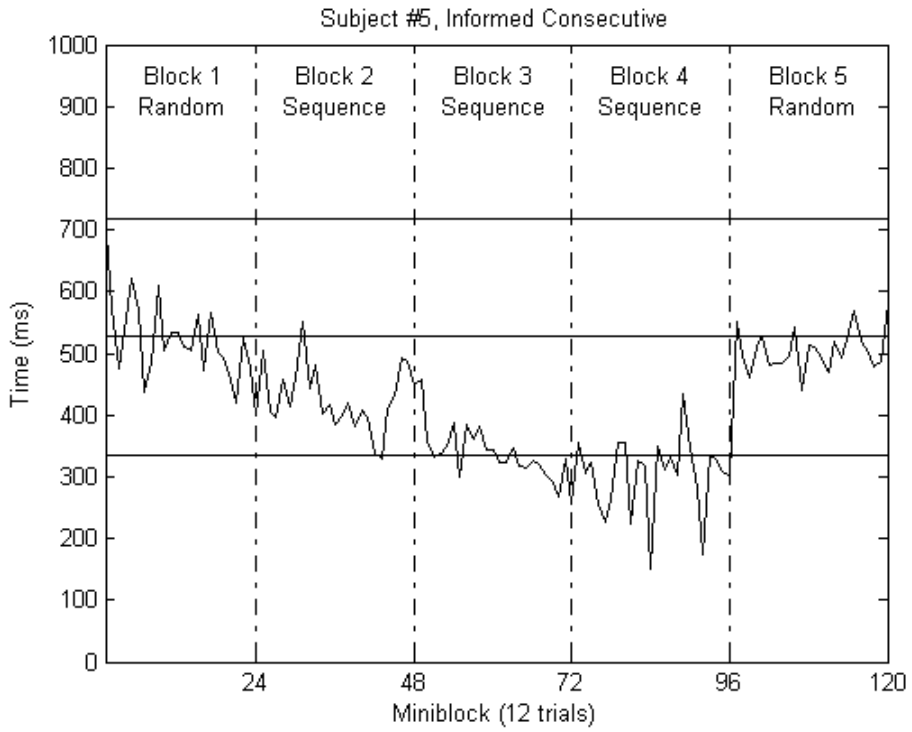


Figure A-18. Subject #5, Informed Consecutive.

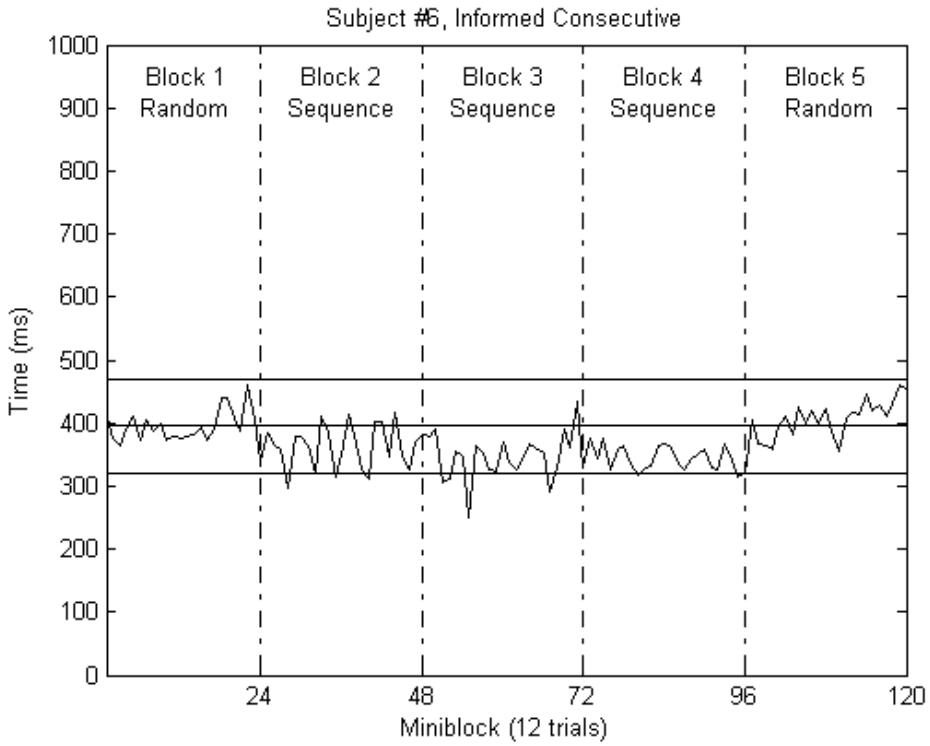


Figure A-19. Subject #6, Informed Consecutive.

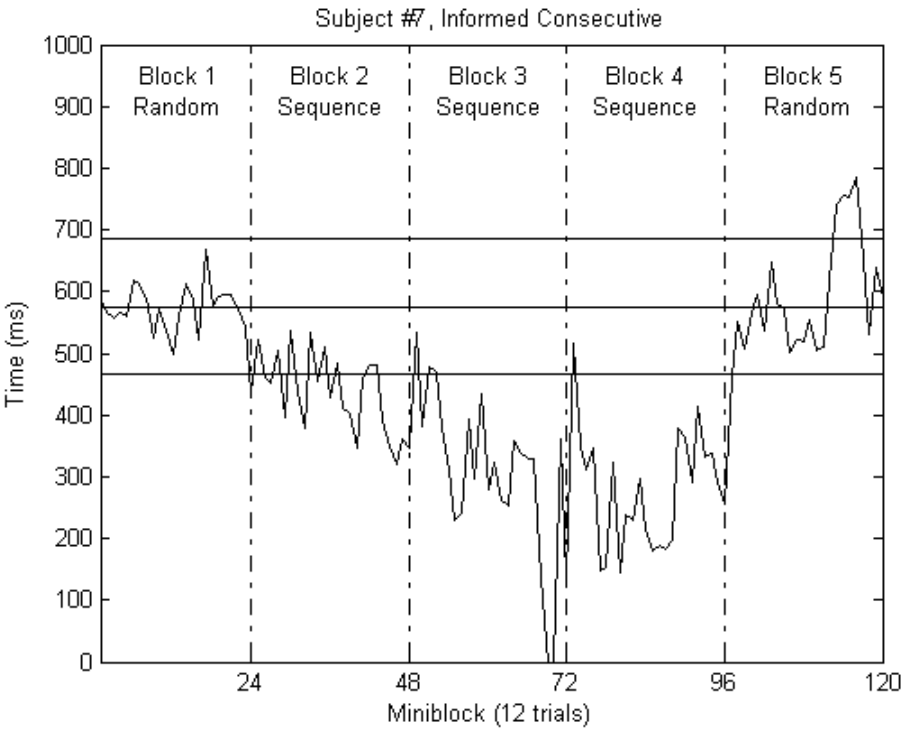


Figure A-20. Subject #7, Informed Consecutive.

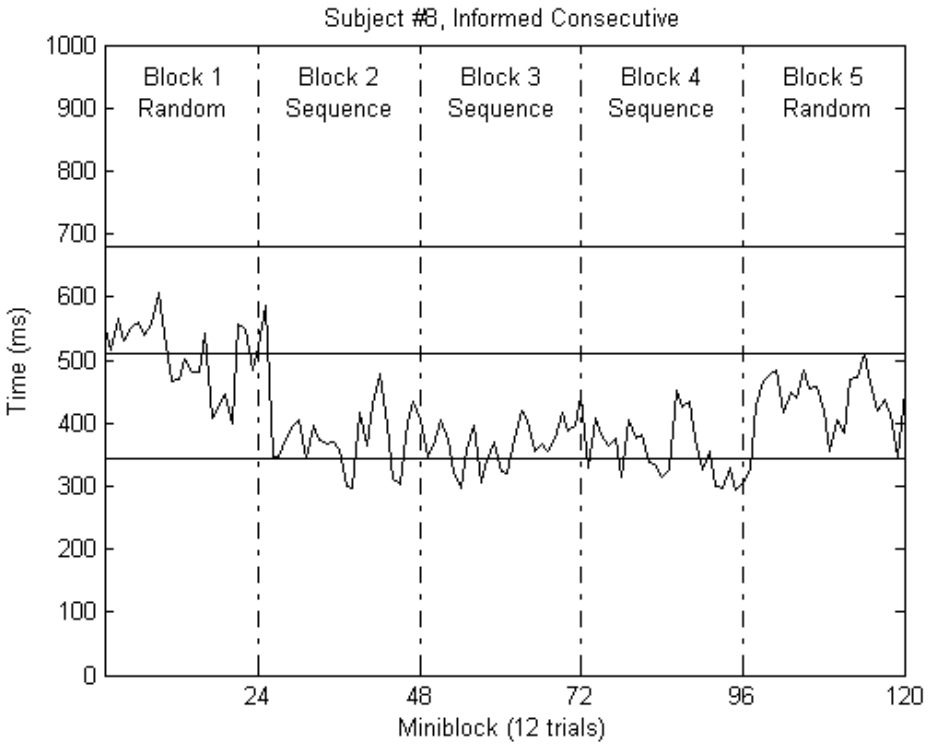


Figure A-21. Subject #8, Informed Consecutive.

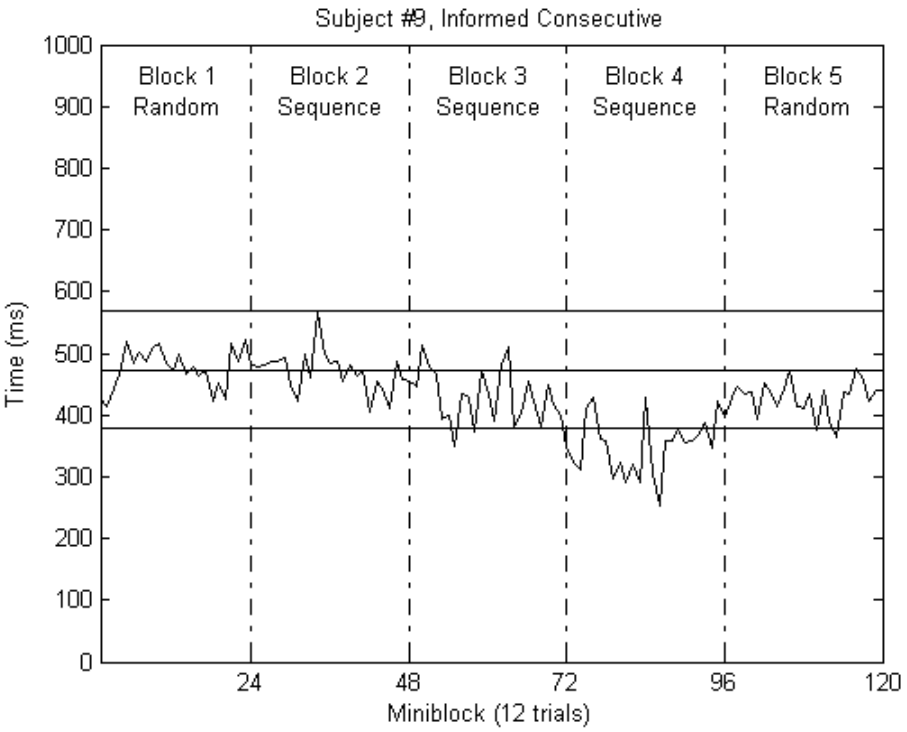


Figure A-22. Subject #9, Informed Consecutive.

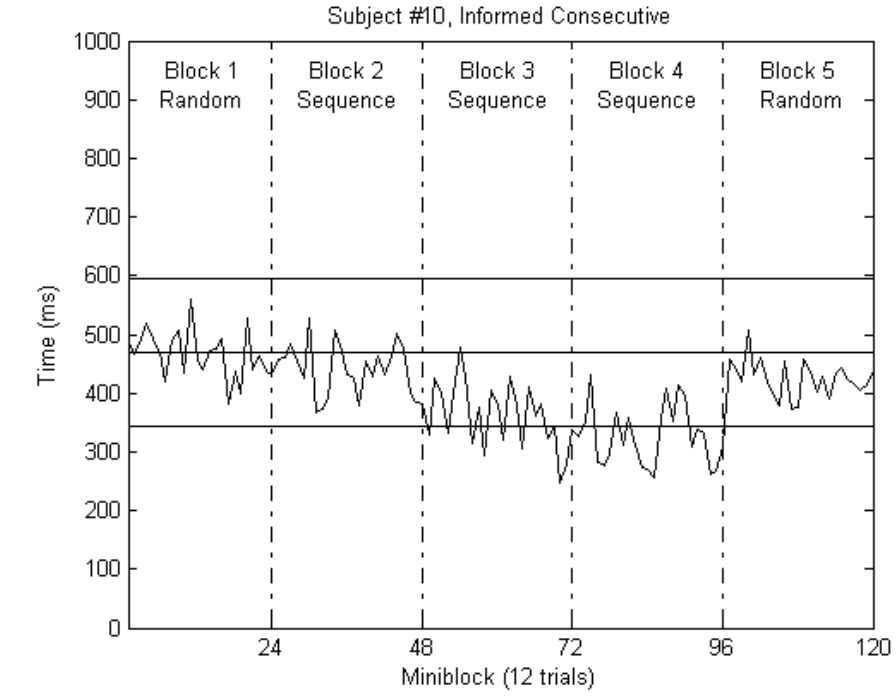


Figure A-23. Subject #10, Informed Consecutive.

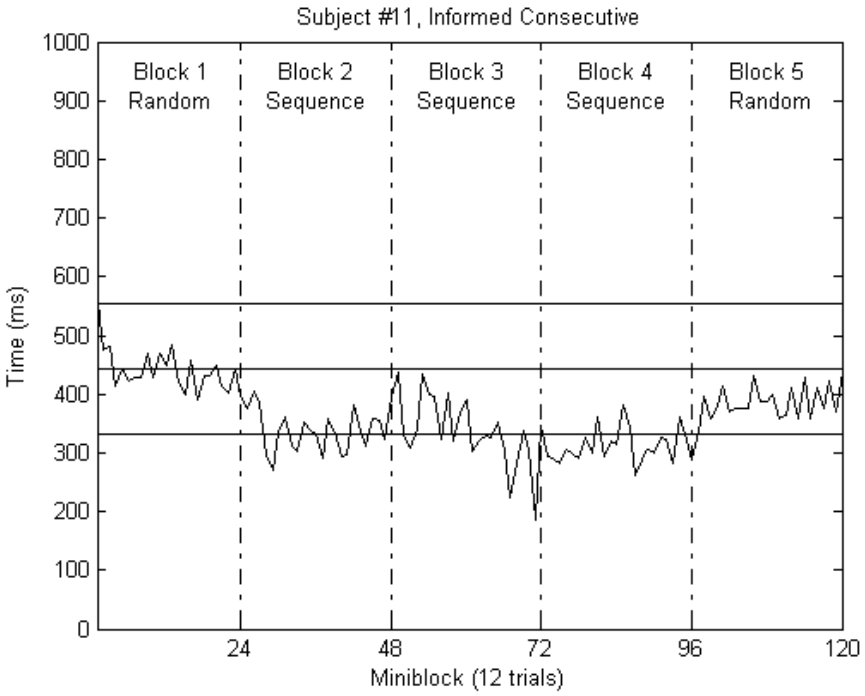


Figure A-24. Subject #11, Informed Consecutive.

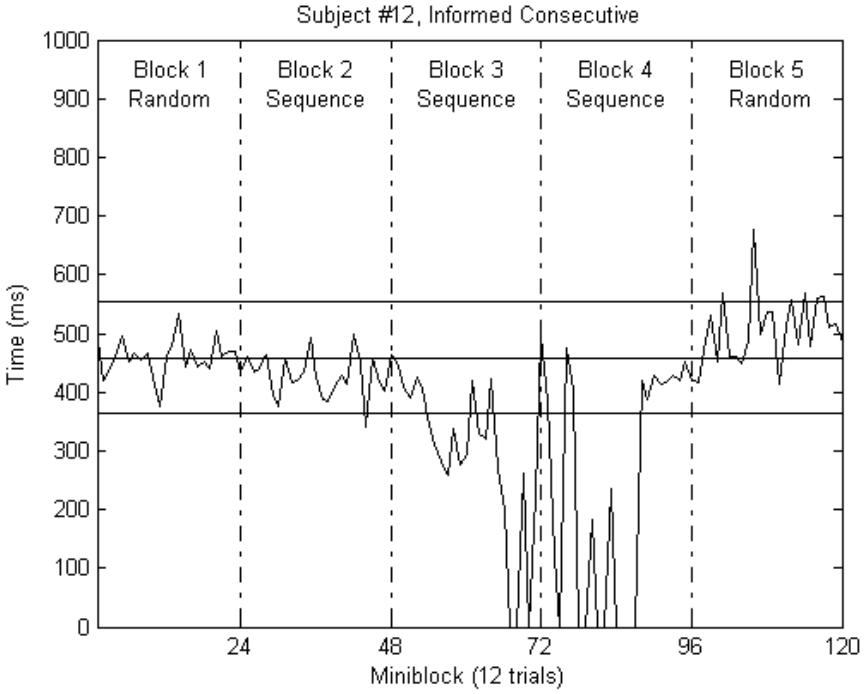


Figure A-25. Subject #12, Informed Consecutive.

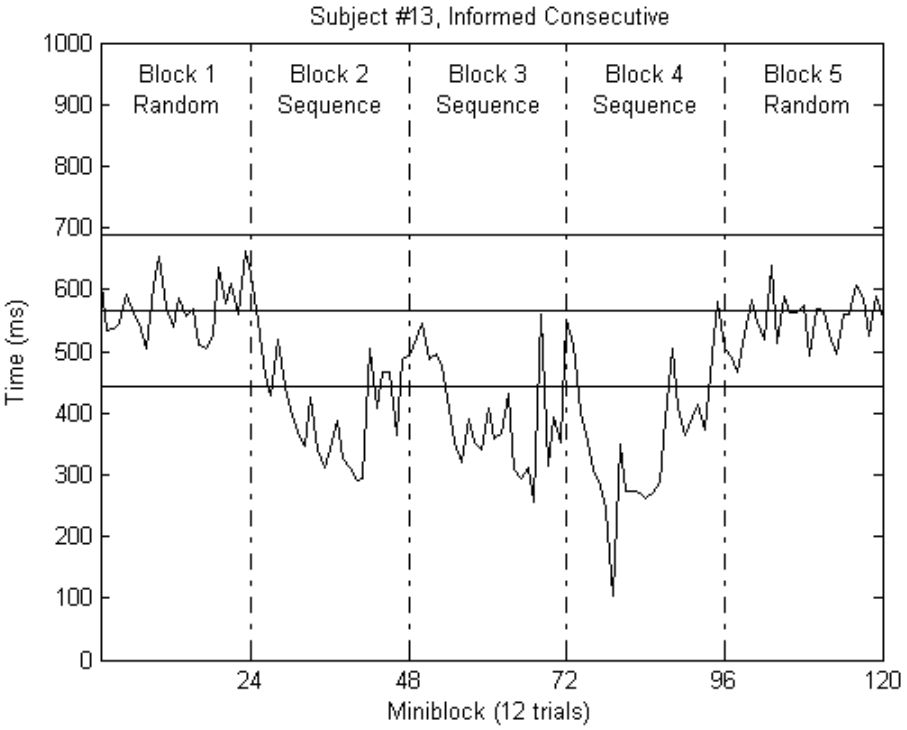


Figure A-26. Subject #13, Informed Consecutive.

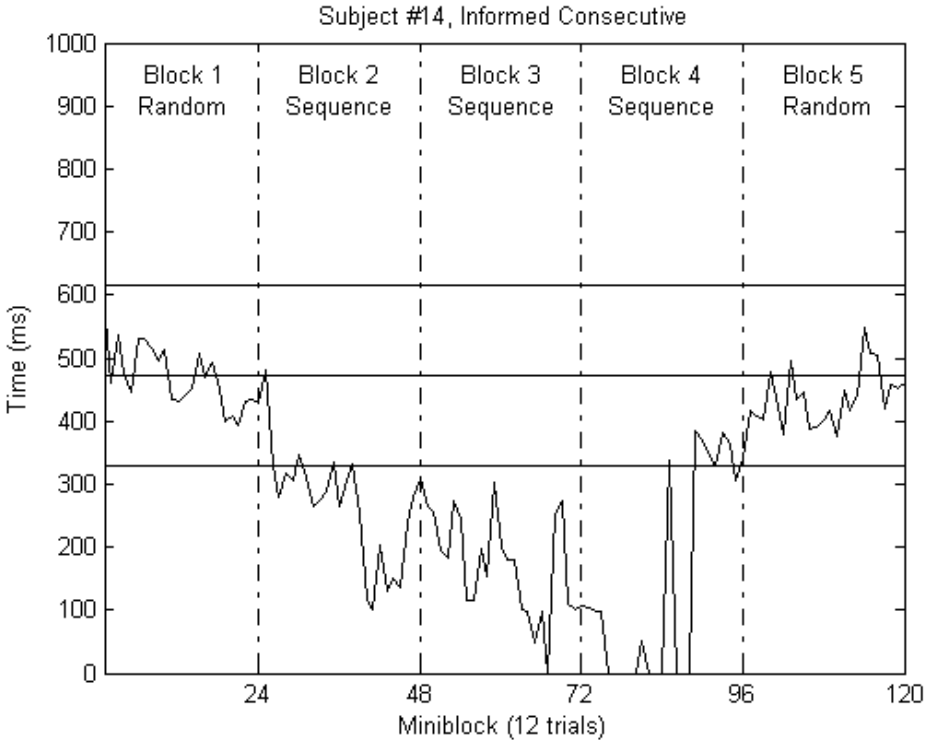


Figure A-27. Subject #14, Informed Consecutive.

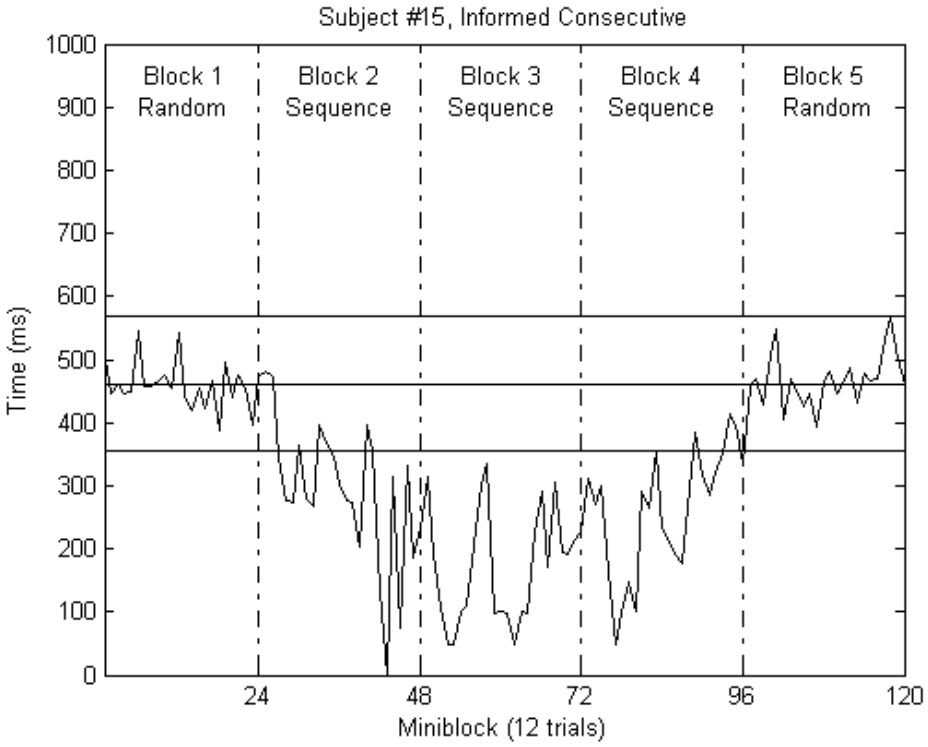


Figure A-28. Subject #15, Informed Consecutive.

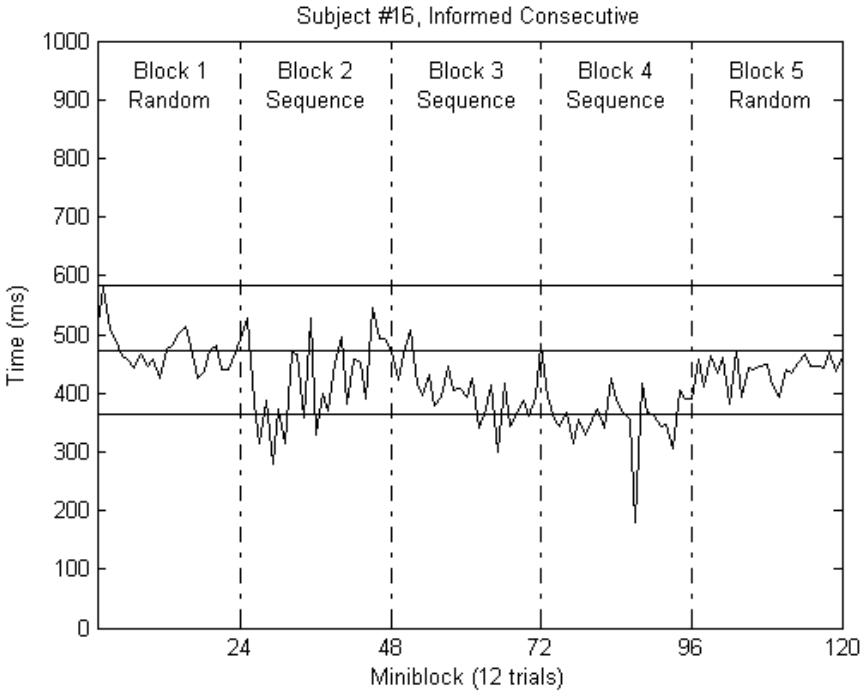


Figure A-29. Subject #16, Informed Consecutive.

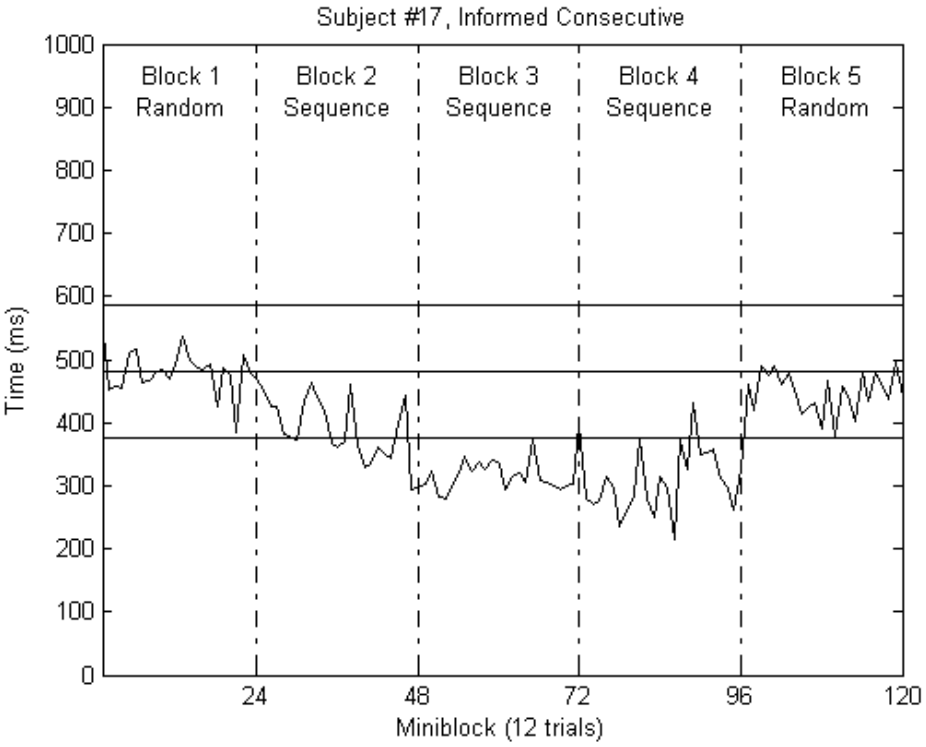


Figure A-30. Subject #17, Informed Consecutive.

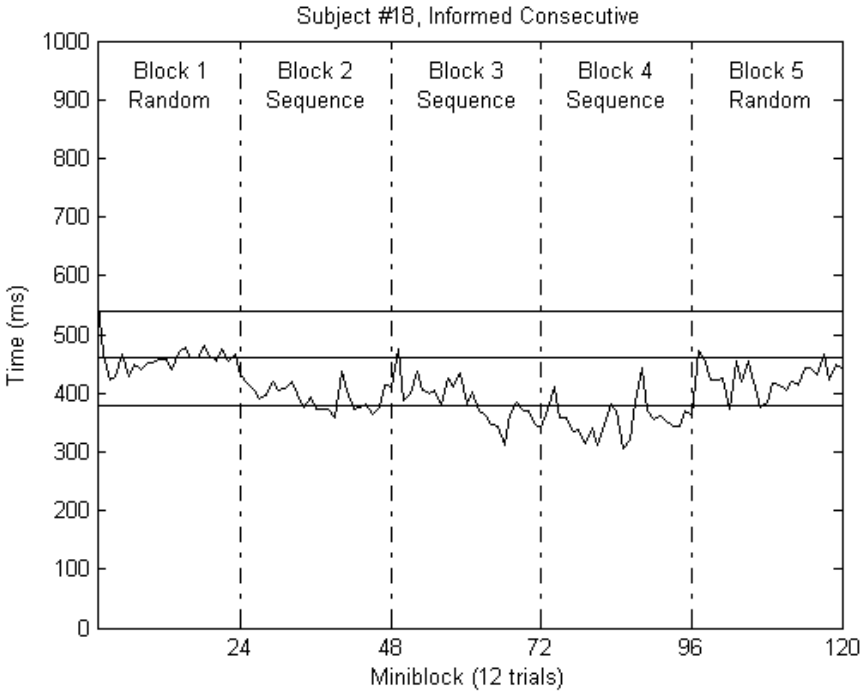


Figure A-31. Subject #18, Informed Consecutive.

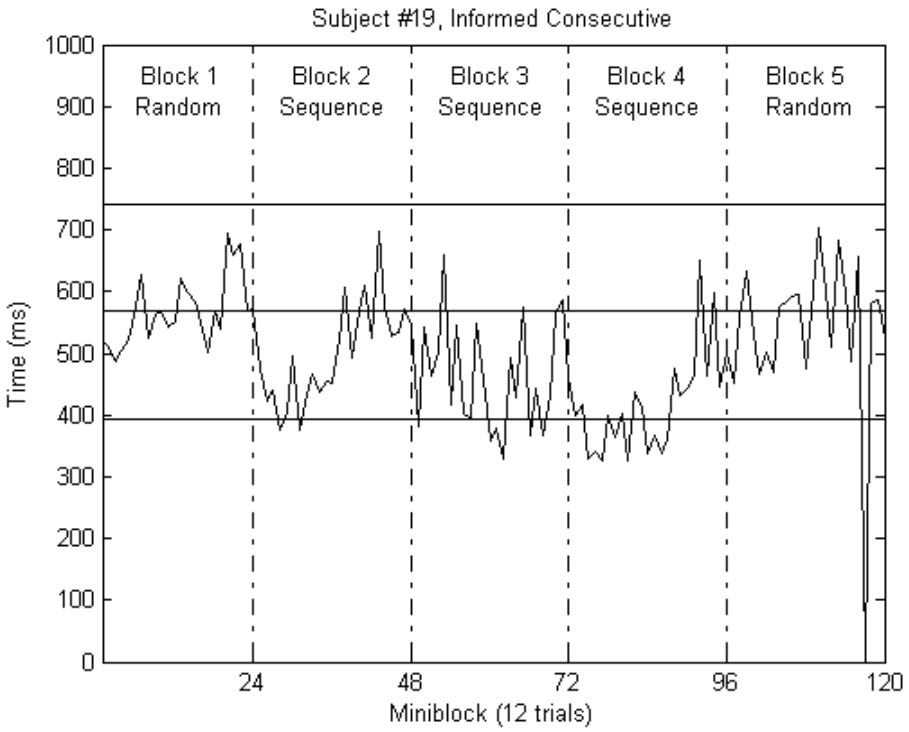


Figure A-32. Subject #19, Informed Consecutive.

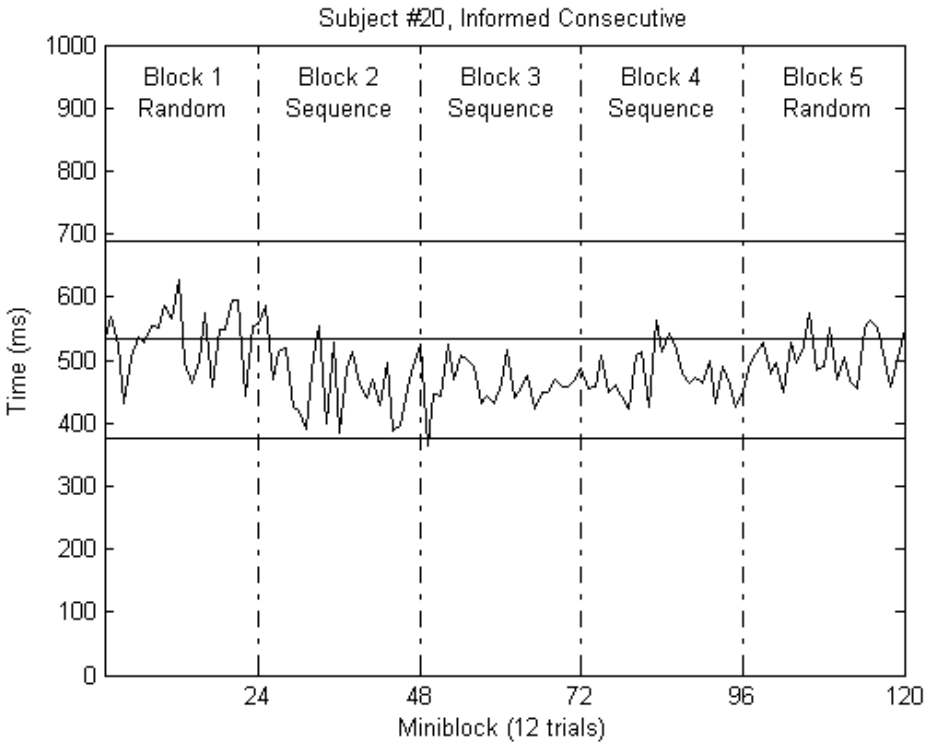


Figure A-33. Subject #20, Informed Consecutive.

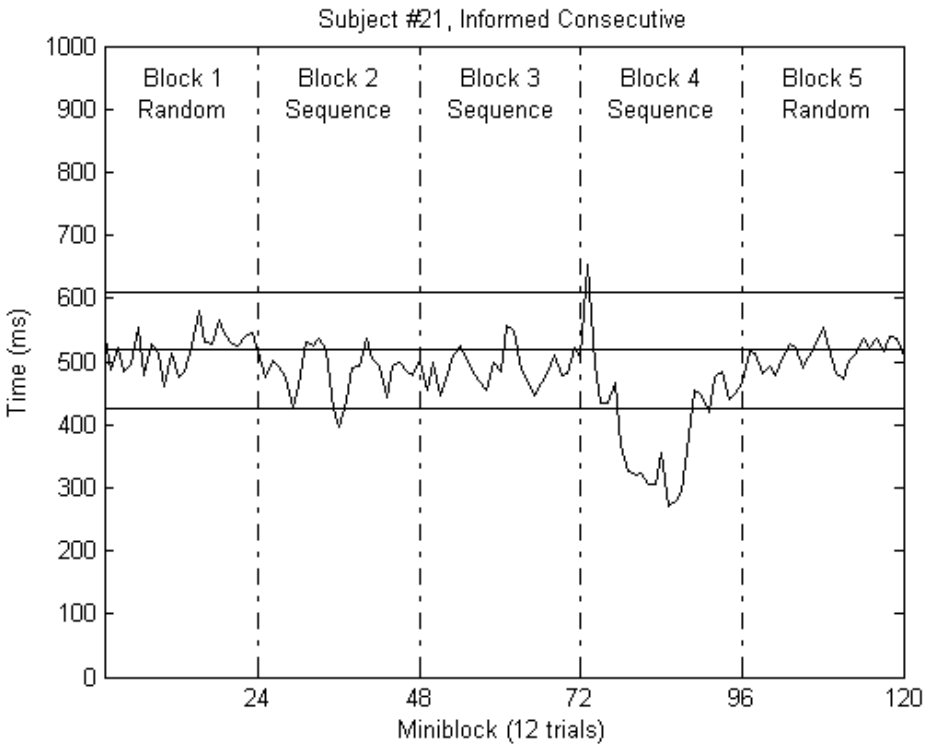
Subject #21, Informed Consecutive
Block 1
Random
Block 2
Sequence
Block 3
Sequence
Block 4
Sequence
Block 5
Random
Time (ms)
1000
900
800
700
600
500
400
300
200
100
0
24
48
72
96
120
Miniblock (12 trials)

APPENDIX B
ANALYSES OF BEHAVIORAL DATA

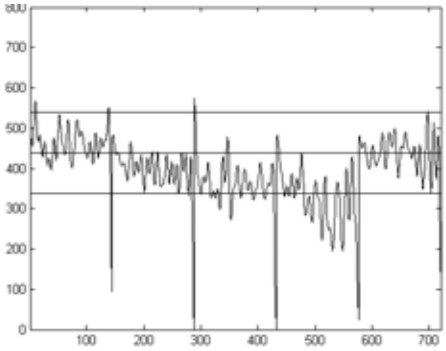

Figure B-1. Young #1, Explicit.

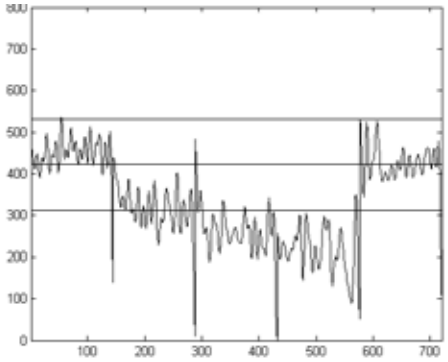

Figure B-2. Young #2, Explicit.

Table B-56. Young #1, Explicit.

| Session | Explicit-Young Participant #1 | | | | |
|---|---|---|---|---|---|
| Block | 1 | 2 | 3 | 4 | 5 |
| Tryon's C | 1.05 | 1.35 | 1.10 | 3.86 | 0.00 |
| Accuracy | 96% | 99% | 96% | 96% | 94% |
| Participant Response Sequence Learned in: | Participant not asked when sequence was learned<br><br>Block 4 | | | | |

Table B-2. Young #2, Explicit.

| Explicit-Young Participant #2 | | | | |
|---|---|---|---|---|
| 1 | 2 | 3 | 4 | 5 |
| 1.42 | -1.72 | 0.93 | 0.50 | 0.79 |
| 97% | 96% | 94% | 91% | 97% |
| Learned sequence in Block 2<br><br>Block 2 | | | | |

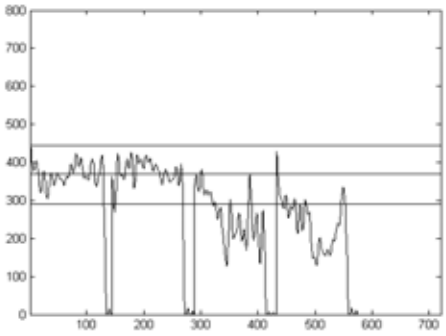

Figure B-3. Young #3, Explicit.

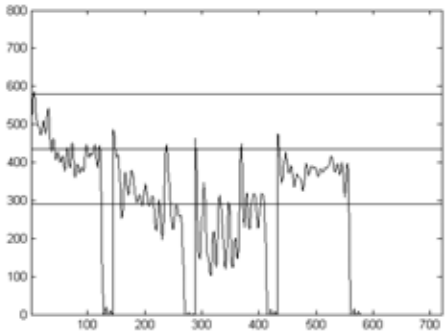

Figure B-4. Young #4, Explicit.

Table B-3. Young #3, Explicit.

| Session | Explicit-Young Participant #3 | | | | |
|---|---|---|---|---|---|
| Block | 1 | 2 | 3 | 4 | 5 |
| Tryon's C | -0.53 | -0.25 | 2.25 | 3.74 | 0.00 |
| Accuracy | 98% | 96% | 95% | 96% | 0% |
| Participant Response Sequence Learned in: | Participant not asked when sequence was learned<br>Block 3 | | | | |

Table B-4. Young #4, Explicit.

| Explicit-Young Participant #4 | | | | |
|---|---|---|---|---|
| **1** | 2 | 3 | 4 | 5 |
| 4.90 | 3.19 | 3.98 | -1.50 | 0.00 |
| 98% | 97% | 95% | 96% | 0% |
| Participant not asked when sequence was learned<br>N/A: sequence from Implicit session accidentally reused | | | | |

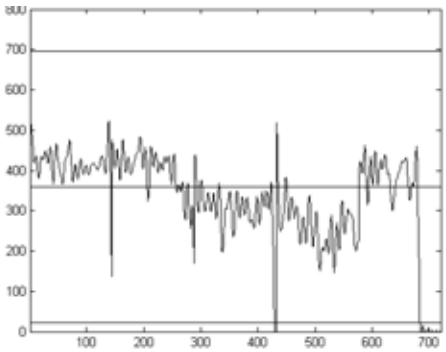

Figure B-5. Young #5, Explicit.

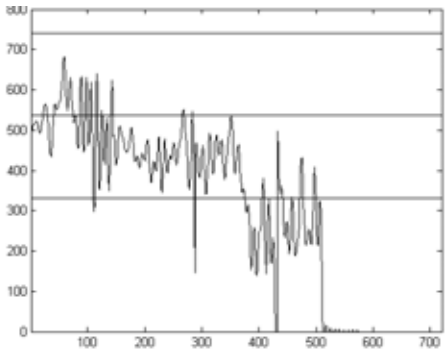

Figure B-6. Young #6, Explicit.

Table B-5. Young #5, Explicit.

| Session | Explicit-Young Participant #5 | | | | |
|---|---|---|---|---|---|
| Block | 1 | 2 | 3 | 4 | 5 |
| Tryon's C | -0.87 | -1.13 | 1.56 | 2.60 | 7.55 |
| Accuracy | 96% | 98% | 95% | 98% | 88% |
| Participant Response Sequence Learned in: | Learned sequence in Block 3<br>Block 3 | | | | |

Table B-6. Young #6, Explicit.

| Explicit-Young Participant #6 | | | | |
|---|---|---|---|---|
| 1 | 2 | 3 | 4 | 5 |
| 1.05 | -0.12 | 5.56 | 0.00 | 0.00 |
| 79% | 97% | 91% | 0% | 0% |
| Learned sequence in Block 3<br>Block 3 | | | | |

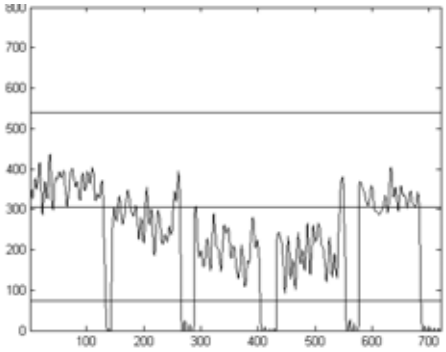

Figure B-7. Young #7, Explicit.

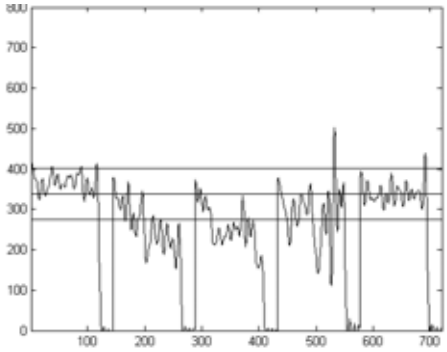

Figure B-8. Young #8, Explicit.

Table B-7. Young #7, Explicit.

| Session | Explicit-Young Participant #7 | | | | |
|---|---|---|---|---|---|
| Block | 1 | 2 | 3 | 4 | 5 |
| Tryon's C | 0.10 | 0.64 | 0.78 | 3.00 | 6.76 |
| Accuracy | 97% | 96% | 94% | 93% | 90% |
| Participant Response Sequence Learned in: | Learned sequence in Block 4<br><br>Block 4 | | | | |

Table B-8. Young #8, Explicit.

| Explicit-Young Participant #8 | | | | |
|---|---|---|---|---|
| 1 | 2 | 3 | 4 | 5 |
| -1.42 | 2.47 | 0.68 | 2.58 | -0.21 |
| 95% | 96% | 92% | 90% | 94% |
| Learned sequence in Block 2<br><br>Block 2 | | | | |

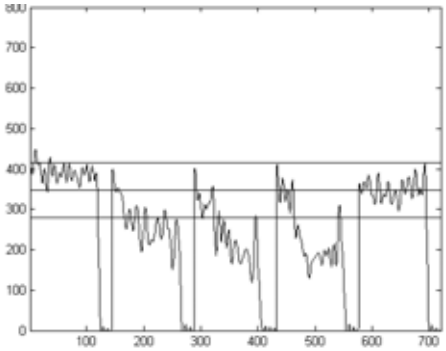

Figure B-9. Young #9, Explicit.

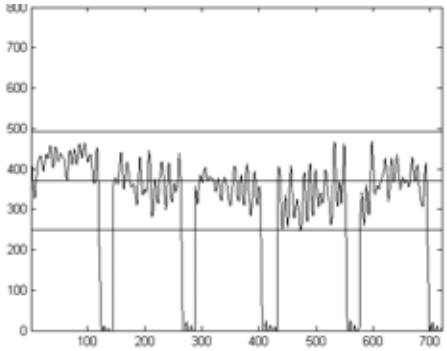

Figure B-10. Young #10, Explicit.

Table B-9. Young #9, Explicit.

| Session | Explicit-Young Participant #9 | | | | |
|---|---|---|---|---|---|
| Block | 1 | 2 | 3 | 4 | 5 |
| Tryon's C | -0.90 | 1.40 | 4.97 | 2.97 | 1.15 |
| Accuracy | 96% | 93% | 96% | 97% | 95% |
| Participant Response Sequence Learned in: | Learned sequence in Block 3<br><br>Block 3 | | | | |

Table B-10. Young #10, Explicit.

| Explicit-Young Participant #10 | | | | |
|---|---|---|---|---|
| 1 | 2 | 3 | 4 | 5 |
| 1.29 | -0.66 | -0.04 | -1.58 | 0.01 |
| 95% | 92% | 93% | 90% | 93% |
| Learned sequence in Block 4<br><br>N/A: no evidence of learning | | | | |

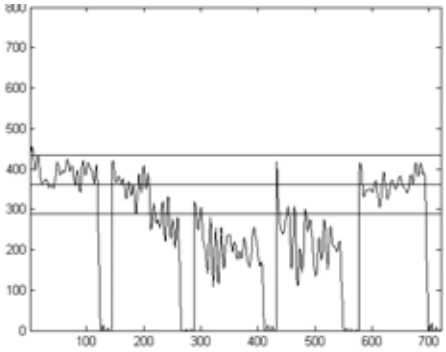

Figure B-11. Young #11, Explicit.

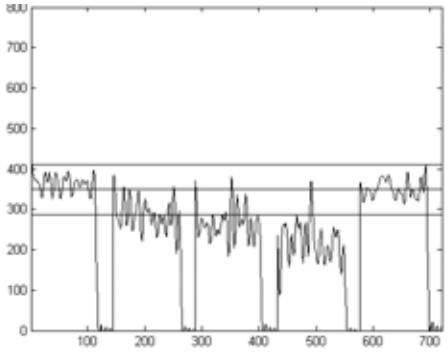

Figure B-12. Young #12, Explicit.

Table B-11. Young #11, Explicit.

| Session | Explicit-Young Participant #11 | | | | |
|---|---|---|---|---|---|
| Block | 1 | 2 | 3 | 4 | 5 |
| Tryon's C | 0.85 | 3.79 | -0.15 | -0.02 | 1.39 |
| Accuracy | 96% | 97% | 90% | 84% | 96% |
| Participant Response Sequence Learned in: | Learned sequence in Block 2<br><br>Block 2 | | | | |

Table B-12. Young #12, Explicit.

| Explicit-Young Participant #12 | | | | |
|---|---|---|---|---|
| 1 | 2 | 3 | 4 | 5 |
| 0.35 | 0.98 | -0.96 | 0.29 | 1.52 |
| 94% | 92% | 88% | 88% | 93% |
| Learned sequence in Block 2<br><br>Block 2 | | | | |

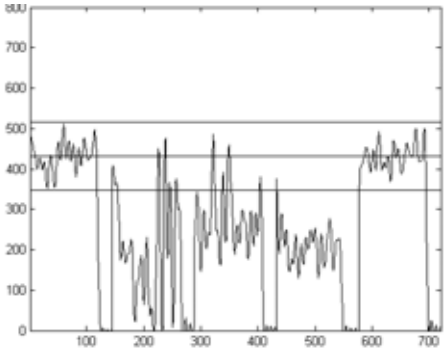

Figure B-13. Young #13, Explicit.

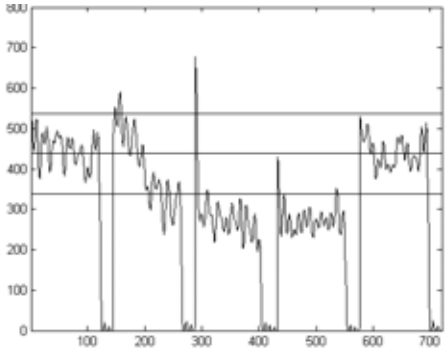

Figure B-14. Young #14, Explicit.

Table B-13. Young #13, Explicit.

| Session | Explicit-Young Participant #13 | | | | |
|---|---|---|---|---|---|
| Block | 1 | 2 | 3 | 4 | 5 |
| Tryon's C | 2.50 | 3.27 | 4.19 | -0.08 | 1.16 |
| Accuracy | 97% | 39% | 90% | 92% | 96% |
| Participant Response<br><br>Sequence Learned in: | Learned sequence in Block 2<br><br>N/A: learning in Block 2, but low accuracy (due to anticipation) | | | | |

Table B-14. Young #14, Explicit.

| Explicit-Young Participant #14 | | | | |
|---|---|---|---|---|
| 1 | 2 | 3 | 4 | 5 |
| 1.29 | 6.19 | 0.78 | 1.15 | 0.30 |
| 97% | 94% | 96% | 99% | 97% |
| Learned sequence in Block 2<br><br>Block 2 | | | | |

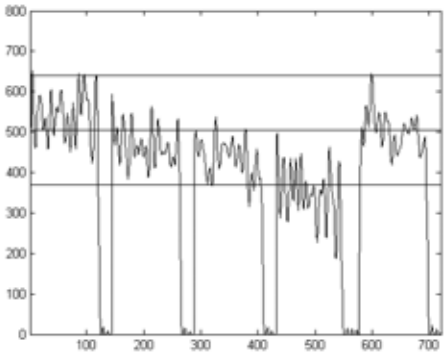

Figure B-15. Young #15, Explicit.

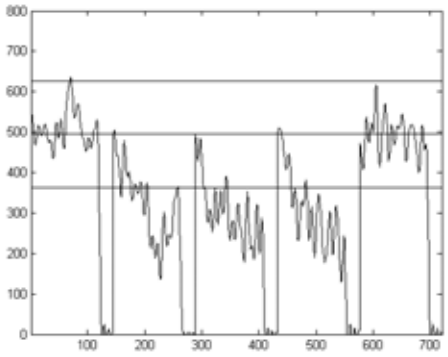

Figure B-16. Young #16, Explicit.

Table B-15. Young #15, Explicit.

| Session | Explicit-Young Participant #15 | | | | |
|---|---|---|---|---|---|
| Block | 1 | 2 | 3 | 4 | 5 |
| Tryon's C | 2.07 | -0.01 | 0.72 | 0.97 | 1.13 |
| Accuracy | 94% | 94% | 93% | 93% | 97% |
| Participant Response Sequence Learned in: | Learned sequence in Block 2<br><br>Block 3 | | | | |

Table B-16. Young #16, Explicit.

| Explicit-Young Participant #16 | | | | |
|---|---|---|---|---|
| 1 | 2 | 3 | 4 | 5 |
| 0.85 | 4.27 | 2.74 | 3.99 | 0.38 |
| 95% | 97% | 92% | 95% | 95% |
| Participant not asked when sequence was learned<br><br>Block 2 | | | | |

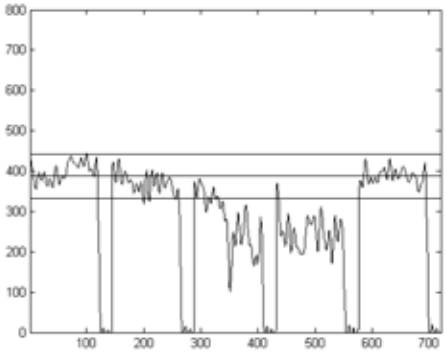

Figure B-17. Young #17, Explicit.

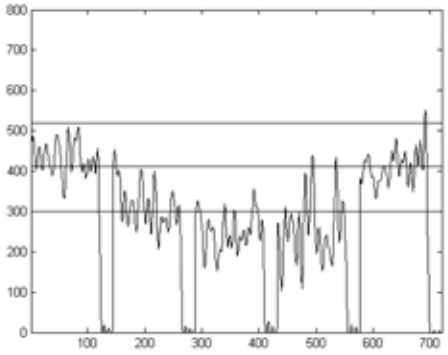

Figure B-18. Young #18, Explicit.

Table B-17. Young #17, Explicit.

| Session | Explicit-Young Participant #17 | | | | |
|---|---|---|---|---|---|
| Block | 1 | 2 | 3 | 4 | 5 |
| Tryon's C | 3.70 | 0.11 | 4.37 | 0.24 | -0.07 |
| Accuracy | 96% | 97% | 96% | 94% | 95% |
| Participant Response Sequence Learned in: | Participant not asked when sequence was learned<br><br>Block 3 | | | | |

Table B-18. Young #18, Explicit.

| Explicit-Young Participant #18 | | | | |
|---|---|---|---|---|
| 1 | 2 | 3 | 4 | 5 |
| 2.79 | 3.86 | 2.26 | 5.53 | 1.46 |
| 95% | 97% | 92% | 95% | 95% |
| Participant not asked when sequence was learned<br><br>Block 2 | | | | |

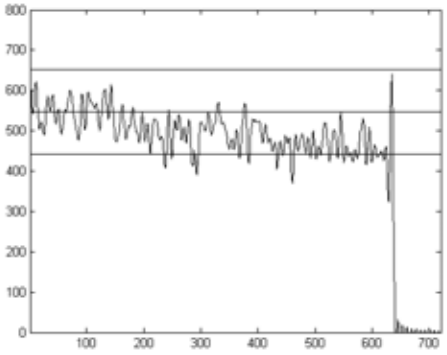

Figure B-19. Young #1, Implicit.

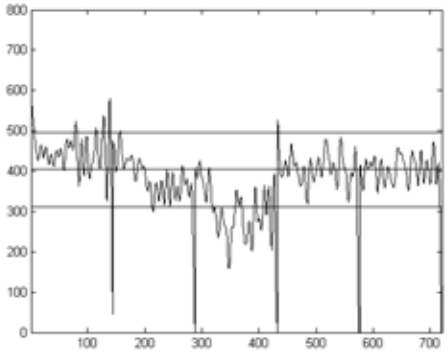

Figure B-20. Young #2, Implicit.

Table B-19. Young #1, Implicit.

| Session | Implicit-Young Participant #1 | | | | |
|---|---|---|---|---|---|
| Block | 1 | 2 | 3 | 4 | 5 |
| Tryon's C | -1.48 | -0.83 | -1.05 | -1.33 | 0.00 |
| Accuracy | 93% | 95% | 94% | 98% | 0% |
| Participant Response Sequence Learned in: | Did not report sequence<br><br>N/A: No evidence of learning | | | | |

Table B-20. Young #2, Implicit.

| Implicit-Young Participant #2 | | | | |
|---|---|---|---|---|
| 1 | 2 | 3 | 4 | 5 |
| 2.24 | 2.07 | 3.18 | 2.68 | -0.46 |
| 95% | 98% | 96% | 98% | 96% |
| Reported sequence during Block 2 but could not reproduce<br><br>Block 3 | | | | |

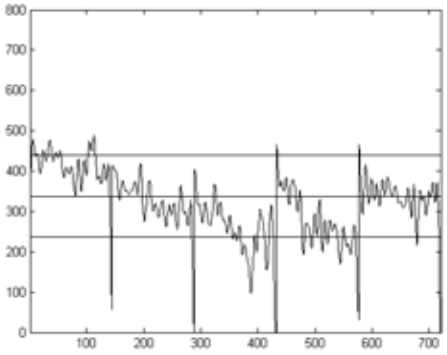

Figure B-21. Young #3, Implicit.

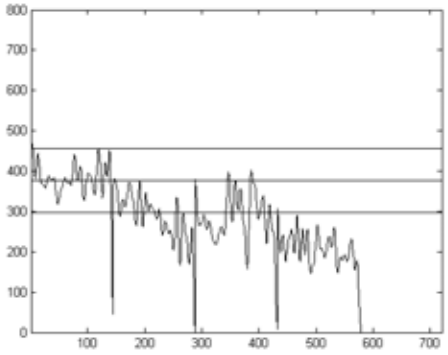

Figure B-22. Young #4, Implicit.

Table B-21. Young #3, Implicit.

| Session | Implicit-Young Participant #3 | | | | |
|---|---|---|---|---|---|
| Block | 1 | 2 | 3 | 4 | 5 |
| Tryon's C | 3.39 | 2.29 | 5.13 | 3.21 | 2.90 |
| Accuracy | 96% | 99% | 94% | 96% | 96% |
| Participant Response Sequence Learned in: | Did not report sequence<br><br>Block 3 | | | | |

Table B-22. Young #4, Implicit.

| Implicit-Young Participant #4 | | | | |
|---|---|---|---|---|
| 1 | 2 | 3 | 4 | 5 |
| 1.26 | 0.63 | 4.46 | 1.49 | 0.00 |
| 96% | 94% | 95% | 94% | 0% |
| Noticed during Block 2 and began explicitly learning<br>N/A: Noticed sequence in block 2 | | | | |

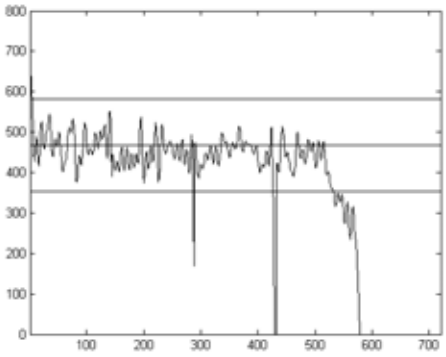

Figure B-23. Young #5, Implicit.

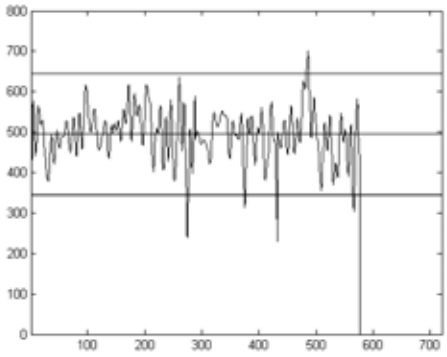

Figure B-24. Young #6, Implicit.

Table B-23. Young #5, Implicit.

| Session | Implicit-Young Participant #5 | | | | |
|---|---|---|---|---|---|
| Block | 1 | 2 | 3 | 4 | 5 |
| Tryon's C | 1.80 | 1.00 | -2.40 | 2.44 | 0.00 |
| Accuracy | 96% | 96% | 97% | 96% | 0% |
| Participant Response Sequence Learned in: | Noticed sequence during Block 4<br>Block 3 | | | | |

Table B-24. Young #6, Implicit.

| Implicit-Young Participant #6 | | | | |
|---|---|---|---|---|
| 1 | 2 | 3 | 4 | 5 |
| 4.04 | -0.86 | -0.56 | 0.65 | 0.00 |
| 97% | 86% | 89% | 81% | 0% |
| Did not report sequence<br>N/A: No evidence of learning | | | | |

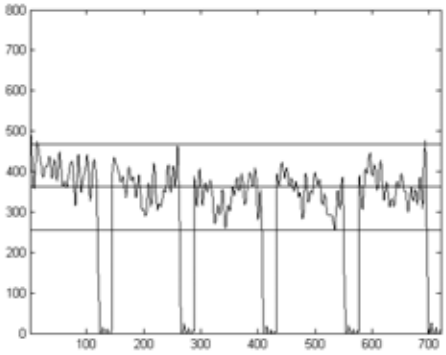

Figure B-25. Young #7, Implicit.

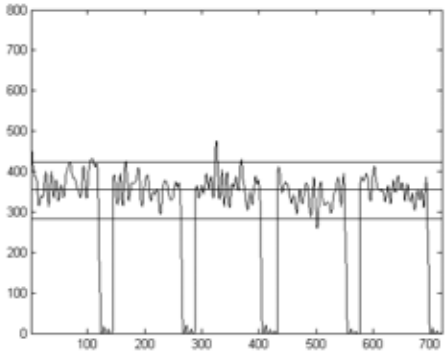

Figure B-26. Young #8, Implicit.

Table B-25. Young #7, Implicit.

| Session | Implicit-Young Participant #7 | | | | |
|---|---|---|---|---|---|
| Block | 1 | 2 | 3 | 4 | 5 |
| Tryon's C | 1.20 | -0.12 | -0.66 | 0.19 | 1.29 |
| Accuracy | 96% | 95% | 97% | 96% | 96% |
| Participant Response Sequence Learned in: | Noticed a sequence but did not try to explicitly learn<br>Block 3 | | | | |

Table B-26. Young #8, Implicit.

| Implicit-Young Participant #8 | | | | |
|---|---|---|---|---|
| 1 | 2 | 3 | 4 | 5 |
| 1.86 | -1.22 | 0.37 | -0.23 | -0.56 |
| 94% | 96% | 95% | 96% | 96% |
| Noticed sequence and could report a portion of it<br>N/A: No evidence of learning | | | | |

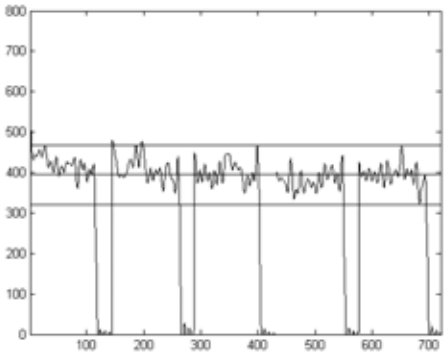

Figure B-27. Young #9, Implicit.

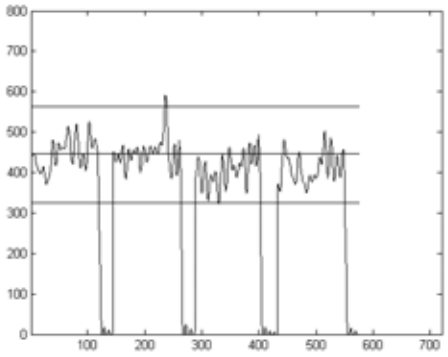

Figure B-28. Young #10, Implicit.

Table B-27. Young #9, Implicit.

| Session | Implicit-Young Participant #9 | | | | |
|---|---|---|---|---|---|
| Block | 1 | 2 | 3 | 4 | 5 |
| Tryon's C | 2.76 | 1.60 | 1.63 | 2.10 | 0.52 |
| Accuracy | 96% | 98% | 96% | 98% | 95% |
| Participant Response | Did not report sequence | | | | |
| Sequence Learned in: | Block 4 | | | | |

Table B-28. Young #10, Implicit.

| Implicit-Young Participant #10 | | | | |
|---|---|---|---|---|
| 1 | 2 | 3 | 4 | 5 |
| 3.97 | -0.52 | 1.95 | -0.73 | 0.00 |
| 96% | 95% | 98% | 90% | 0% |
| Noticed a sequence but did not try to explicitly learn | | | | |
| Block 3 | | | | |

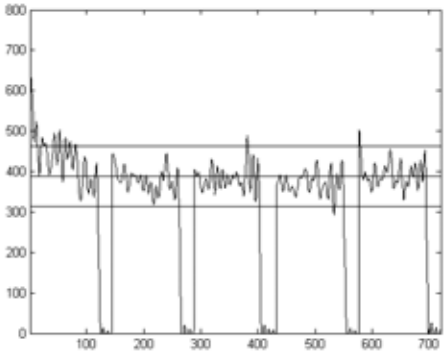

Figure B-29. Young #11, Implicit.

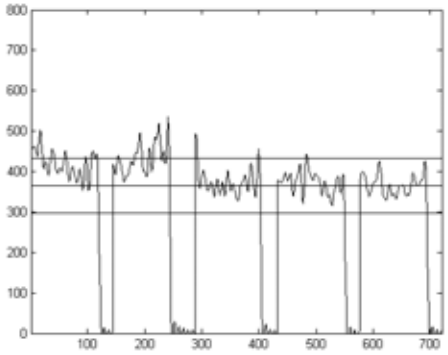

Figure B-30. Young #12, Implicit.

Table B-29. Young #11, Implicit.

| Session | Implicit-Young Participant #11 | | | | |
|---|---|---|---|---|---|
| Block | 1 | 2 | 3 | 4 | 5 |
| Tryon's C | 4.02 | 0.56 | 1.25 | 2.22 | -0.13 |
| Accuracy | 95% | 96% | 92% | 96% | 95% |
| Participant Response | Noticed sequence during Block 4 | | | | |
| Sequence Learned in: | N/A: Noticed sequence in same block as RT improvement | | | | |

Table B-30. Young #12, Implicit.

| Implicit-Young Participant #12 | | | | |
|---|---|---|---|---|
| 1 | 2 | 3 | 4 | 5 |
| 2.20 | 8.90 | 1.24 | 1.51 | 0.43 |
| 96% | 84% | 98% | 95% | 95% |
| Noticed sequence during Block 3 | | | | |
| N/A: No evidence of Learning | | | | |

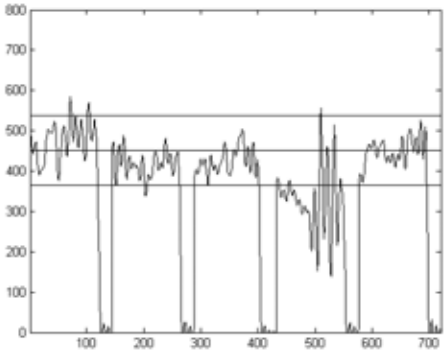

Figure B-31. Young #13, Implicit.

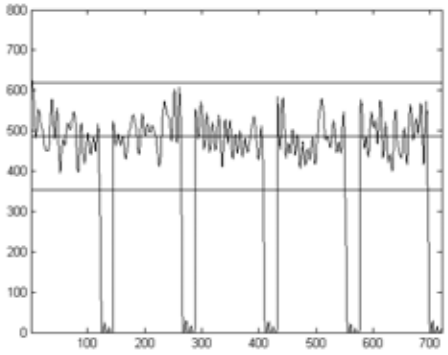

Figure B-32. Young #14, Implicit.

Table B-31. Young #13, Implicit.

| Session | Implicit-Young Participant #13 | | | | |
|---|---|---|---|---|---|
| Block | 1 | 2 | 3 | 4 | 5 |
| Tryon's C | 3.25 | 1.24 | 2.74 | 4.53 | 1.96 |
| Accuracy | 97% | 97% | 97% | 87% | 96% |
| Participant Response | Noticed sequence during "first run"; unclear if Block 2 or 4 | | | | |
| Sequence Learned in: | N/A: Unclear if Block 2 is implicit or explicit learning | | | | |

Table B-32. Young #14, Implicit.

| Implicit-Young Participant #14 | | | | |
|---|---|---|---|---|
| 1 | 2 | 3 | 4 | 5 |
| 2.28 | -0.43 | -0.89 | -1.30 | 1.01 |
| 95% | 93% | 93% | 97% | 94% |
| Did not report sequence | | | | |
| N/A: No evidence of learning | | | | |

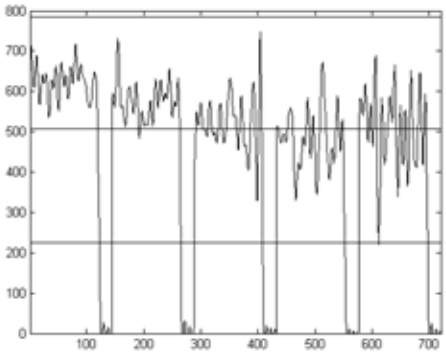

Figure B-33. Young #15, Implicit.

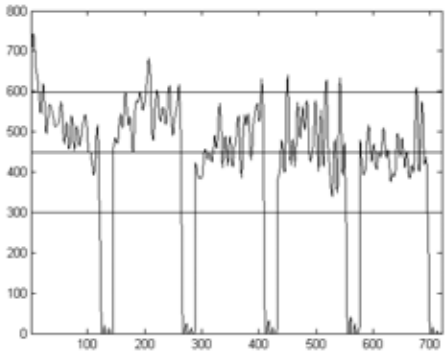

Figure B-34. Young #16, Implicit.

Table B-33. Young #15, Implicit.

| Session | Implicit-Young Participant #15 | | | | |
|---|---|---|---|---|---|
| Block | 1 | 2 | 3 | 4 | 5 |
| Tryon's C | 0.07 | -2.02 | -1.45 | 0.19 | 0.18 |
| Accuracy | 77% | 83% | 82% | 90% | 76% |
| Participant Response | Noticed sequence during Block 2 | | | | |
| Sequence Learned in: | N/A: No evidence of learning. | | | | |

Table B-34. Young #16, Implicit.

| Implicit-Young Participant #16 | | | | |
|---|---|---|---|---|
| 1 | 2 | 3 | 4 | 5 |
| 4.65 | 2.27 | -0.51 | 2.52 | 1.20 |
| 96% | 93% | 93% | 91% | 96% |
| Noticed sequence during Block 2 but ignored. Many incorrect elements in reported sequence. | | | | |
| N/A: No evidence of learning. | | | | |

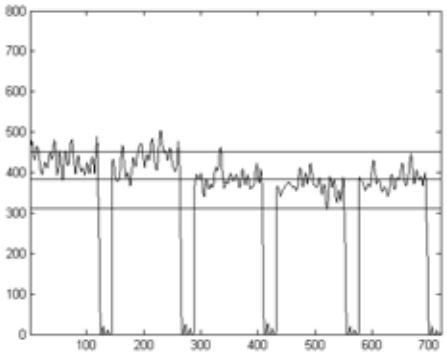

Figure B-35. Young #17, Implicit.

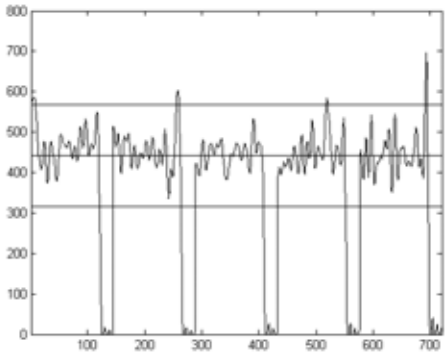

Figure B-36. Young #18, Implicit.

Table B-35. Young #17, Implicit.

| Session | Implicit-Young Participant #17 | | | | |
|---|---|---|---|---|---|
| Block | 1 | 2 | 3 | 4 | 5 |
| Tryon's C | 0.39 | 1.84 | -0.17 | 1.58 | 0.77 |
| Accuracy | 98% | 95% | 96% | 98% | 97% |
| Participant Response | Noticed sequence during Block 4 | | | | |
| Sequence Learned in: | N/A: Noticed sequence in same block as RT improvement | | | | |

Table B-36. Young #18, Implicit.

| Implicit-Young Participant #18 | | | | |
|---|---|---|---|---|
| 1 | 2 | 3 | 4 | 5 |
| 1.16 | 1.99 | 0.61 | 2.37 | 2.08 |
| 97% | 95% | 94% | 94% | 94% |
| Did not notice sequence | | | | |
| N/A: No evidence of learning. | | | | |

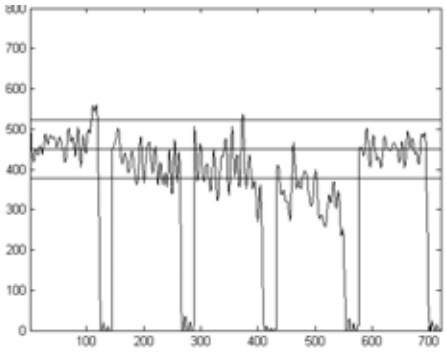

Figure B-37. Senior #1, Explicit.

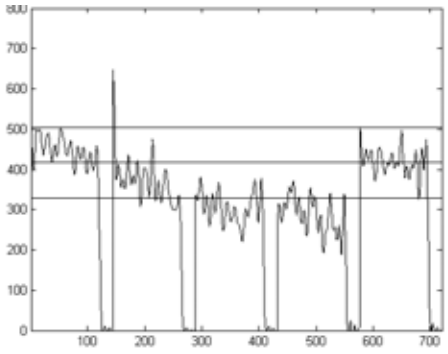

Figure B-38. Senior #2, Explicit.

Table B-37. Senior #1, Explicit.

| Session | Explicit-Senior Participant #1 | | | | |
|---|---|---|---|---|---|
| Block | 1 | 2 | 3 | 4 | 5 |
| Tryon's C | 1.99 | 0.11 | 2.32 | 1.18 | 1.03 |
| Accuracy | 0.95 | 0.95 | 0.95 | 0.94 | 0.94 |
| Participant Response | Participant reported improved sequence knowledge with each block. | | | | |
| Sequence Learned in: | Block 2 | | | | |

Table B-38. Senior #2, Explicit.

| Explicit-Senior Participant #2 | | | | |
|---|---|---|---|---|
| 1 | 2 | 3 | 4 | 5 |
| 1.54 | 2.36 | 2.19 | 2.43 | 0.62 |
| 0.98 | 0.98 | 0.96 | 0.96 | 0.96 |
| Participant reported knowing (Block 2) 6/12 trials; (B3) 9/12; (B4) all 12. | | | | |
| Block 2 | | | | |

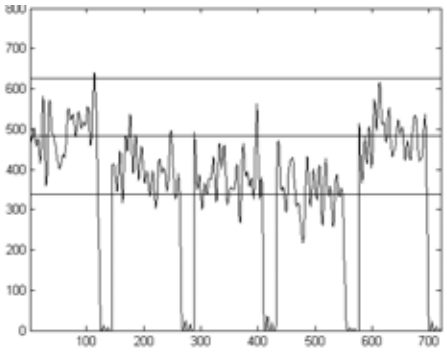

Figure B-39. Senior #3, Explicit.

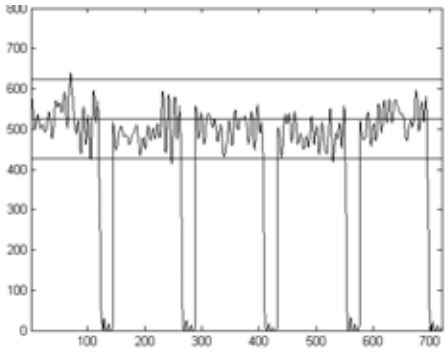

Figure B-40. Senior #4, Explicit.

Table B-39. Senior #3, Explicit.

| Session | Explicit-Senior Participant #3 | | | | |
|---|---|---|---|---|---|
| Block | 1 | 2 | 3 | 4 | 5 |
| Tryon's C | 1.10 | -1.20 | 0.19 | -1.14 | 1.07 |
| Accuracy | 0.93 | 0.91 | 0.93 | 0.91 | 0.95 |
| Participant Response | Participant felt he learned some of sequence in Block 2, most in 3. | | | | |
| Sequence Learned in: | Block 2 | | | | |

Table B-40. Senior #4, Explicit.

| Explicit-Senior Participant #4 | | | | |
|---|---|---|---|---|
| 1 | 2 | 3 | 4 | 5 |
| 3.17 | 1.22 | -0.73 | 0.08 | 1.49 |
| 0.84 | 0.93 | 0.91 | 0.95 | 0.93 |
| Participant reported learning sequence but could not report. "I have to see it to follow it." | | | | |
| N/A: No evidence of learning | | | | |

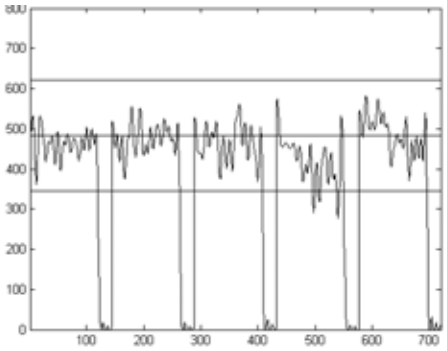

Figure B-41. Senior #5, Explicit.

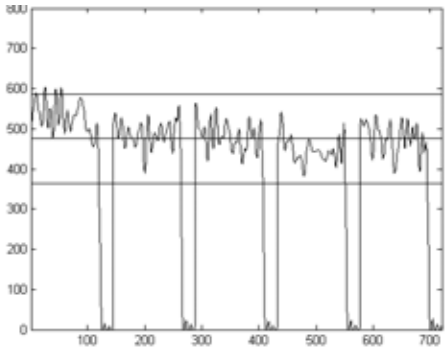

Figure B-42. Senior #6, Explicit.

Table B-41. Senior #5, Explicit.

| Session | Explicit-Senior Participant #5 | | | | |
|---|---|---|---|---|---|
| Block | 1 | 2 | 3 | 4 | 5 |
| Tryon's C | 2.66 | 2.02 | 3.03 | 2.48 | 3.98 |
| Accuracy | 0.97 | 0.96 | 0.99 | 0.98 | 0.96 |
| Participant Response | Participant felt she knew "up to a third of sequence" in Block 4. | | | | |
| Sequence Learned in: | Block 4 | | | | |

Table B-42. Senior #6, Explicit.

| Explicit-Senior Participant #6 | | | | |
|---|---|---|---|---|
| 1 | 2 | 3 | 4 | 5 |
| 1.86 | -0.69 | -0.65 | -1.73 | 0.65 |
| 0.94 | 0.95 | 0.91 | 0.93 | 0.93 |
| Participant reported knowing 4 elements during Block 4. | | | | |
| Block 4 | | | | |

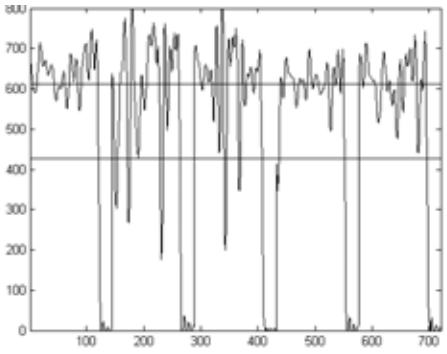

Figure B-43. Senior #7, Explicit.

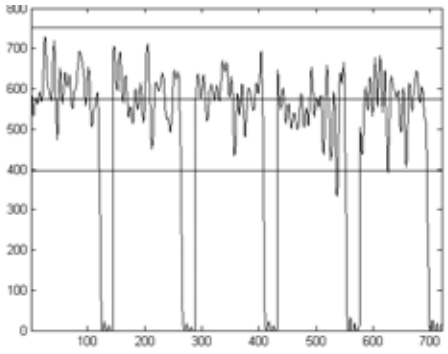

Figure B-44. Senior #8, Explicit.

Table B-43. Senior #7, Explicit.

| Session | Explicit-Senior Participant #7 | | | | |
|---|---|---|---|---|---|
| Block | 1 | 2 | 3 | 4 | 5 |
| Tryon's C | -0.47 | 2.36 | 3.55 | -1.08 | 1.00 |
| Accuracy | 0.87 | 0.60 | 0.76 | 0.88 | 0.92 |
| Participant Response | Participant did not try to learn sequence. "When I do, I make lots of mistakes and press the wrong fingers." | | | | |
| Sequence Learned in: | N/A: Too many missed responses | | | | |

Table B-44. Senior #8, Explicit.

| Explicit-Senior Participant #8 | | | | |
|---|---|---|---|---|
| 1 | 2 | 3 | 4 | 5 |
| 1.21 | -0.83 | 0.57 | -0.17 | 0.61 |
| 0.77 | 0.78 | 0.72 | 0.69 | 0.72 |
| Participant tried but could not learn sequence. "I don't know why, but I just can't learn it." | | | | |
| N/A: Too many missed responses | | | | |

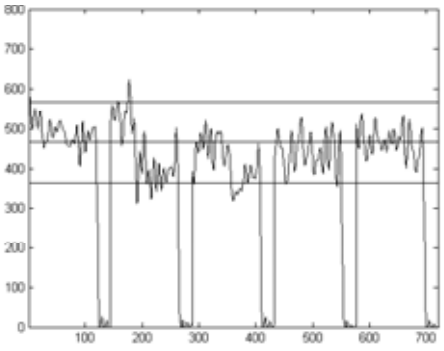

Figure B-45. Senior #9, Explicit

Table B-45. Senior #9, Explicit.

| Session | Explicit-Senior Participant #9 | | | | |
|---|---|---|---|---|---|
| Block | 1 | 2 | 3 | 4 | 5 |
| Tryon's C | -1.02 | 4.34 | 1.90 | 2.52 | -0.25 |
| Accuracy | 0.97 | 0.97 | 0.96 | 0.95 | 0.96 |
| Participant Response | Participant learned "about 20%" of sequence by Block 4. "I found that I did better when I didn't try [to learn sequence] and just focused on pressing the buttons when the fingers lit up. | | | | |
| Sequence Learned in: | Block 3 | | | | |

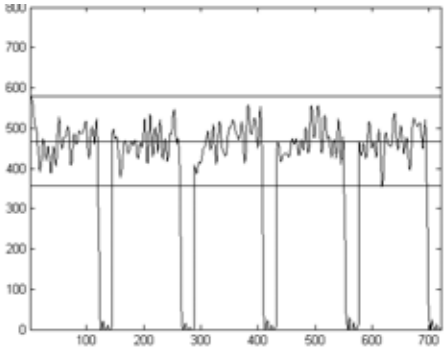

Figure B-46. Senior #1, Implicit.

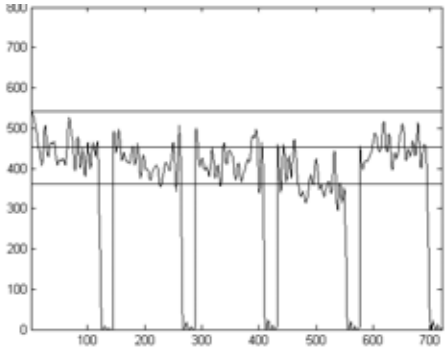

Figure B-47. Senior #2, Implicit.

Table B-46. Senior #1, Implicit.

| Session | Implicit-Senior Participant #1 | | | | |
|---|---|---|---|---|---|
| Block | 1 | 2 | 3 | 4 | 5 |
| Tryon's C | 1.48 | 0.23 | 0.79 | -0.22 | 1.48 |
| Accuracy | 0.88 | 0.93 | 0.94 | 0.95 | 0.92 |
| Participant Response | Participant thought he saw pattern but could not describe it. | | | | |
| Sequence Learned in: | N/A: No evidence of learning | | | | |

Table B-47. Senior #2, Implicit.

| Implicit-Senior Participant #2 | | | | |
|---|---|---|---|---|
| 1 | 2 | 3 | 4 | 5 |
| -0.28 | 0.98 | 0.94 | 3.67 | -0.28 |
| 0.95 | 0.96 | 0.98 | 0.99 | 0.96 |
| Participant noticed pattern in beginning of Block 4; began explicitly learning it. | | | | |
| Block 2 | | | | |

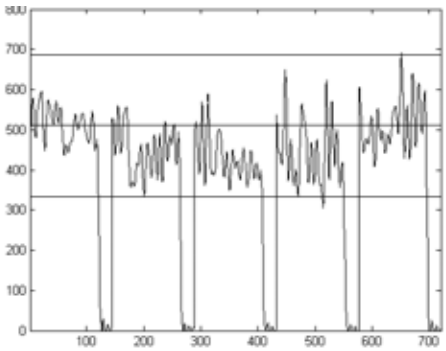

Figure B-48. Senior #3, Implicit.

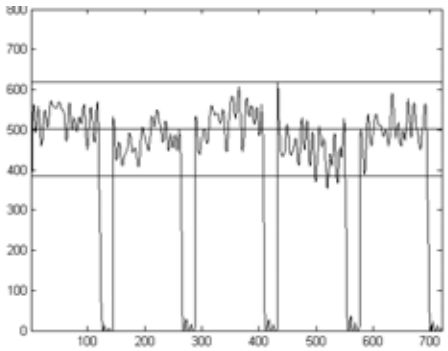

Figure B-49. Senior #4, Implicit.

Table B-48. Senior #3, Implicit.

| Session | Implicit-Senior Participant #3 | | | | |
|---|---|---|---|---|---|
| Block | 1 | 2 | 3 | 4 | 5 |
| Tryon's C | 1.47 | -0.51 | -1.69 | 1.09 | 1.47 |
| Accuracy | 0.97 | 0.94 | 0.97 | 0.94 | 0.91 |
| Participant Response | Participants noticed parts of sequence but thought it changed. | | | | |
| Sequence Learned in: | Block 3 | | | | |

Table B-49. Senior #4, Implicit.

| Implicit-Senior Participant #4 | | | | |
|---|---|---|---|---|
| 1 | 2 | 3 | 4 | 5 |
| -0.04 | 2.83 | 1.26 | -0.71 | -0.04 |
| 0.93 | 0.97 | 0.87 | 0.73 | 0.94 |
| Participant did not notice sequence. “Either [trials] are getting slower or I’m betting better.” | | | | |
| Block 2 | | | | |

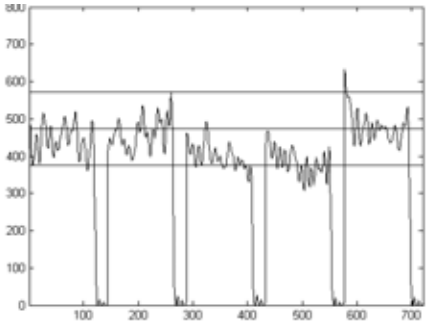

Figure B-50. Senior #5, Implicit.

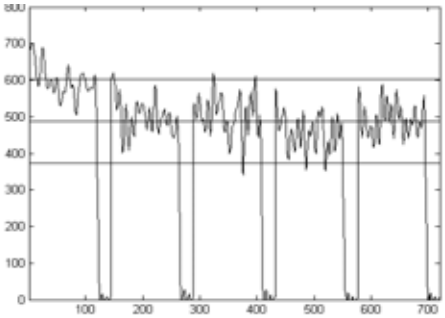

Figure B-51. Senior #6, Implicit.

Table B-50. Senior #5, Implicit.

| Session | Implicit-Senior Participant #5 | | | | |
|---|---|---|---|---|---|
| Block | 1 | 2 | 3 | 4 | 5 |
| Tryon's C | 1.64 | 1.23 | -0.10 | 0.34 | 1.64 |
| Accuracy | 0.97 | 0.96 | 0.98 | 0.98 | 0.95 |
| Participant Response | Participant did not notice sequence. "I'm getting faster. My fingers know where to go." | | | | |
| Sequence Learned in: | Block 3 | | | | |

Table B-51. Senior #6, Implicit.

| Implicit-Senior Participant #6 | | | | |
|---|---|---|---|---|
| 1 | 2 | 3 | 4 | 5 |
| 0.93 | 2.26 | 0.25 | 0.91 | 0.93 |
| 0.91 | 0.92 | 0.89 | 0.92 | 0.90 |
| Participant thought he saw patterns "but they disappeared when I looked for them." | | | | |
| Block 4 | | | | |

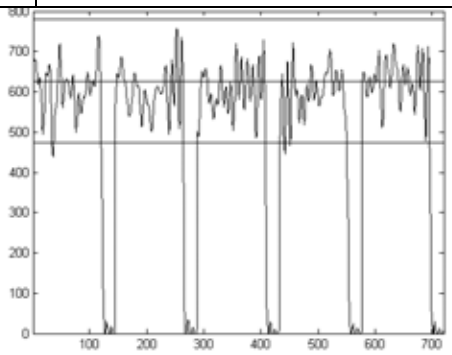

Figure B-52. Senior #7, Implicit.

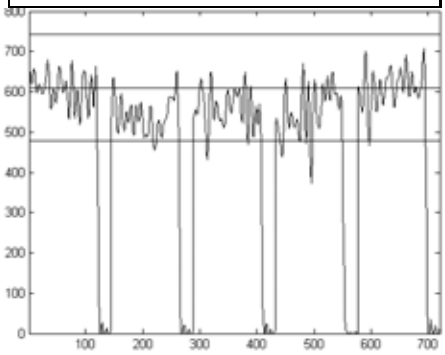

Figure B-53. Senior #8, Implicit.

Table B-52. Senior #7, Implicit.

| Session | Implicit-Senior Participant #7 | | | | |
|---|---|---|---|---|---|
| Block | 1 | 2 | 3 | 4 | 5 |
| Tryon's C | 1.13 | 0.98 | -1.62 | -0.70 | 1.13 |
| Accuracy | 0.83 | 0.90 | 0.89 | 0.87 | 0.82 |
| Participant Response | Participant noticed that trials "repeats itself a little" but did not try to learn. "The brain automatically finds patterns. Don't ask me to tell you what it is." | | | | |
| Sequence Learned in: | N/A: No evidence of learning. | | | | |

Table B-53. Senior #8, Implicit.

| Implicit-Senior Participant #8 | | | | |
|---|---|---|---|---|
| 1 | 2 | 3 | 4 | 5 |
| 0.97 | -1.31 | -1.19 | 0.87 | 0.97 |
| 0.89 | 0.96 | 0.87 | 0.83 | 0.84 |
| Participant did not notice any patterns. | | | | |
| Block 2 | | | | |

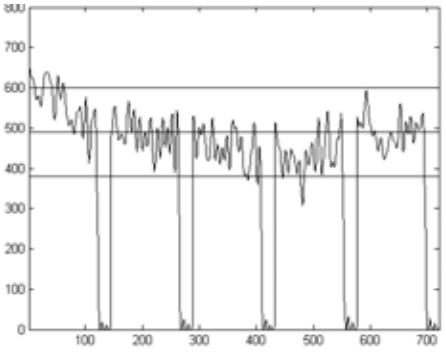


Figure B-54. Senior #9, Implicit.

Table B-54. Senior #9, Implicit.

| Session | Implicit-Senior Participant #9 | | | | |
|---|---|---|---|---|---|
| Block | 1 | 2 | 3 | 4 | 5 |
| Tryon's C | 2.98 | -0.22 | -0.23 | 0.84 | 2.98 |
| Accuracy | 0.96 | 0.96 | 0.93 | 0.98 | 0.94 |
| Participant Response | Participant noticed sequence toward end of Block 3. "It repeats itself over and over." | | | | |
| Sequence Learned in: | N/A: RT improvements occurred after explicit awareness of sequence | | | | |

APPENDIX C
CORRELATIONAL HISTOGRAMS

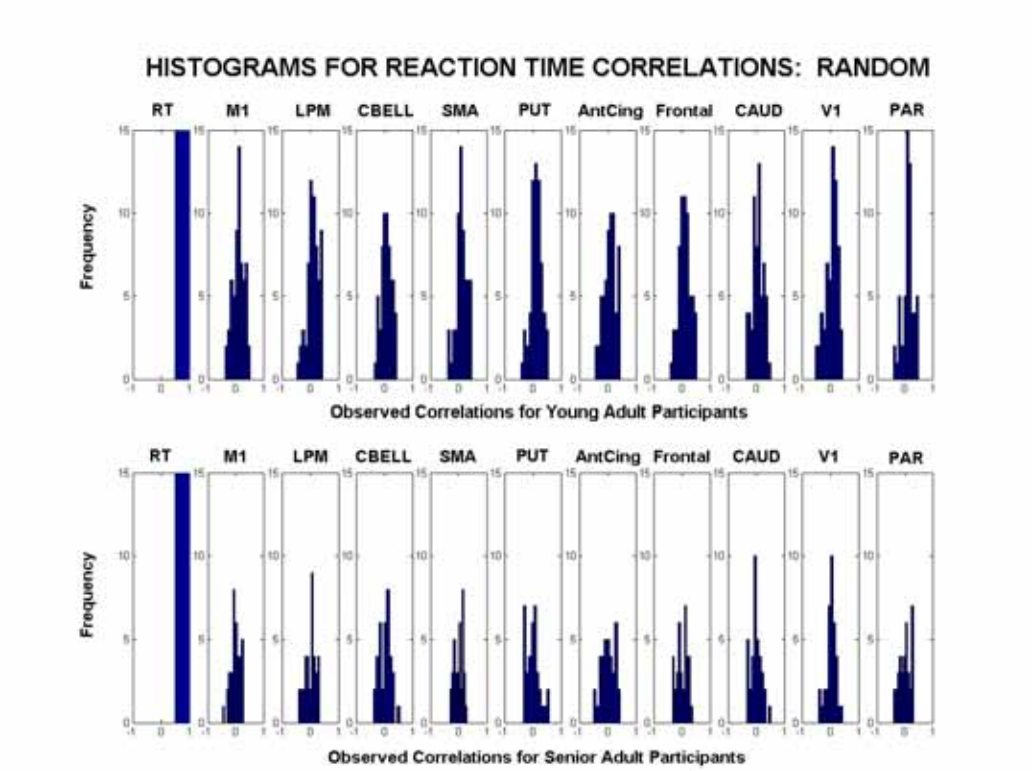


Figure C-1. Random Correlation Histograms by Age: Reaction Time

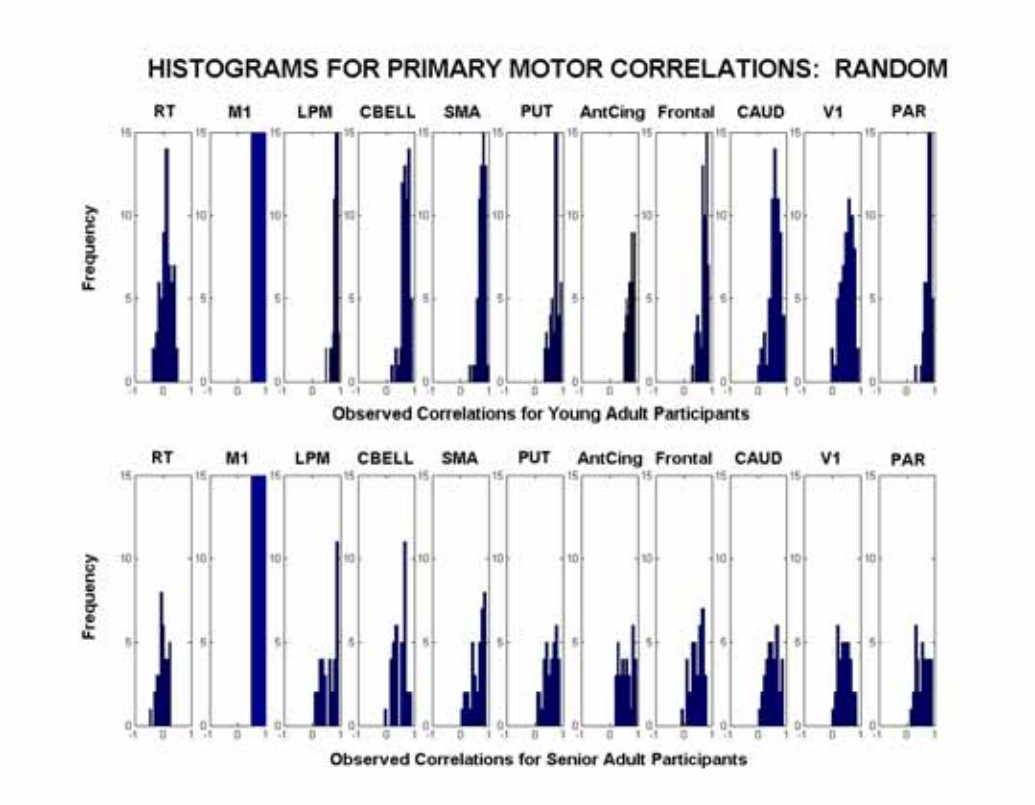


Figure C-2. Random Correlation Histograms by Age: Primary Motor

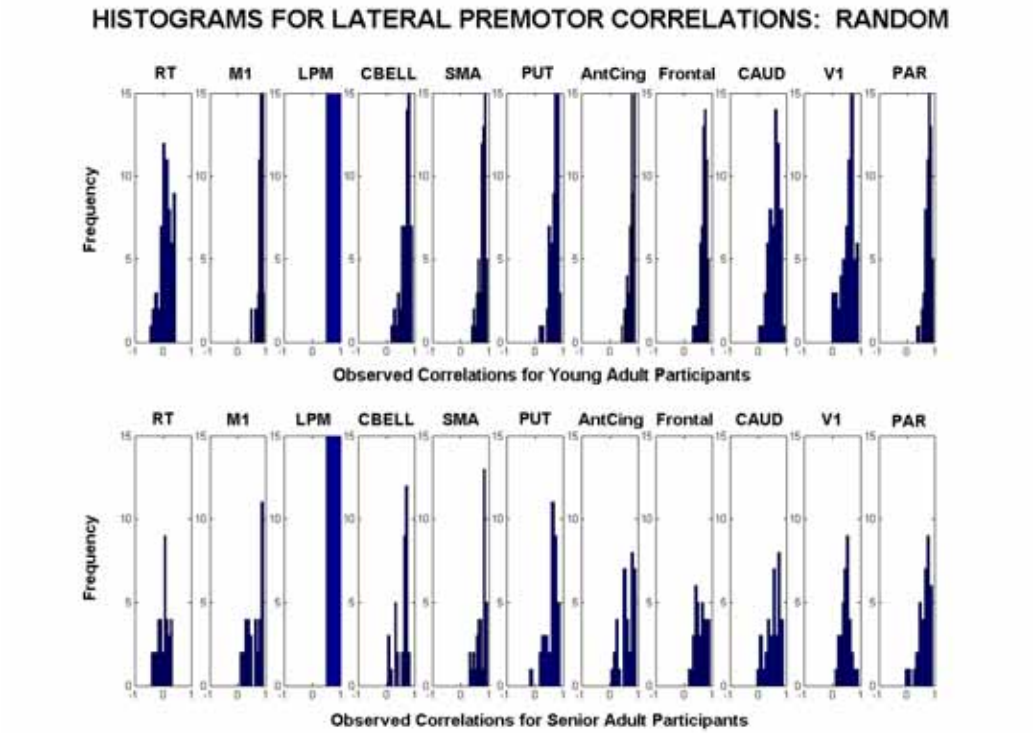


Figure C-3. Random Correlation Histograms by Age: Lateral Premotor

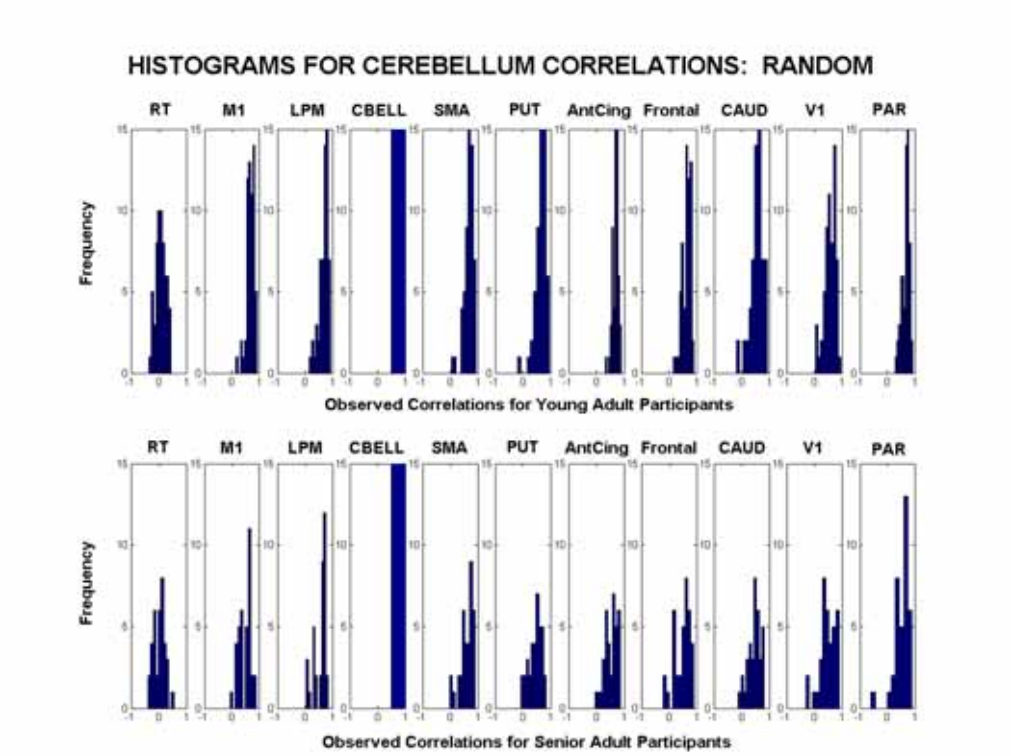


Figure C-4. Random Correlation Histograms by Age: Cerebellum

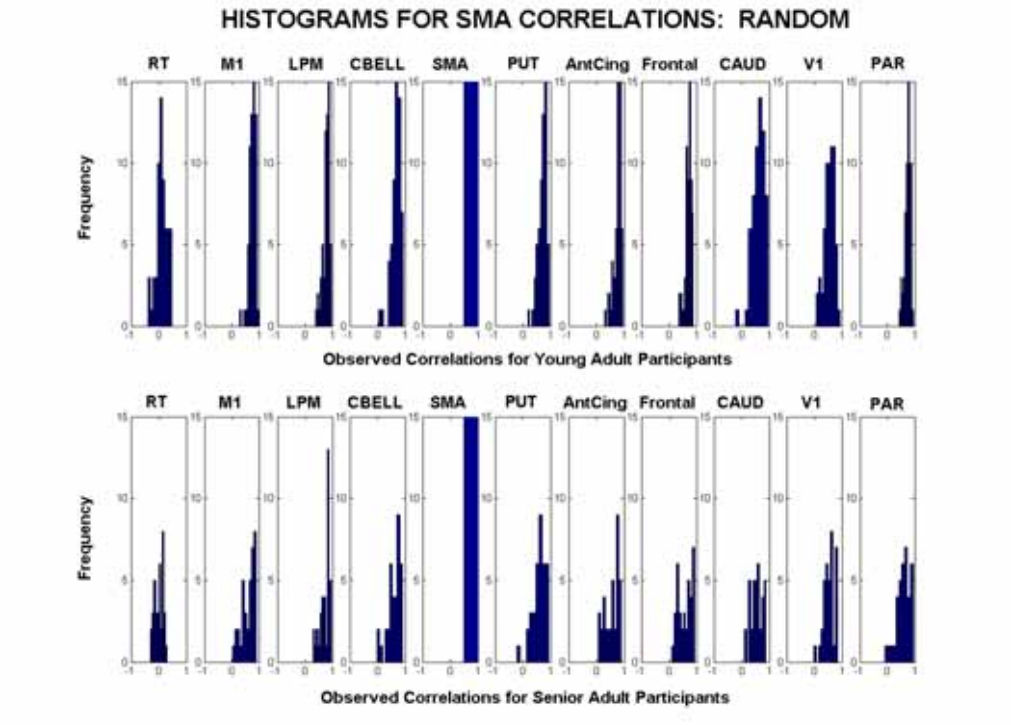


Figure C-5. Random Correlation Histograms by Age: SMA

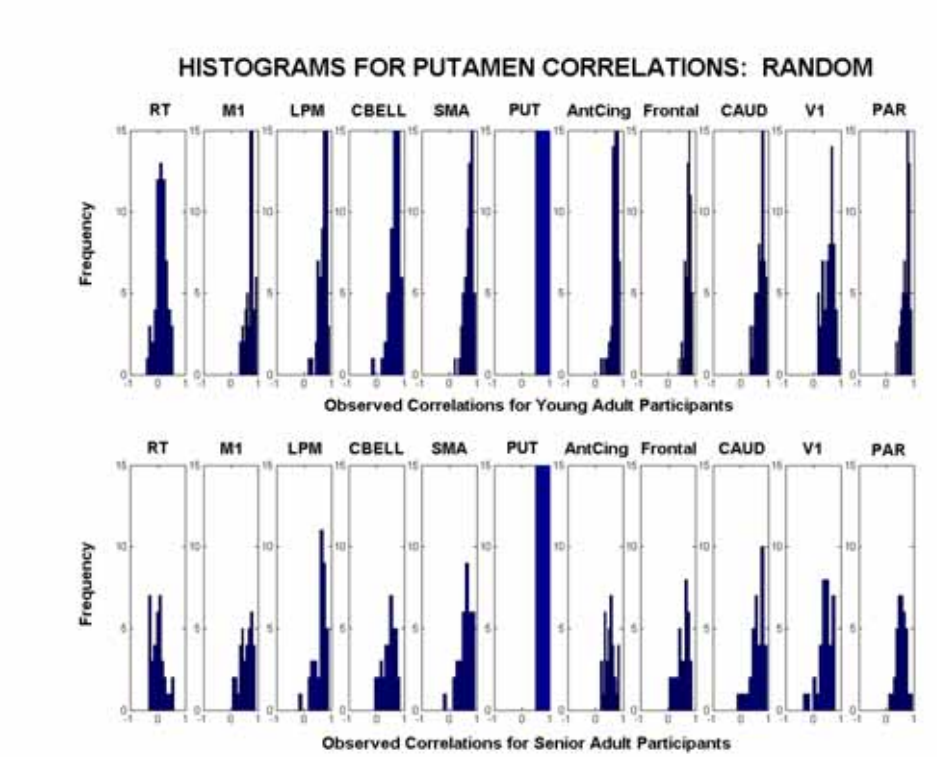


Figure C-6. Random Correlation Histograms by Age: Putamen

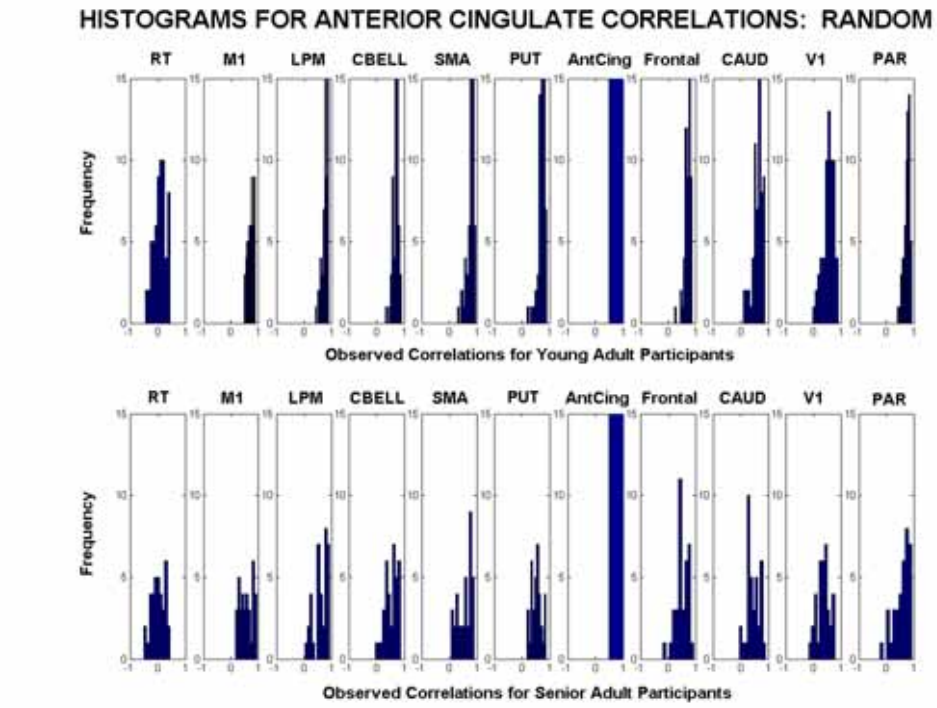


Figure C-7. Random Correlation Histograms by Age: Anterior Cingulate

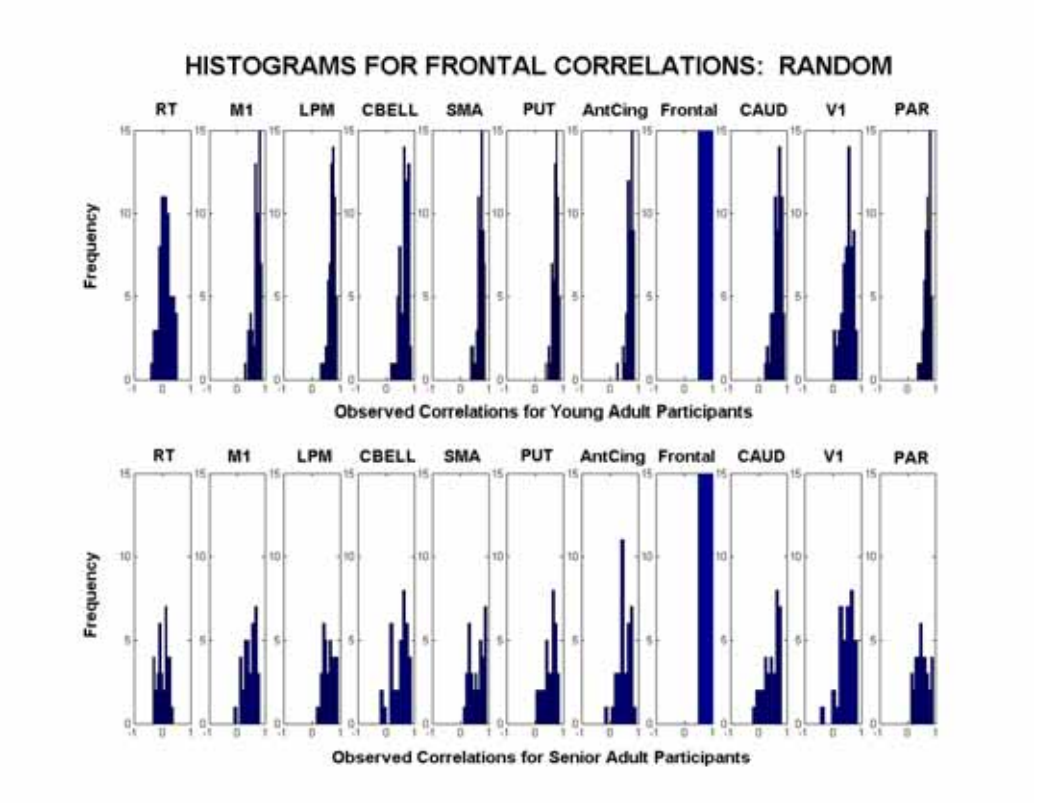


Figure C-8. Random Correlation Histograms by Age: Frontal

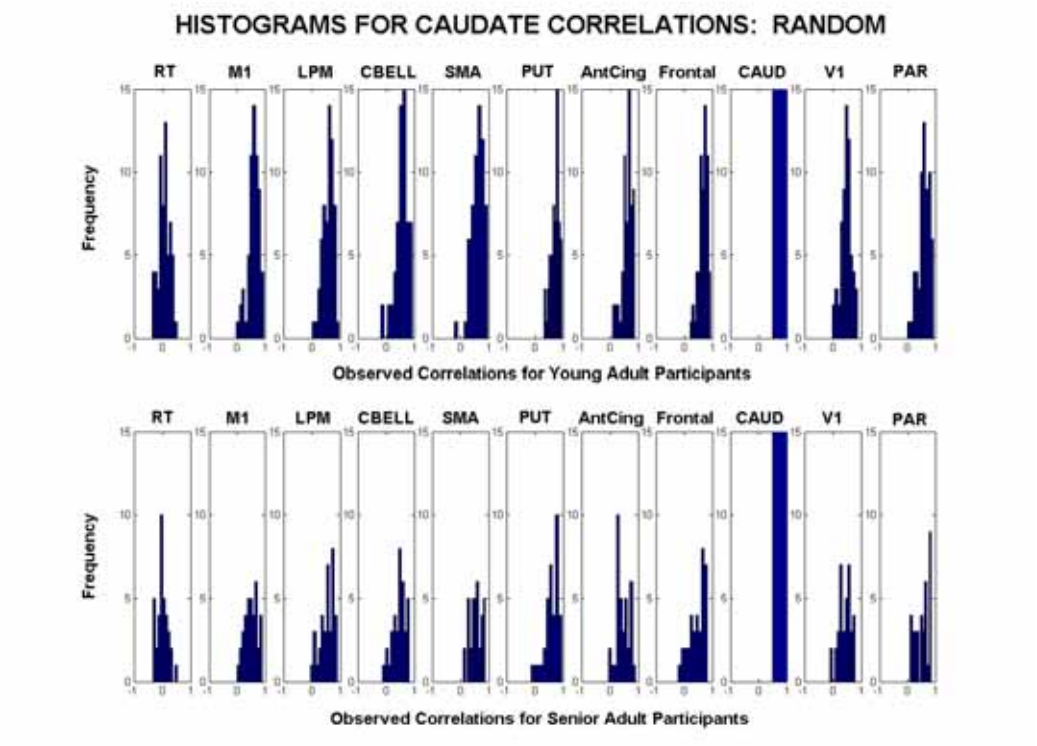


Figure C-9. Random Correlation Histograms by Age: Caudate

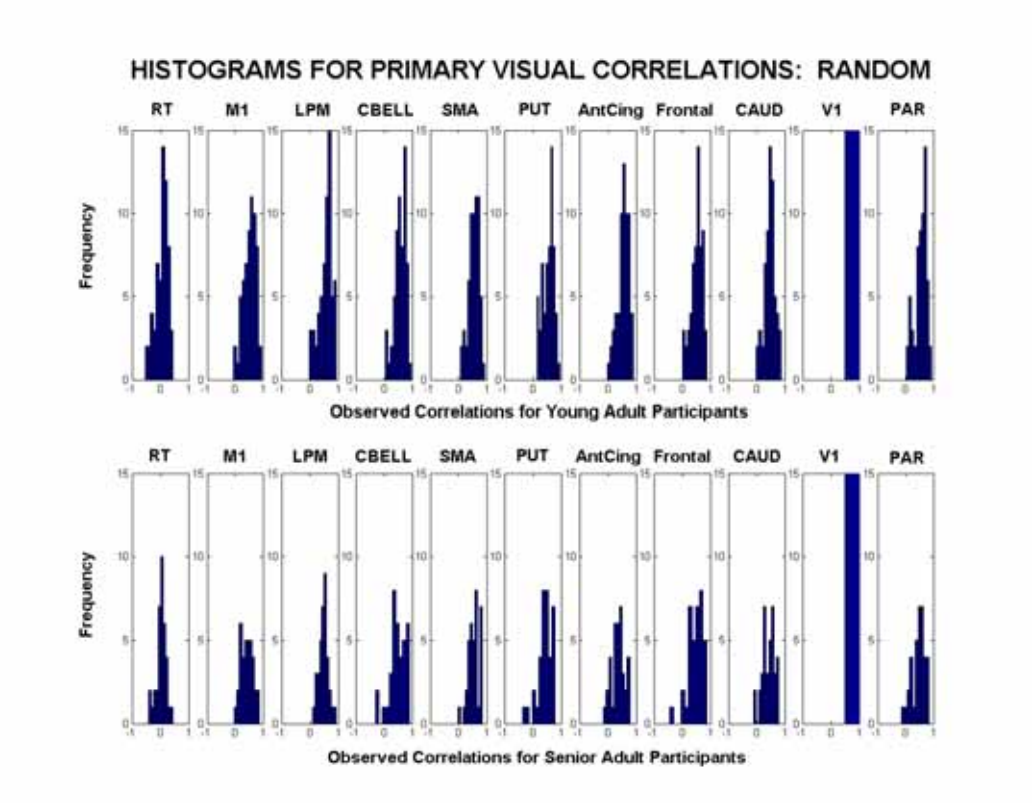


Figure C-10. Random Correlation Histograms by Age: Calcarine Fissure

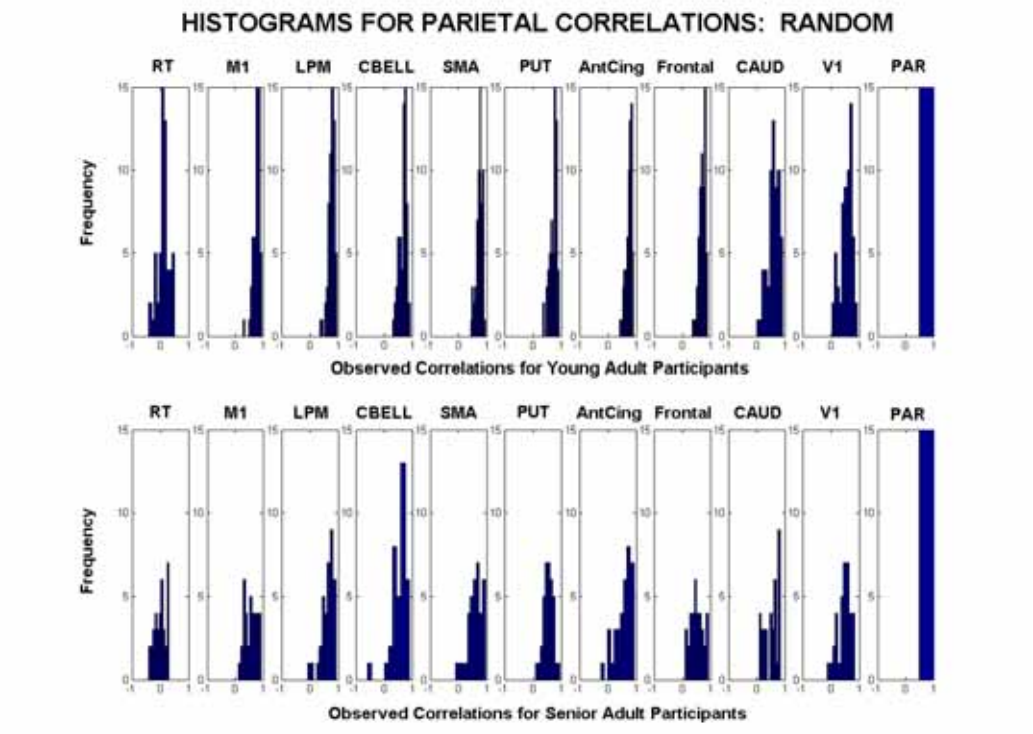


Figure C-11. Random Correlation Histograms by Age: Parietal

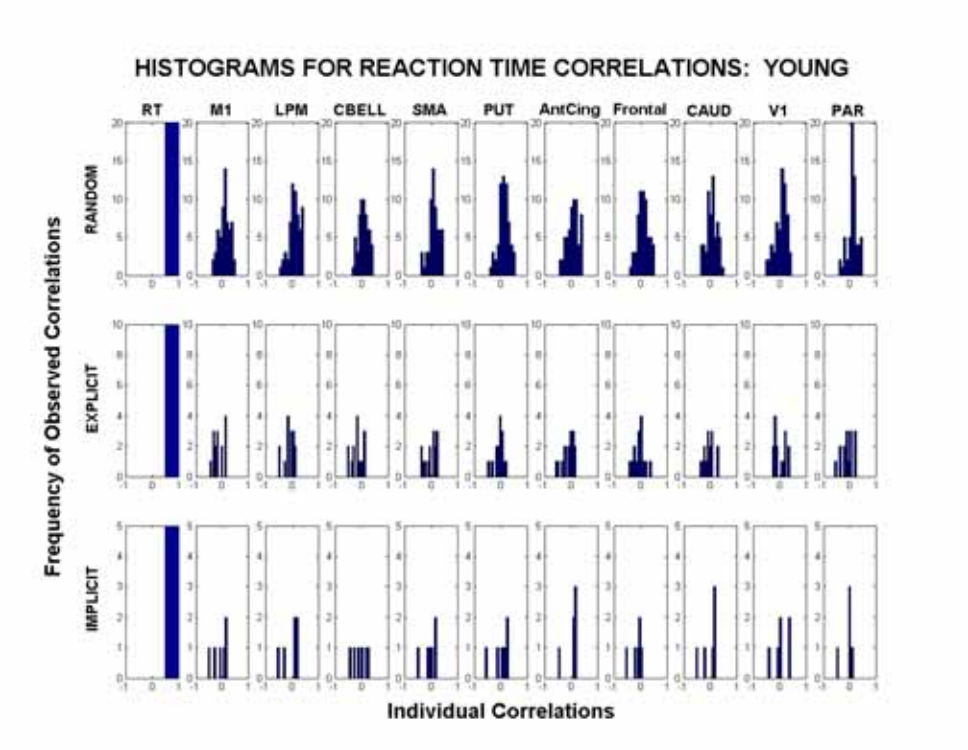


Figure C-12. Young Correlations by Learning Condition: Reaction Time

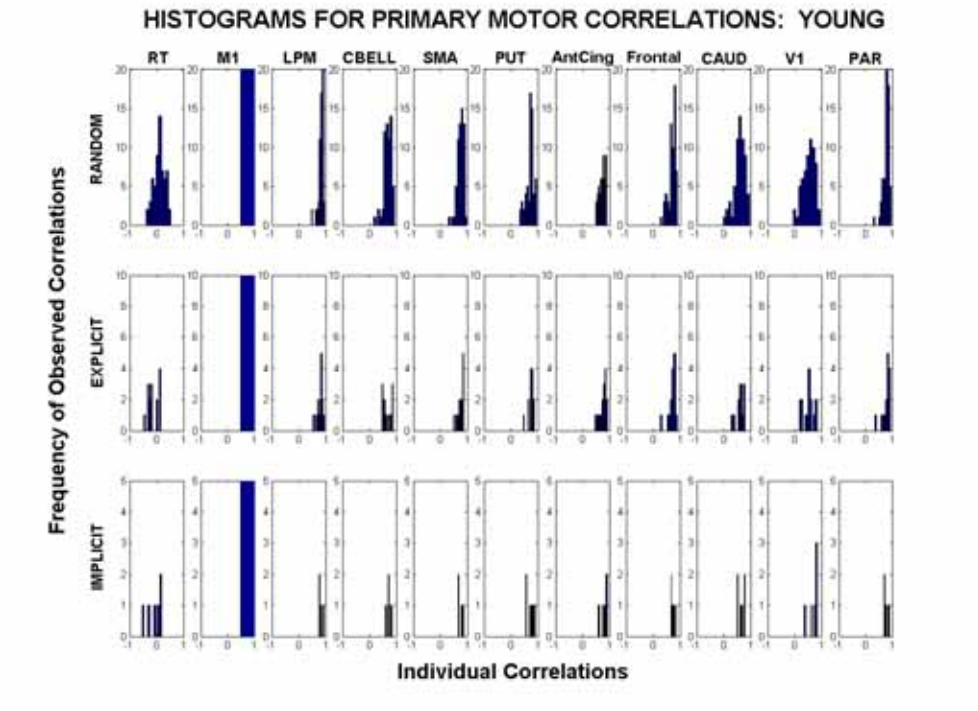


Figure C-13. Young Correlations by Learning Condition: Primary Motor

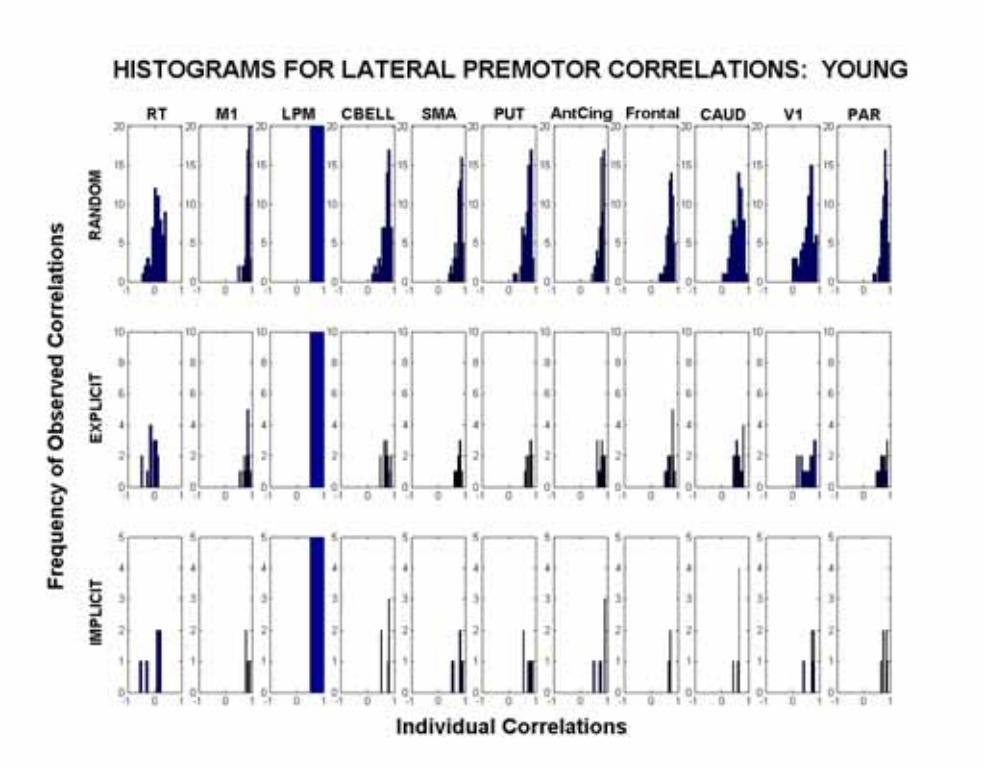


Figure C-14. Young Correlations by Learning Condition: Lateral Premotor

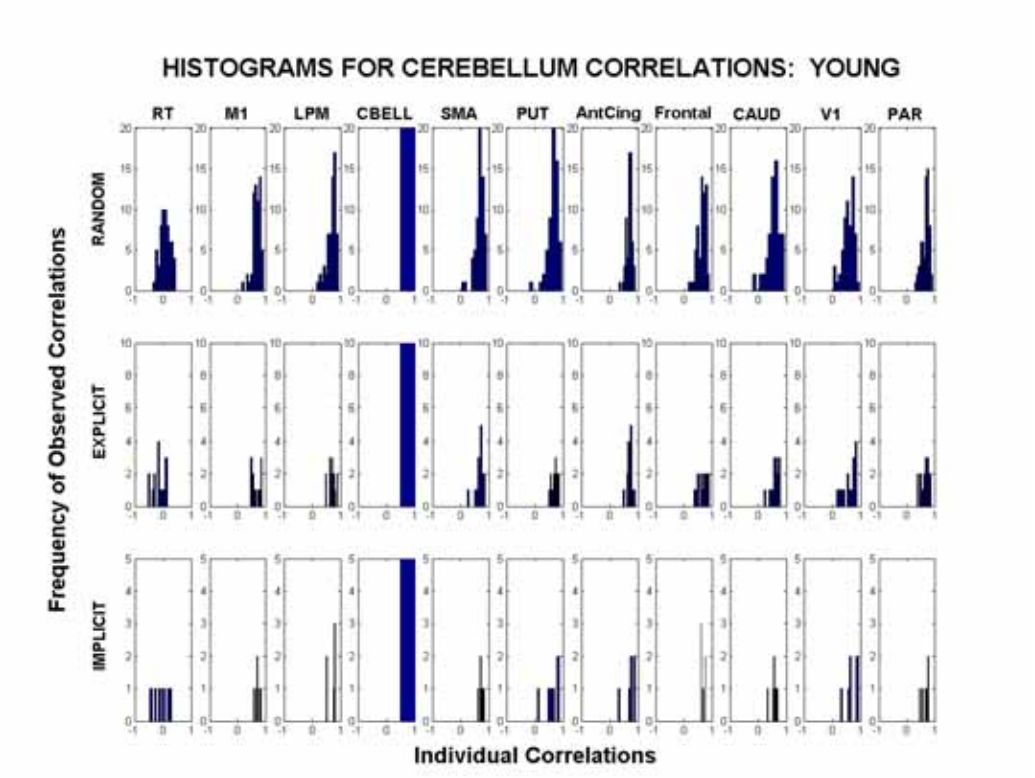


Figure C-15. Young Correlations by Learning Condition: Cerebellum

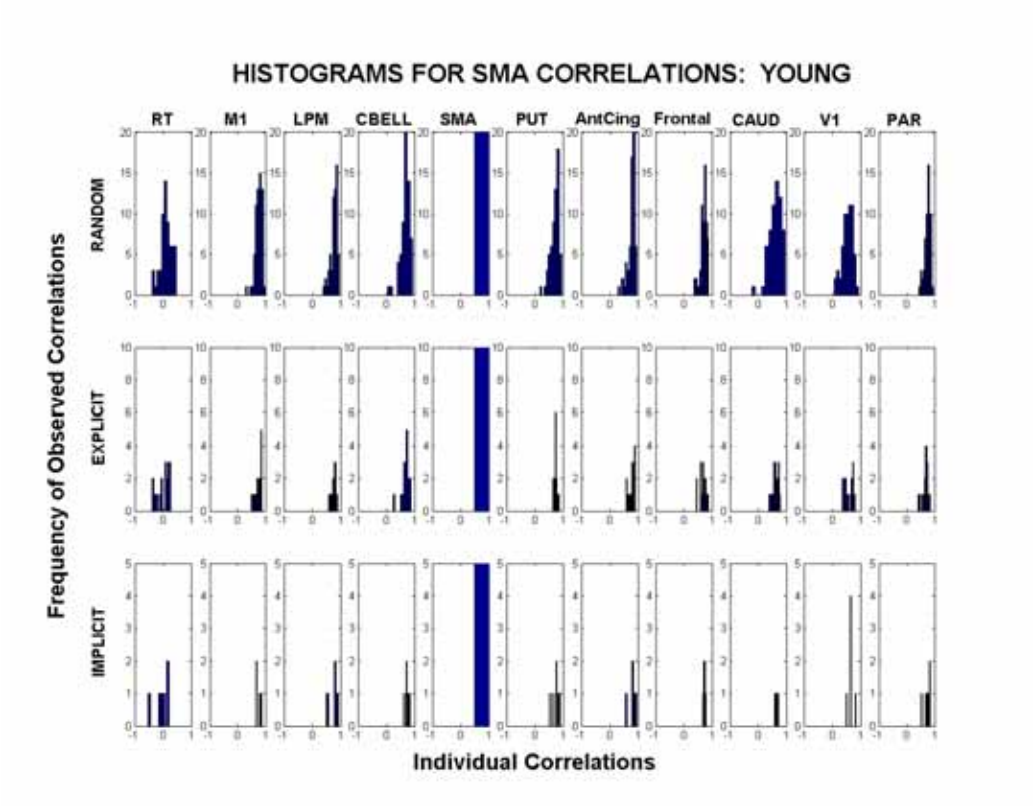


Figure C-16. Young Correlations by Learning Condition: SMA

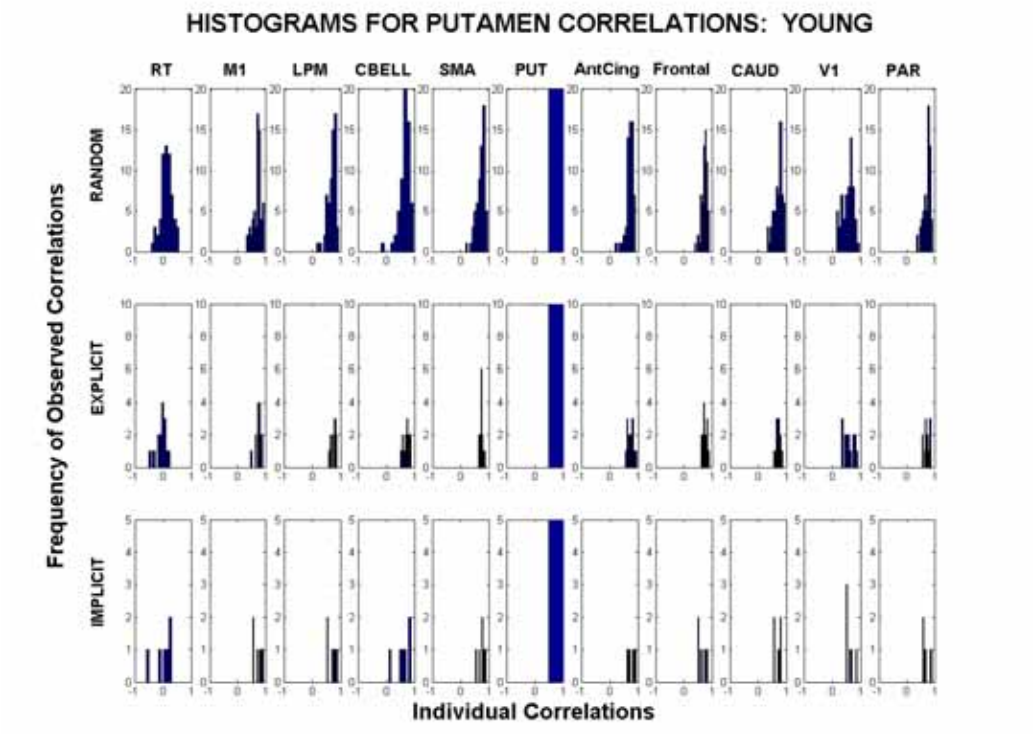


Figure C-17. Young Correlations by Learning Condition: Putamen

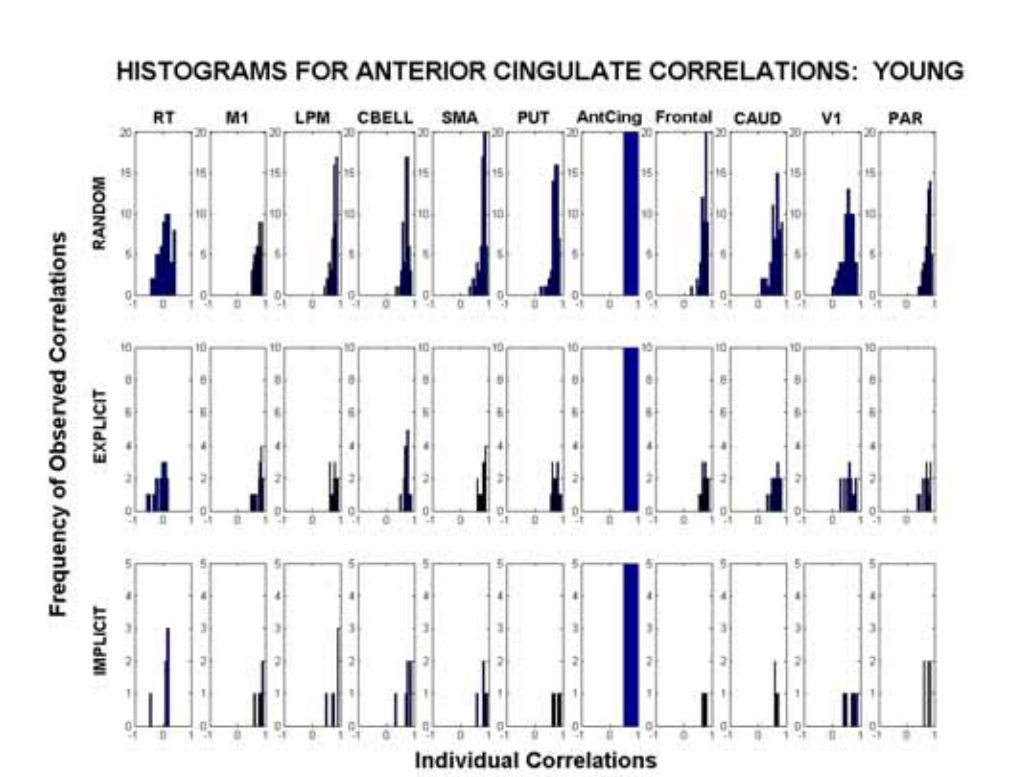


Figure C-18. Young Correlations by Learning Condition: Anterior Cingulate

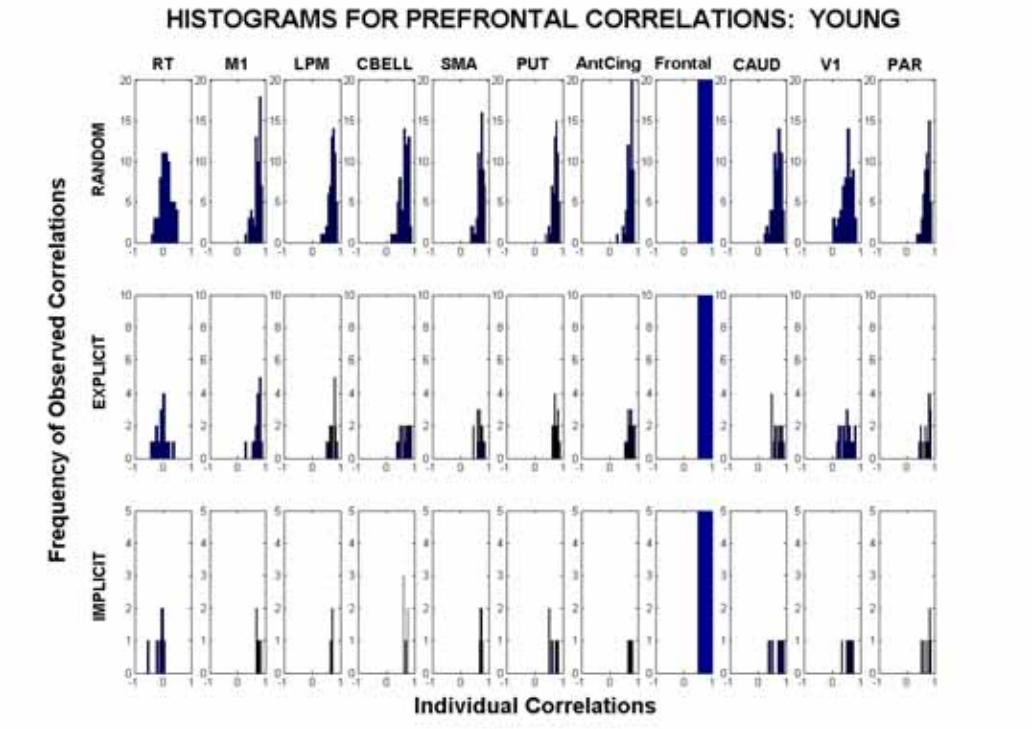


Figure C-19. Young Correlations by Learning Condition: Prefrontal

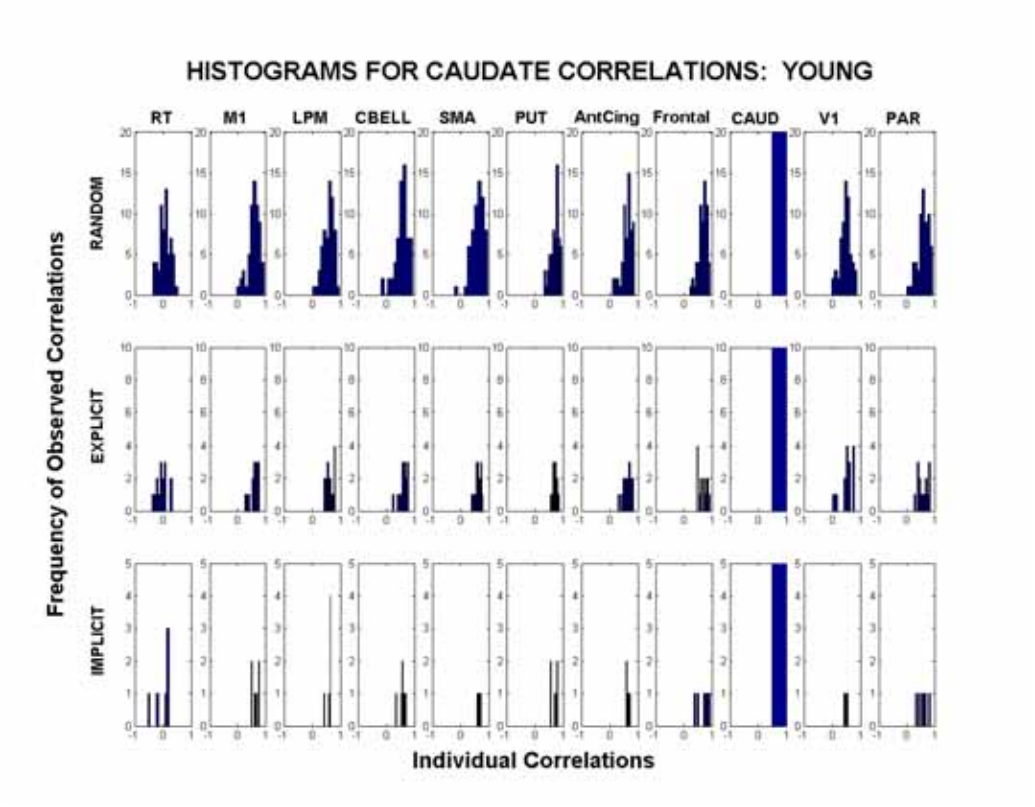


Figure C-20. Young Correlations by Learning Condition: Caudate

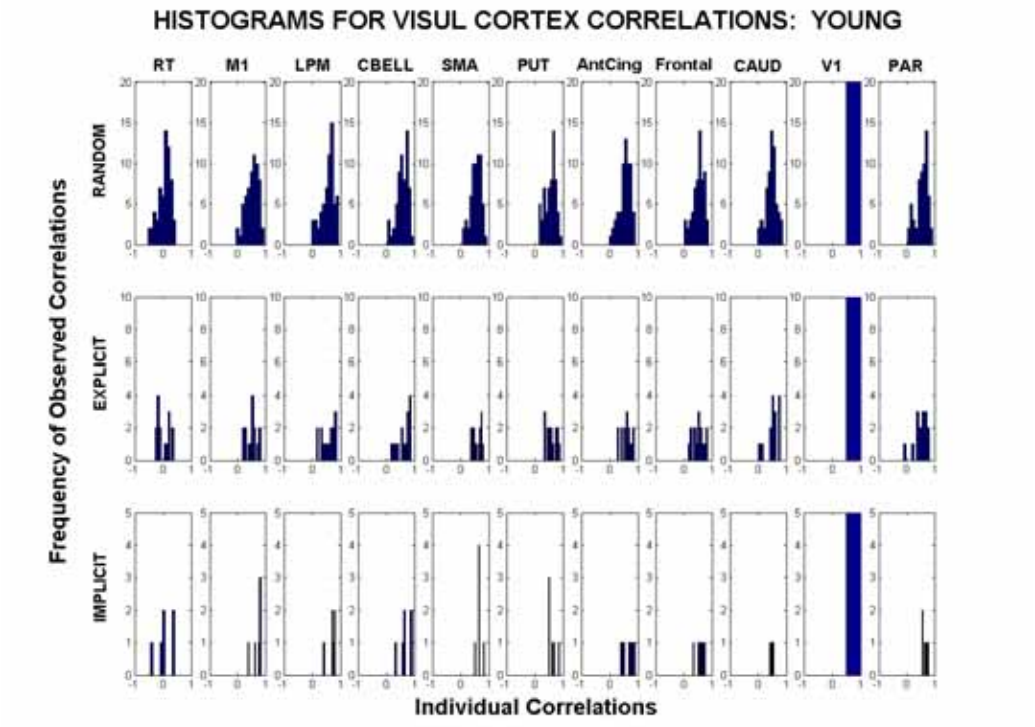


Figure C-21. Young Correlations by Learning Condition: Calcarine Fissure

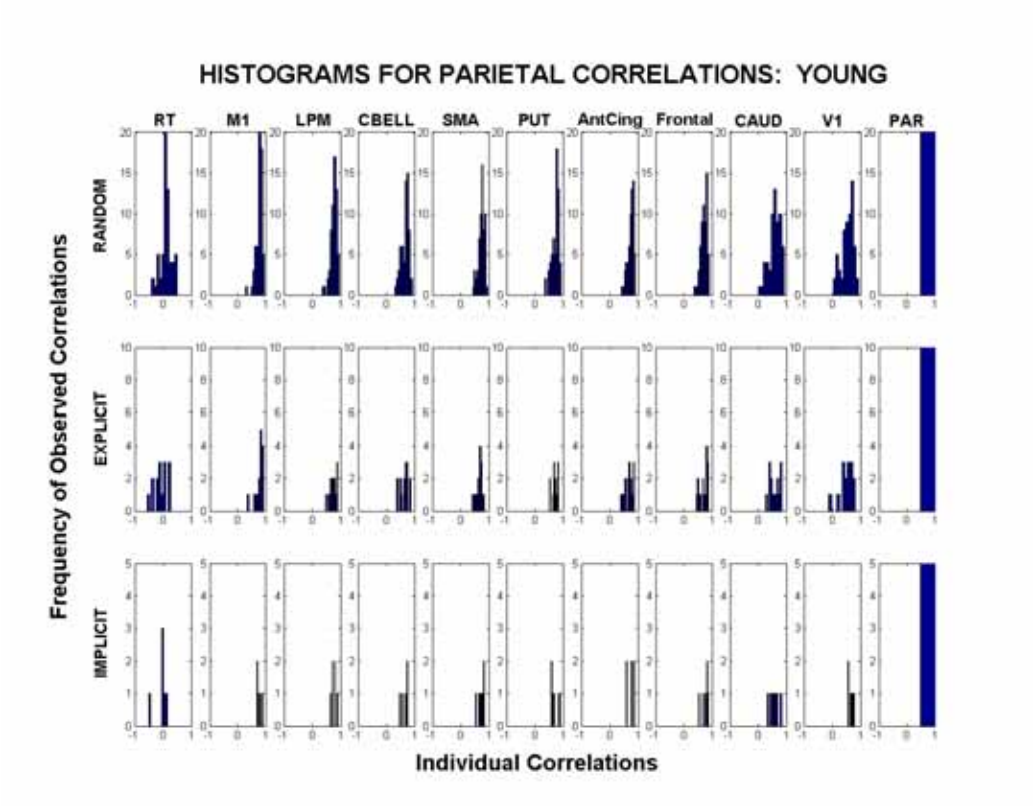


Figure C-22. Young Correlations by Learning Condition: Parietal

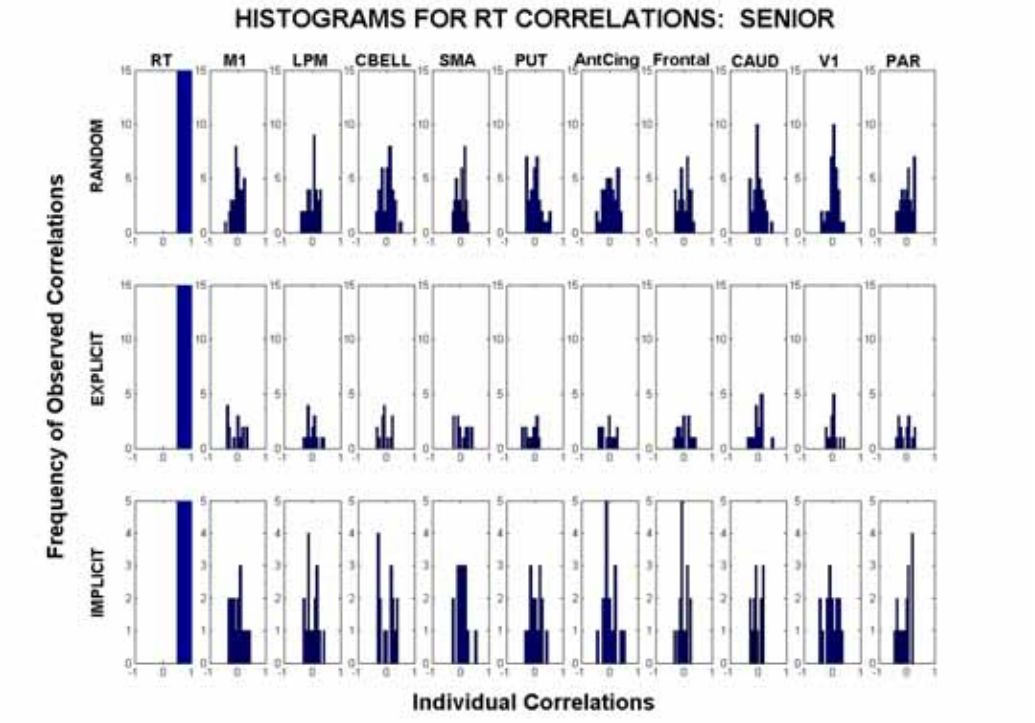


Figure C-23. Senior Correlations by Learning Condition: Reaction Time

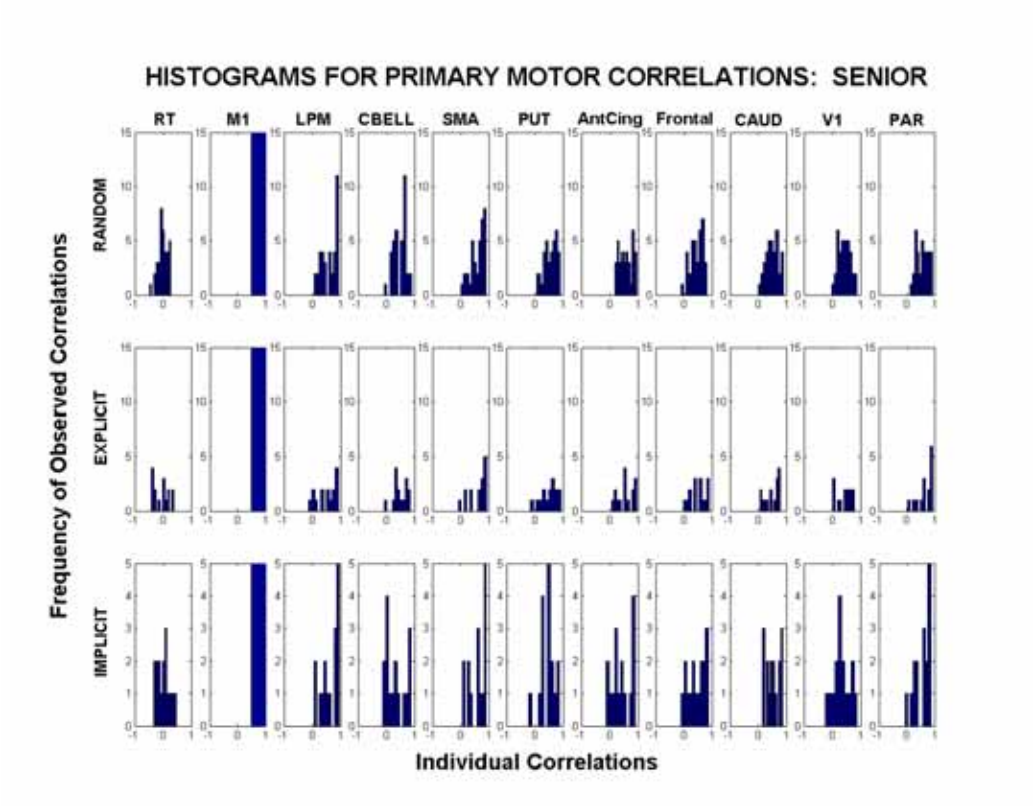


Figure C-24. Senior Correlations by Learning Condition: Primary Motor

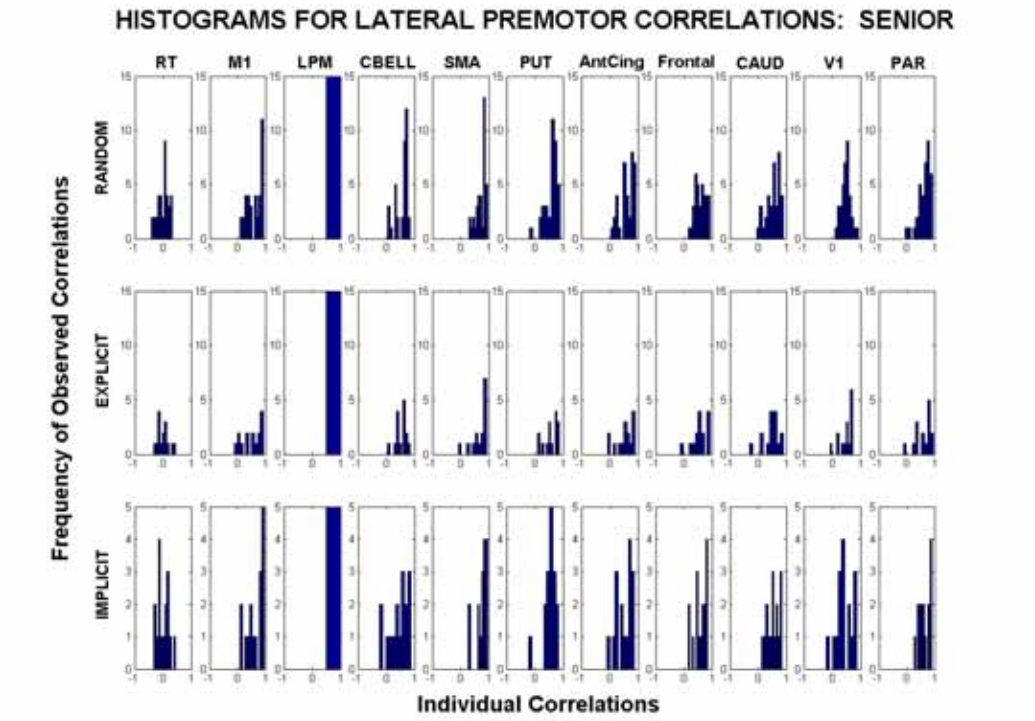


Figure C-25. Senior Correlations by Learning Condition: Lateral Premotor

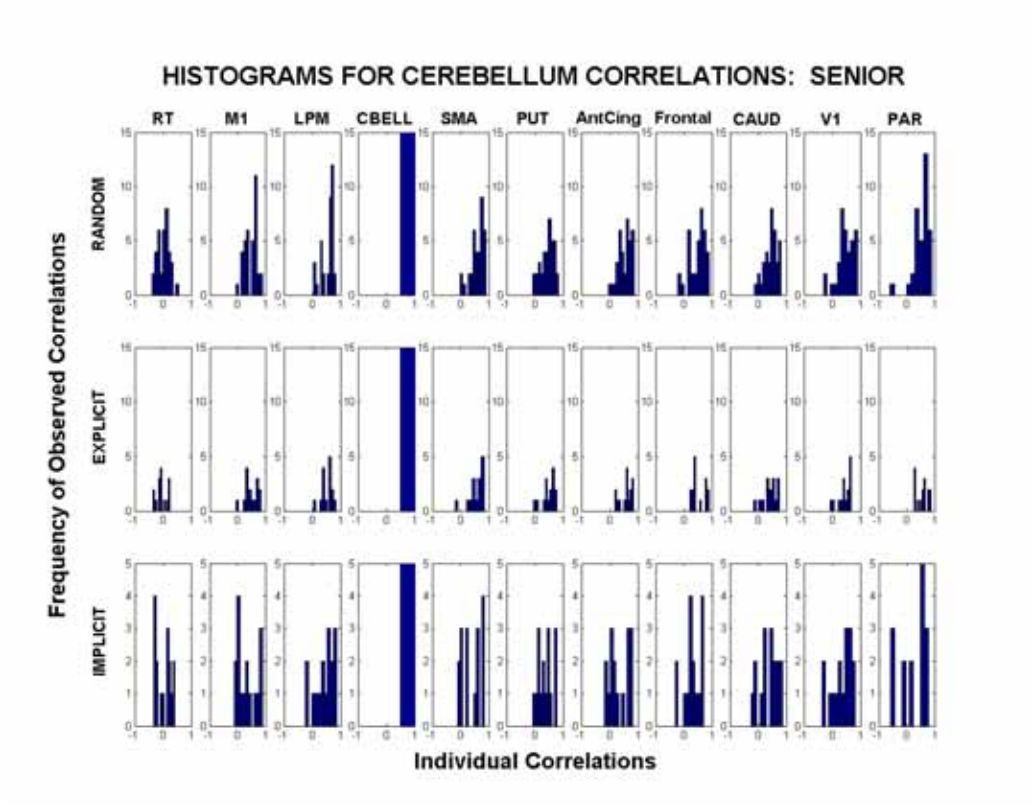


Figure C-26. Senior Correlations by Learning Condition: Cerebellum

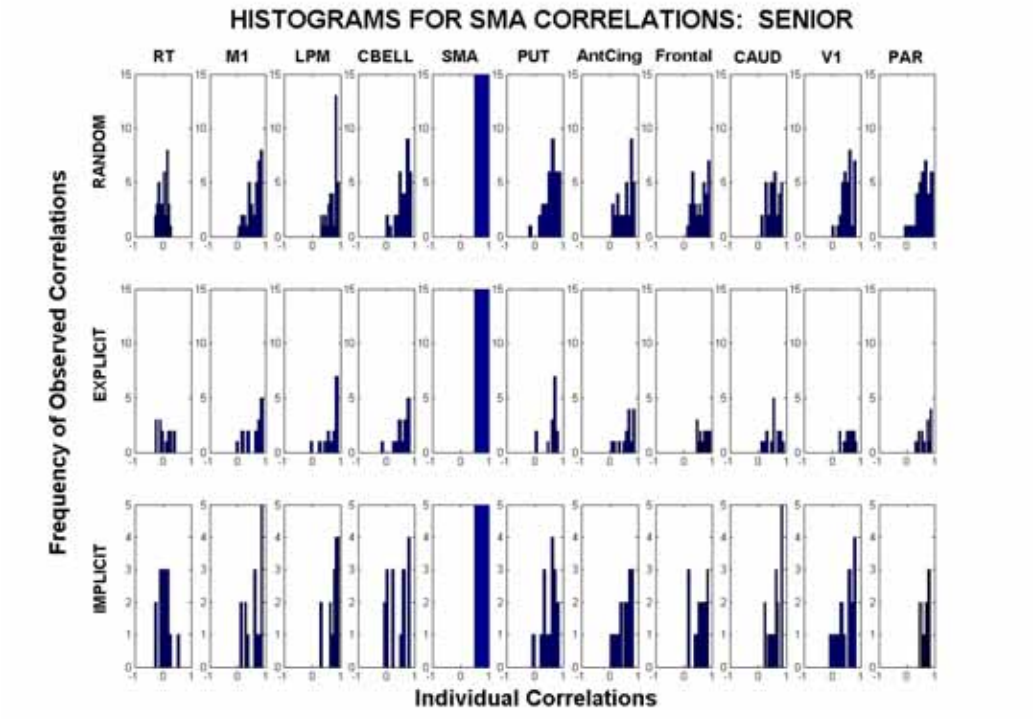


Figure C-27. Senior Correlations by Learning Condition: SMA

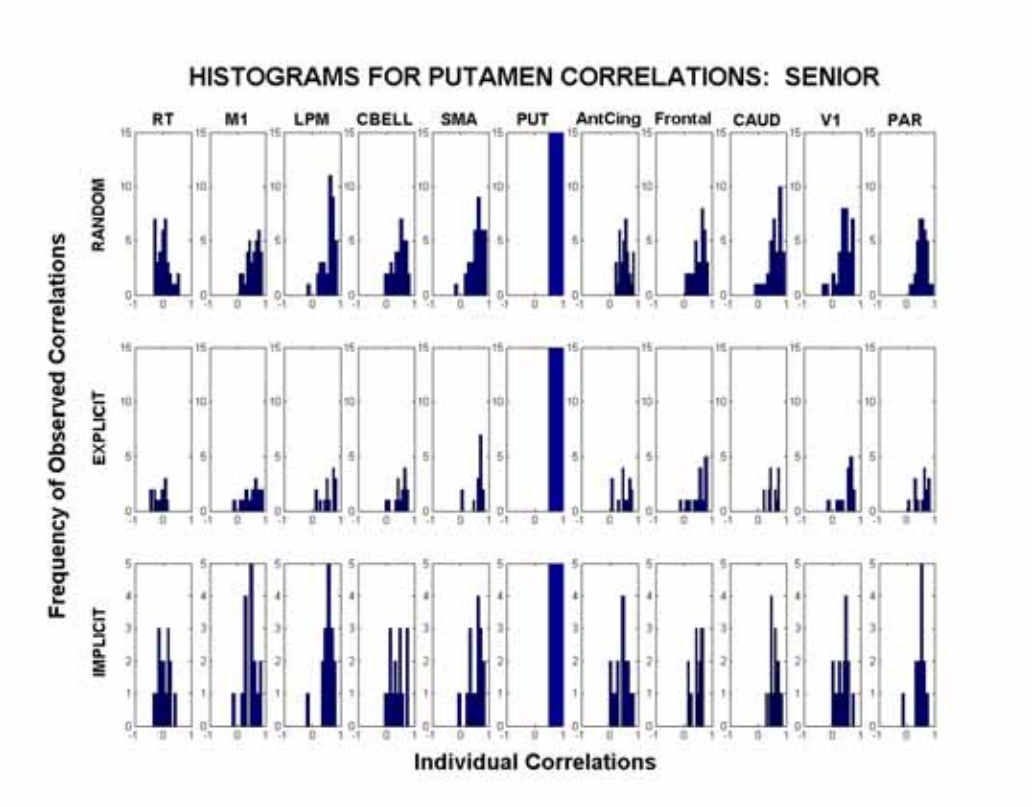


Figure C-28. Senior Correlations by Learning Condition: Putamen

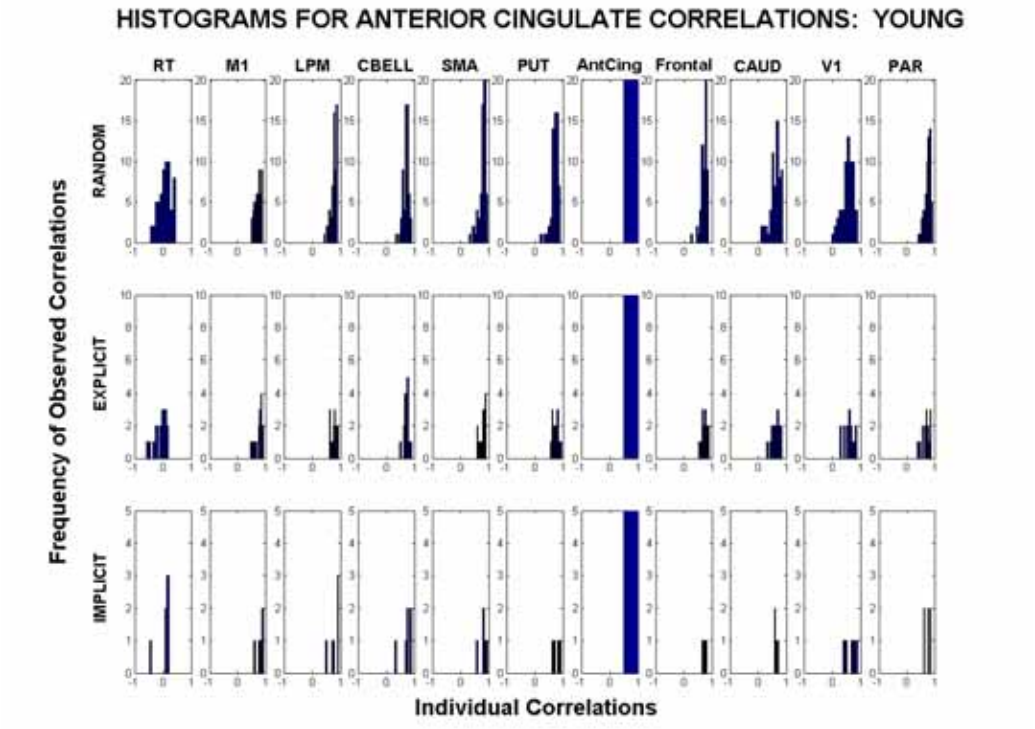


Figure C-29. Senior Correlations by Learning Condition: Anterior Cingulate

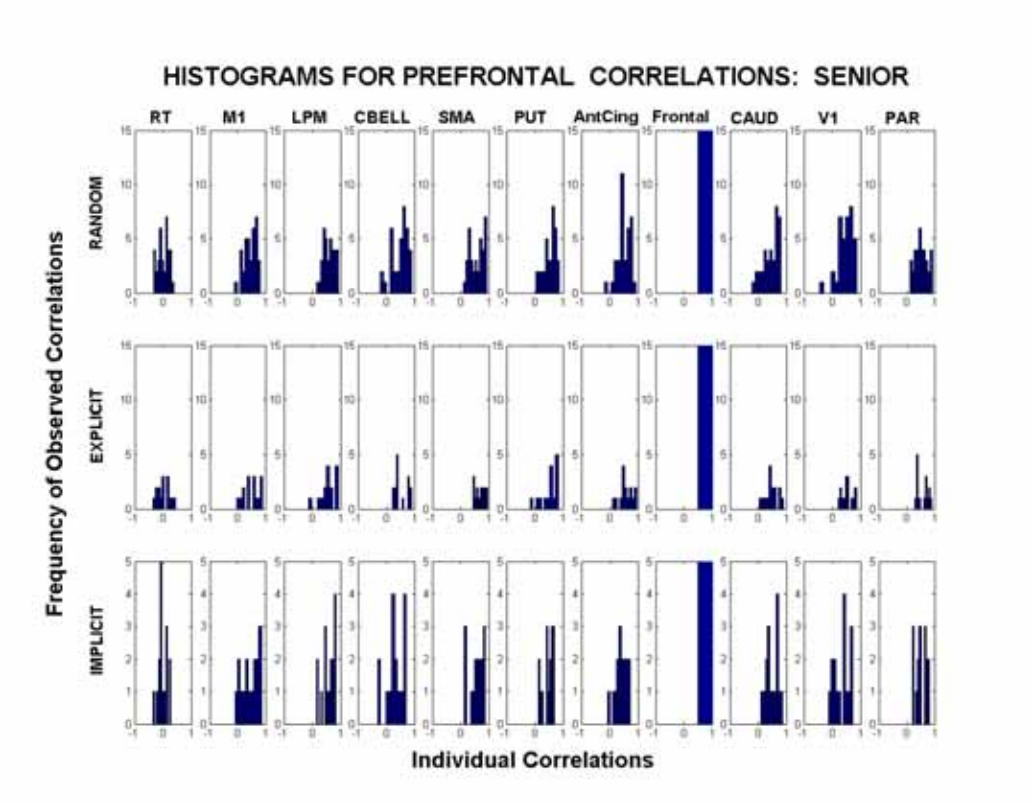


Figure C-30. Senior Correlations by Learning Condition: Prefrontal

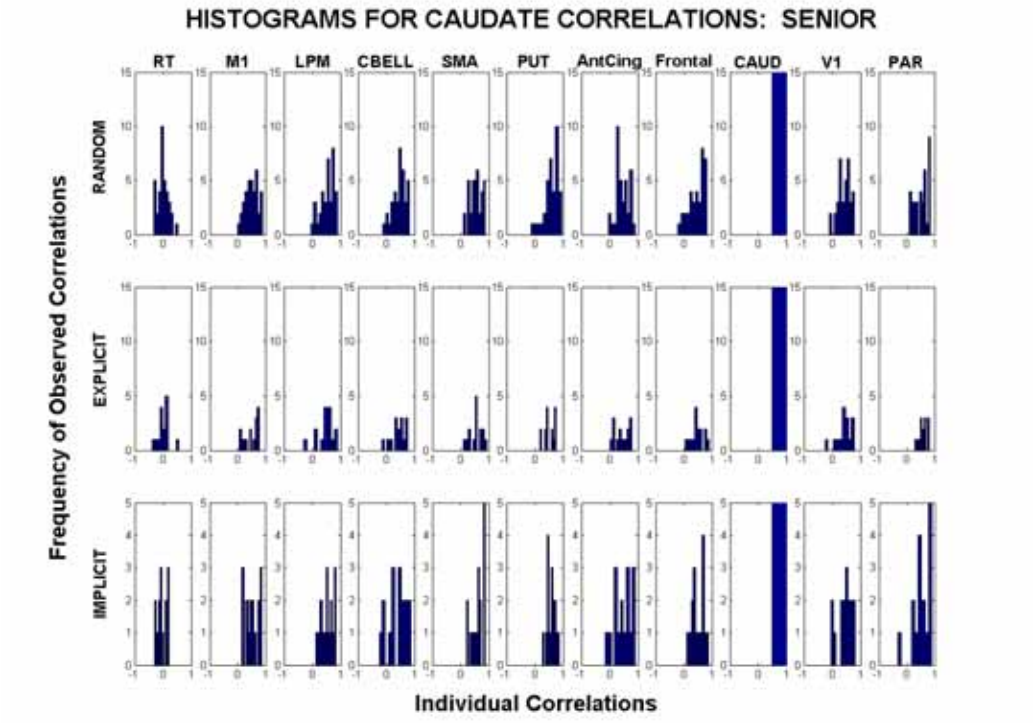


Figure C-31. Senior Correlations by Learning Condition: Caudate

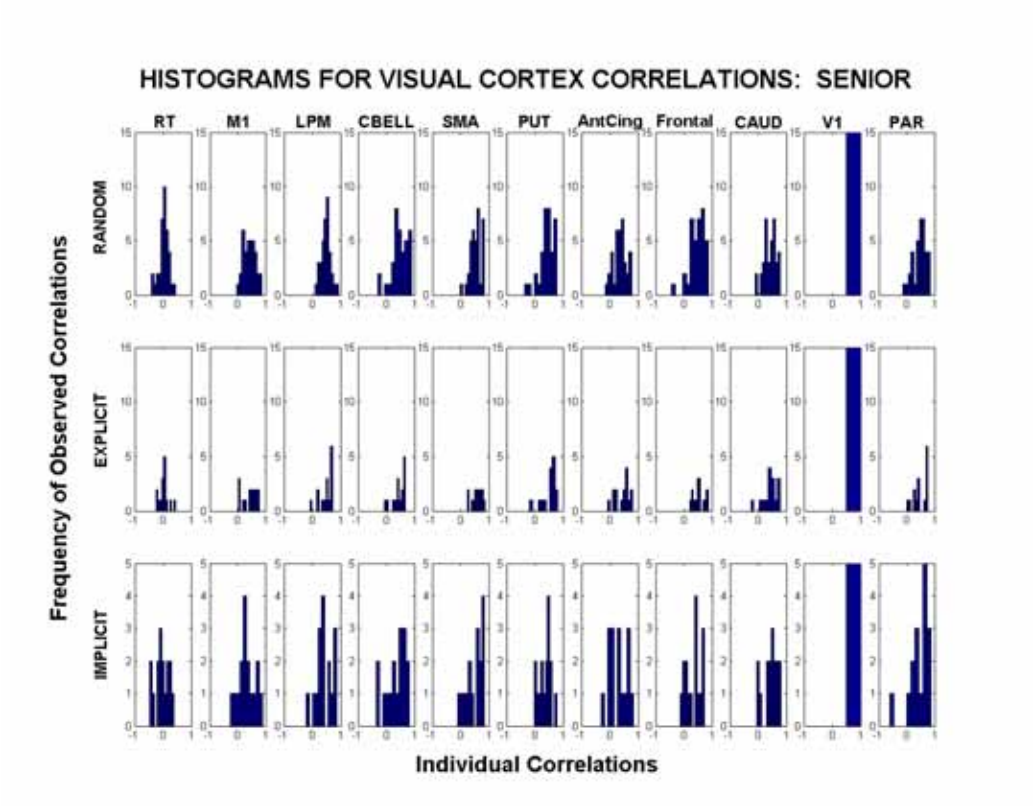


Figure C-32. Senior Correlations by Learning Condition: Calcarine Fissure

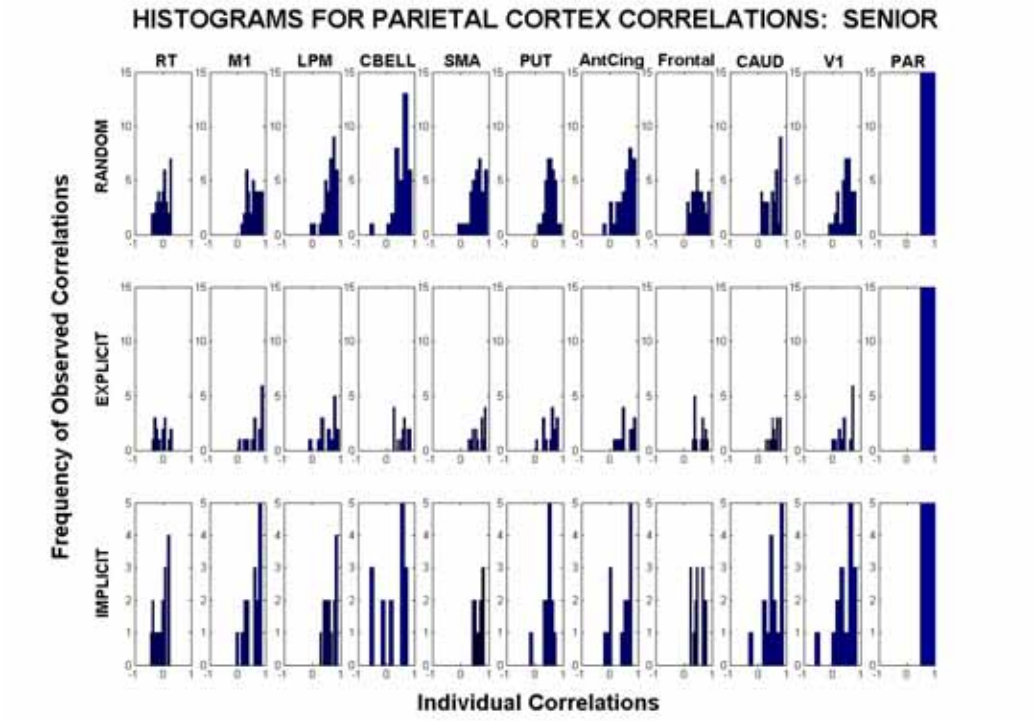


Figure C-33. Senior Correlations by Learning Condition: Parietal Cortex

REFERENCES

Ackerman, P. L., & Cianciolo, A. T. (2000). Cognitive, perceptual-speed, and psychomotor determinants of individual differences during skill acquisition. Journal of Experimental Psychology: Applied, 6, 259-290.

Ackerman, P. L., Kyllonen, P. C., & Roberts, R. D. (1999). Learning and individual differences: Process, trait, and content determinants. American Psychological Association.

Aizenstein, H. J., Nebes, R. D., Meltzer, C. C., Fukui, M. B., Williams, R. L., Saxton, J., Houck, P. R., Carter, C. S., Reynolds, C. F. & DeKosky, S. T. (2002). The relation of white matter hyperintensities to implicit learning in healthy older adults. International Journal of Geriatric Psychiatry, 17, 664-669.

Alexander, G. E., & Crutcher, M. D. (1990). Preparation for movement: Neural representations of intended direction in three motor areas of the monkey. Journal of Neurophysiology, 64, 133-150.

Amos, A. (2000). A computational model of information processing in the frontal cortex and basal ganglia. Journal of Cognitive Neuroscience, 12, 505-519.

Andersen, B. B., Gundersen, H. J., & Pakkenberg, B. (2003). Aging of the human cerebellum: a stereological study. Journal of Comparative Neuroscience, 466, 356-365.

Anderson, B., & Rutledge, V. (1996). Age and hemisphere effects on dendritic strucure. Brain, 119, 1983-1990.

Awad, I., Spetzler, R., Hodak, J., Awad, C. A., & Carey, R. (1986). Incidental subcortical lesions identified on magnetic resonance imaging in the elderly. Correlation with age and cerebrovascular risk factors. Stroke, 17, 1084-1089.

Barbas, H. and Pandya, D. N. (1987). Architecture and frontal cortical connections of the premotor cortex (area 6) in the rhesus monkey. Journal of Comparative Neurology, 286, 353-375.

Bartzokis, G., Beckson, M., Hance, D. B., Marx, P., Foster, J. A. and Marder, S. R. (1997). MR evaluation of age-related increase of brain iron in young adult and older normal males. Magnetic Resonance Imaging, 15, 29-35

Birren, J. E. & Schaie, K. W. (Eds.). (2001). Handbook on the Psychology of Agin. San Diego, California: Academic Press.

Biswal, B., Yetkin, F. Z., Haughton, V. M. and Hyde, J. S. (1995). Functional connectivity in the motor cortex of resting human brain using echo-planar MRI. Magnetic Resonance in Medicine, 30, 161-173.

Brodmann, K. (1909). Vergleichende Lokalisationslehre der Grohirnrinde in Ihren Prinzipien Dargestellt auf Grund des Zellenbaues. Barth, Leipzig. [English translation: Garey, L.J. 1994. Brodmann's Localisation in the Cerebral Cortex. Smith-Gordon, London.]

Blood, A. J. & Zatorre, R. J. (2001). Intensely pleasurable responses to music correlate with activity in brain regions implicated in reward and emotion. Proceedings of the National Academy of Science, 98, 11818-11823.

Brown, J. W. (1972). Aphasia, apraxia, and agnosia. Clinical and theoretical aspects. Springfield, Illinois: Charles C. Thomas.

Buckner, R. L., Snyder, A. Z., Sanders, A. L., Raichle, M. E. and Morris, H. C. (2000). Functional brain imaging of young, nondemented, and demented older adults. Journal of Cognitive Neuroscience, Supplement 2, 24-34.

Buchsbaum, B. R., Greer, S., Chang, W. L., & Berman, K. F. (2005). Meta-analysis of neuroimaging studies of the Wisconsin card-sorting task and component processes. Human Brain Mapping, 25, 35-45.

Cabeza, R. (2002). Hemispheric asymmetry reduction in older adults: the HAROLD model. Psychology and Aging, 17, 85-100.

Cabeza, R. and Nyberg, L. (2000). Imaging cognition II: an empirical review of 275 PET and fMRI studies. Journal of Cognitive Neuroscience, 12(1), 1-47.

Cajade-Law, A., Cohen, H., Heier, L. (1993). Vascular causes of white matter disease. Neuroimaging Clinics of North America, 3, 361-378.

Carter, C. S., MacDonald, A. W. III, Ross, L. L., & Stenger, V. A. (2001). Anterior cingulate cortex activity and impaired self-monitoring of performance nn patients with schizophrenia: an event-related fMRI study. The American Journal of Psychiatry, 158, 1423-1428.

Chimowitz, M. I., Awad, I. A. and Furlan, A. H. (1989). Periventricular lesions of MRI. Facts and theories. Current Concepts of Cerebrovascular Disease and Stroke, 24, 7-12.

Coffey, C. E., Wilkinson, W. E., Parashos, I. A. *et al.* (1992). Quantitative cerebral anatomy of the aging human brain: A cross-sectional study using magnetic resonance imaging. Neurology, 42, 527-536.

Creasey, H. and Rapoport, S. I. (1985). The aging human brain. Annuals of Neurology, 17, 2-10.

Damasio, H., Grabowski, T., Frank, R., Galaburda, A. M., & Damasio, A. R. (1994). The return of Phineas Gage: clues about the brainf rom the skull of a famous patient. Science, 256, 1159.

Deiber, M.-P., Passingham, R. E., Colebatch, J. G., Friston, K. J., Nixon, P. D. and Frackowiak, R. S. J. (1991). Cortical areas and the selection of movement: a study with positron emission tomography. Experimental Brain Research, 84, 393-402.

Dolcos, F., Rice, H. J., & Cabeza, R. (2002). Hemispheric asymmetry and aging: right hemisphere decline or asymmetry reduction. Neuroscience and Biobehavioral Reviews, 26, 819-825.

Dum, R. P. and Strick, P. L. (1991). The origin of corticospinal projections from the premotor areas in the frontal lobe. Journal of Neuroscience, 11, 667-689.

Erdler, M., Windischberger, C., Lanzenberger, R., Edward, V., Gartus, A., Deeckle, L. and Beisteiner, R. (2001). Dissociation of supplementary motor area and primary motor cortex in human subjects when comparing index and little finger movements with functional magnetic resonance imaging. Neuroscience Letters, 313, 5-8.

Esri, M. M., Hyman, B. T., Beyreuther, K. (1997). Ageing and the dementias. *In* Graham, D.L. and Lantos, P.L. (eds): Greenfield's Neuropathology, ed 6. New York, Oxfort University Press, vol 1, pp 153-233.

Feeney, J. J., Howard, J. H. J., & Howard, D. V. (2002). Implicit learning of higher order sequences in middle age. Psychology & Aging, 17, 351-355.

Frensch, P. A., & Miner, C. S. (1994). Effects of presentation rate and individual differences in short-term memory capacity on an indirect measure of serial learning. Memory & Cognition, 22, 95-110.

Frensch, P. A., & Miner, C. S. (1995). The role of working memory in implicit sequence learning. Journal for Experimental Psychology, 42, 545-575.

Friston, K. J., Holmes, A. P., Poline, J. B., Grasby, P. J., Williams, S. C., Frackowiak, R.S., & Turner, R. (1995). Analysis of fMRI time-series revisited. Neuroimage, 2, 45-53.

Gado, M., Hughes, C. P., Dnazinger, W. (1982). Volumetric measurements of the cerebrospinal fluid spaces in demented subjects and controls. Radiology, 144, 535-538.

Ge, Y., Grossman, R. I., Babb, J. S., Rabin, M. L., Mannon, L. J. and Kolson, D. L. (2002). Age-Related Total Gray Matter and White Matter Changes in Normal Adult Brain. Part I: Volumetric MR Imaging Analysis. American Journal of Neuroradiology, 23, 1327-1333.

Geshwind, N. (1965). Disconnexion syndromes in animals and man. I. Brain, 88, 237-294.

Goldman-Rakic, P. S., Selemon, L. D., & Schwartz, M. L. (1984). Dual pathways connecting the dorsolateral prefrontal cortex with the hippocampal formation and parahippocampal cortex in the rhesus monkey. Neuroscience, 12, 719-743.

Gordon, A. M., Lee, J.-H., Flament, D., Ugurbil, K. and Ebner, T. J. (1998). Functional magnetic resonance imaging of motor, sensory, and posterior parietal cortical areas during performance of sequential typing movements. Experimental Brain Research, 121, 153-166.

Grafton, S. T., Hazeltine, E. and Ivry, R. (1995). Functional mapping of sequence learning in normal humans. Journal of Cognitive Neuroscience, 7, 497-510.

Graybiel, A. M. (1990). Neurotransmitters and neuromodulators in the basal ganglia. Trends in Neuroscience, 13, 244-254.

Hallet, M. and Massquoi, S. G. (1993). Physiologic studies of dysmetria in patients with cerebellar deficits. Canadian Journal of Neurological Science, Supplement 3, S83-92.

Halsband, U. and Passingham, R. E. (1985). Premotor cortex and the conditions for movement in monkeys (*Macaca mulatta*). Behavioral Brain Research, 18, 269-276.

Harrington, D. L, & Haaland, K. Y. (1991). Sequencing in Parkinson's disease: Abnormalities in programming and controlling movement. Brain, 114, 99-115.

Harrington, D. L, & Haaland, K. Y. (1998). Temporal processing in the basal ganglia. Neuropsychology, 12, 3-12.

Hazeltine, E., Grafton, S. T. and Ivry, R. (1997). Attention and stimulus characteristics determined the locus of motor sequence encoding: A PET study. Brain, 120, 123-140.

He, G., Mao, J., Perry, A. S., Gao, J.-H., Fox, P. T. and Liu, Y. (2001). The temporal constancy of resting brain activity implicated in fMRI studies. Proceedings of the International Society for Magnetic Resonance in Medicine.

He, G., Tan, L.-H., Tang, Y., James, G. A., Wright, P., Eckert, M., Fox, P. T. & Liu, Y. (2003). Modulation of neural connectivity during tongue movement and Chinese "pin-yin" speech. Human Brain Mapping, 18, 222-232.

Hesselmann, V., Zaro, W. O., Wedekind, C., Krings, T., Schulte, O., Kugel, H., Krug, B., Klug, N. and Lackner, K. J. (2001). Age related signal decrease in functional magnetic resonance imaging during motor stimulation in humans. Neuroscience Letters, 308, 141-144.

Hikosaka, O. (1998) Neural systems for control of voluntary action--a hypothesis. Advances in Biophysics, 35, 81-102.

Honda, M., Deiber, M.-P., Ibáñez, V., Pascual-Leone, A., Zhuang, P. and Hallett, M. (1998). Dynamic cortical involvement in implicit and explicit motor sequence learning: A PET study. Brain, 121, 2159-2173.

Hoshi, E., Tremblay, L., Feger, J., Carras, P. L., & Strick, P. L. (2005). The cerebellum communicates with the basal ganglia. *8*(11), 1491-1493.

Howard, D. V. and Howard, J. H. (1992). Adult age differences in the rate of learning serial patterns: Evidence from direct and indirect tests. Psychology and Aging, 7, 232-241.

Howard, D. V. and Howard, J. H. (1989). Age differences in learning serial patterns: direct versus indirect measures. Psychology and Aging, 4, 357-364.

Howard, J. H. and Howard, D. V. (1997). Age differences in implicit learning of higher order dependencies in serial patterns. Psychology and Aging, 12, 634-656.

Howard, D. V., Howard, J.H., Japikse, K., DiYanni, C., Thompson, A., & Somberg, R. (2004). Implicit sequence learning: effects of level of structure, adult age, and extended practice. Psychology and Aging, 19, 79-92.

Huettel, S. A., Singerman, J. and McCarthy, G. (2001). The effects of aging upon the hemodynamic response measured by functional MRI. NeuroImage, 13, 161-175

Hutchins, K. D., Martino, A. M. and Strick, P. L. (1988). Corticospinal projections from the medial wall of the hemisphere. Experimental Brain Research, 71, 667-672.

Ivry, R. B., & Keele, S. W. (1989). Timing functions of the cerebellum. Journal of Cognitive Neuroscience, 1, 136-152.

Jernigan, T., Archibald, S., Berhow, M. (1991). Cerebral structure on MRI, part I: Localization of age-related changes. Biological Psychiatry, 29, 55-67.

Jernigan, T. L., Archibald, S. L., Fennema-Notestine, C., Gamst, A. C., Stout, J. C., Bonner, J. and Hesselink, J. R. (2001). Effects of age on tissues and regions of the cerebrum and cerebellum. Neurobiology of Aging, 22, 581-594.

Kakade, S., & Dayan, P. (2002). Acquisition and extinction in autoshaping. Psychological Review, 109, 533-544.

Ketonen, L. (1998). Neuroimaging of the aging brain. Neurological Clinics, 16, 581-598.

Lawrence, D. G. and Kuypers, H. G. J. M. (1968). The functional organization of the motor system in the monkey. I. The effects of bilateral pyramidal lesions. Brain, 91, 1-14.

Laforce, R and Doyon, J. (2002). Differential role for the striatum and cerebellum in response to novel movements using a motor learning paradigm. Neuropsychologia, 40, 512-517.

Liu, Y., Gao, J.-H., Liotti, M., Pu, Y. and Fox, P. T. (1999). Temporal dissociation of parallel processing in the human subcortical outputs. Nature, 400, 364-367.

Liu, Y., Pu, Y., Gao, J.-H., Parsons, L. M., Xiong, J., Liotti, M., Bower, J. M. and Fox, P. T. (2000). The human red nucleus and lateral cerebellum in cooperative roles supporting sensory discrimination. Human Brain Mapping, 10, 147-159.

Madden, D. J. (2001). Speed and timing of behavioral processes. In J.E. Birren & K.W. Schaie (Eds.), Handbook of the Psychology of Aging (5th ed., pp. 288-312). New York: Academic Press.

Mann, M. A. (1994). Vulnerability of specific neurons to aging. In Neurodegenerative Diseases (Ed. D.B. Calne), Philadelphia, W.B. Saunders, pp. 15-31.

Martin, W. R., Ye, F. Q. and Allen, P. S. (1998). Increasing striatal iron content associated with normal aging. Movement Disorders, 13, 281-286.

Martino, A. M. and Strick, P. L. (1987). Corticospinal projections originate from the arcuate premotor area. Brain Research, 404, 307-312.

Mattay, V. S., Fera, F., Tessitore, A., Hariri, A. R., Das, S., Callicott, J. H. and Weinberger, D. R. (2002). Neurophysiological correlates of age-related changes in human motor function. Neurology, 58, 630-635.

Mayr, U. (1996). Spatial attention and implicit sequence learning: Evidence for independent learning of spatial and nonspatial sequences. Journal of Experimental Psychology: Learning, Memory, and Cognition, 22, 350-364.

Mehagnoul-Schipper, D. J., van der Kallen, B. F., Colier, W. N., van der Sluijs, M. C., van Erning, L. J., Thijssen, H. O., Oeseburg, B., Hoefnagels, W. H. and Jansen, R.W. (2002). Simultaneous measurements of cerebral oxygenation changes during brain activation by near-infrared spectroscopy and functional magnetic resonance imaging in healthy young and elderly subjects. Human Brain Mapping, 16, 14-23.

Miller, E. K., & Cohen, J. D. (2001). An integrative theory of prefrontal cortex function. Annual Review of Neuroscience, 24, 167-202.

Miyachi S., Hikosaka, O., & Lu, X. (2002). Differential activation of monkey striatal neurons in the early and late stages of procedural learning. Experimental Brain Research, 146, 122-126.

Miyachi S., Hikosaka, O., Miyashita, K., Kárádi, Z. & Rand, M. K. (1997). Differential roles of monkey striatum in learning of sequential hand movements. Experimental Brain Research, 115, 1-5.

Morecraft, R. J., Geula, C., & Mesulam, M. M. (1992). Cytoarchitecture and neural afferents of orbitofrontal cortex in the brain of the monkey. The Journal of Comparative Neurology, 323, 341-358.

Muakkassa, K. F. & Strick, P. L. (1979). Frontal lobe inputs to primate motor cortex: evidence for four somatotopically organized 'premotor areas'. Brain Research, 177, 176-182.

Müller, R.-A., Kleinhans, N., Pierce, K., Kemmotsu, N. & Courchesne, E. (2002). Functional MRI of motor sequence acquisition: effects of learning stage and performance. Cognitive Brain Research, 14, 277-293.

Nakamura, K., Sakai, K. & Hikosaka, O. (1999). Effects of local inactivation of monkey medial frontal cortex in learning of sequential procedures. Journal of Neurophysiology, 82, 1063-1068.

Nakamura, K., Sakai, K. & Hikosaka, O. (1998). Neuronal activity in medial frontal cortex during learning of sequential procedures. Journal of Neurophysiology, 80, 2671-2687.

Napier, J. R. (1961). Prehensility and opposability in the hands of primates. Symposia of the Zoological Society of London, 5, 115-132.

Nissen, M. J., & Bullemer, P. (1987). Attentional requirements of learning: Evidence from performance measures. Cognitive Psychology, 19, 1-32.

O'Doherty, J., Rolls, E. T., Francis, S., Bowtell, R., McGlone, F., Kobal, Renner, B., & Ahne, G. (2000). Sensory-specific satiety-related olfactory activation of the human orbitofrontal cortex. Neuroreport, 4, 893-897.

Oldfield, R. (1971). The assessment and analysis of handedness: the Edinburgh inventory. Neuropsychologia, 9, 97-113.

Owen, A. M., McMillan, K. M., Laird, A. R., & Bullmore, E. (2005). N-back working memory paradigm: a meta-analysis of normative functional neuroimaging studies. Human Brain Mapping, 25, 46-59.

Pantoni, L. & Garcia, H. H. (1995). The significance of cerebral white matter abnormalities 100 years after Binswanger's report: A review. Stroke, 26, 1293-1301.

Passingham, R. E. (1987). From where does motor cortex get its instructions? In: Neural and Behavioral Approaches to Higher Brain Function, (Ed. S. Wise) Wiley, New York, pp. 67-97.

Passingham, R. E. (1988). Premotor cortex and preparation for movement. Experimental Brain Research, 70, 590-596.

Passingham, R. E. (1989). The origins of human intelligence. In: Human Origins, (Ed. J.R. Durant) Oxford University Press, pp. 123-136.

Penfield, W. (1938). The cerebral cortex in man: 1. The cerebral cortex and consciousness. Archives of Neurology and Psychiatry , 40, 417-442.

Petrides, M. (1982). Motor conditional associative-learning after selective prefrontal lesions in the monkey. Behavioral Brain Research, 5, 407-413.

Petrides, M. (1987). Conditional learning and primate frontal lobes. In: The Frontal Lobes Revisited (Ed. E. Perecman), IBRN press, New York, pp. 91-108.

Petrides, M. & Pandya, D. N. (1984). Projections to the frontal lobe from the posterior-parietal region in the rhesus monkey. Journal of Comparative Neurology, 273, 52-66.

Poldrack, R. A. & Gabrieli, J. D. (2001). Characterizing the neural mechanisms of skill learning and repetition priming: evidence from mirror reading. Brain, 124, 67-82.

Ramnani, N., Toni, I., Passingham, R. E., & Haggard, P. (2001). The cerebellum and parietal cortex play a specific role in coordination: a PET study. Neuroimage, 14, 899-911.

Ranganathan, V. K., Siemionow, V., Sahgal, V. & Yue, G. H. (2001). Effects of aging on hand function. Journal of the American Geriatric Society, 49, 1478-1484.

Rauch, S. L., Savage, C. R., Brown, H. D., Curran, T., Alpert, N. M., Kendrick, A., Fischman, A. J. & Kosslyn, S. M. (1995). A PET investigation of implicit and explicit sequence learning. Human Brain Mapping, 3, 271-286.

Raz, N., Gunning-Dixon, F., Head, D., Williamson, A., & Acker, J. D. (2001). Age and sex differences in the cerebellum and the ventral pons: a prospective MR study of healthy adults. American Journal of Neuroradiology, 22, 1161-1167.

Reber, A. S. (1967). Implicit Learning of Artificial Grammers. Journal of Verbal Learning and Verbal Behavior, 6, 855-863.

Reber, A. S., & Allen, R. (2000). Individual differences in implicit learning: Implications for the evolution of consciousness. In R. G. Kunzendorf & B. Wallace (Eds.), Individual differences in conscious experience. (pp. 227-247): John Benjamins Publishing Company.

Reber, A. S., Walkenfeld, F. F., & Hernstadt, R. (1991). Implicit and explicit learning: Individual differences and IQ. Journal of Experimental Psychology: Learning, Memory, & Cognition, 17, 888-896.

Resnick, S. M., Goldszal, A. F., Davatzikos, C., Golski, S., Kraut, M. A., Metter, E. J., Bryan, N. & Zonderman, A. B. (2000). One-year Age Changes in MRI Brain Volumes in Older Adults. Cerebral Cortex, *10*(5), 464-472.

Rijntjes, M., Buechel, C., Kiebel, S. & Weiller, C. (1999). Multiple somatotopic representations in the human cerebellum. Neuroreport, 10, 3653-3658.

Ross, M. H., Yurgelun-Todd, D. A., Renshaw, P. F., Maas, L. C., Mendelson, J. H., Mello, N. K., Cohen, M. D., & Levin, J. M. (1997). Age-related reduction in functional MRI response to photic stimulation. Neurology, 48, 173-176.

Samson, F. E. & Nelson, S. R. (2000). The aging brain, metals and oxygen free radicals. Cellular and Molecular Biology, 46, 699-707.

Schochet, S. S. (1998). Neuropathology of aging. Neurologic Clinics, 16, 569-580.

Schugens, M. M., Breitenstein, C., Ackermann, H. & Daum, I. (1998). Role of the striatum and the cerebellum in motor skill acquisition. Behavioral Neurology, 11, 149-157.

Seitz, R. J., & Binkofski, F. (2003). Modular organization of parietal lobe functions as revealed by functional activation studies. Advances in Neurology, 93, 281-292.

Shewhart, W. A. (1931). Economic control of quality of manufactured product. New York: D. van Nostrand Company, Inc.

Solodkin, A., Hlustik, P., Chen, E. E., & Small, S. L. (2004). Fine modulation in network activation during motor execution and motor imagery. Cerebral Cortex, 14, 1246-1255.

Small, S. L., Hlustik, P., Noll, D. C., Genovese, C. & Solodkin, A. (2002). Cerebellar hemispheric activation ipsilateral to the paretic hand correlates with functional recovery after stroke. Brain, 125, 1544-1557.

Small, D. M., Zatorre, R. J., Dagher, A., Evans, A. C., & Jones-Gotman, M. (2001). Changes in brain activity related to eating chocolate: from pleasure to aversion. Brain, 124, 1720-1733.

Smith, A. C., Frank, L. M., Wirth, S., Yanike, M., Hu, D., Kubota, Y., Graybiel, A. M., Suzuki, W.A., & Brown, E.N. (2004). Dynamic Analysis of Learning in Behavioral Experiments. The Journal of Neuroscience, 24, 447-461.

Stadler, M. A., & Frensch, P. A. (Eds.). (1998). Handbook of Implicit Learning. Thousand Oaks, California: SAGE Publications, INC.

Strick, P. L. & Hoover, J. E. (1999). The organization of cerebellar and basal ganglia outputs to primary motor cortex as revealed by retrograde transneuronal transport of herpes simplex virus type 1. Journal of Neuroscience, 19, 1446-1463.

Strub, R. L. & Black, W. F. (1977). The Mental Status Examination in Neurology. Philadelphia: F.A. Davis Co.

Squire, L. R., & Zola, S. M. (1996), Structure and function of declarative and nondeclarative memory systems. Proceedings of the National Academy of Sciences USA, 93, 13515-13522.

Sullivan, E. V., Mathalon, D. H., Zipursky, R. B., Kersteen-Tucker, Z., Knight, R. T., & Pfefferbaum, A. (1993). Factors of the Wisconsin Card Sorting Test as measures of frontal-lobe function in schizophrenia and in chronic alcoholism. Psychiatry Research, 46, 175-199.

Swainson, R., Cunnington, R., Jackson, G. M., Rorden, C., Peters, A. M., Morris, P.G., & Jackson, S. R. (2003). Cognitive control mechanisms revealed by ERP and fMRI: evidence from repeated task-switching. Journal of Cognitive Neuroscience, 15, 785-799.

Tang, Y., Whitman, G. T., Lopez, I. & Baloh, R. W. (2001). Brain volume changes on longitudinal magnetic resonance imaging in normal older people. Journal of Neuroimaging, 11, 393-400.

Tanji, J. (1996). The supplementary motor area in the cerebral cortex. Neuroscience Research, 19, 251-268.

Tataranni, P. A., Gautier, J.-F., Chen, K., Uecker, A., Bandy, D., Salbe, A. D., Pratley, R. E., Lawson, M., Reiman, E. M., & Ravussin E. (1999). Neuroanatomical correlates of hunger and satiation in humans using positron emission tomography. Proceedings of the National Academy of Science of the United States of America, 96(, 4569-4574.

Terry, R. D., DeTeresa, R. & Hansen, L. A. (1987). Neocortical cell counts in human adult aging. Annuals of Neurology, 21, 530-539.

Theoret, H., Haque, J. & Pascual-Leone, A. (2001). Increased variability of paced finger tapping accuracy following repetitive magnetic stimulation of the cerebellum in humans. Neuroscience Letters, 306, 29-32.

Toni, I., Krams, M, Turner, R. & Passingham, R. E. (1998). The time course of changes during motor sequence learning: a whole-brain fMRI study. Neuroimage, 8, 50-61.

Tower, S. S. (1940). Pyramidal lesions in the monkey. Brain, 63, 36-90.

Tryon, W. W. (1982) A Simplified time-series analysis for evaluating treatment interventions. Journal of Applied Behavioral Analysis, 15, 423-429.

Twitchell, T. E. (1951). The restoration of motor function following hemiplegia in man. Brain, 74, 443-480.

Volkow, N. D., & Fowler, J. S. (2000). Addiction, a disease of compulsion and drive: involvement of the orbitofrontal cortex. Cerebral Cortex, 10, 318-325.

Willingham, D. B., Salidis, J., & Gabrieli, J. D. E. (2002). Direct comparison of neural systems mediating conscious and unconscious skill learning. Journal of Neurophysiology, 88, 1451-1460

Ye, N. (Ed.). (2003). Handbook of data mining. Mahwah, N.J.: Lawren Erlbaum Assoc.

Yousry, T., Schmid, U., Alkadhi, H., Schmidt, D., Peraud, A., Buettner, A., & Winkler, P. (1997). Localization of the motor hand area to a knob on the precentral gyrus. A new landmark. Brain, *120*, 141-157.

Zhang, Z. Andersen, A., Grondin, R., Barber, T., Avison, R., Gerhardt, G. & Gash, D. (2001). Pharmacological MRI Mapping of Age-Associated Changes in Basal Ganglia Circuitry of Awake Rhesus Monkeys. NeuroImage, 14, 1159–1167.

Zhuang, J. C., LaConte, S. M., Peltier, S., Zhang, K., & Hu, X. (2005). Connectivity exploration with structural equation modeling: an fMRI study of bimanual motor coordination. NeuroImage, 25, 462-470.

Zilles, K., Eickhoff, S., & Palomero-Gallagher, N. (2003). The human parietal cortex: a novel approach to its architectonic mapping. Advances in Neurology, 93, 1-21.

# BIOGRAPHICAL SKETCH

George Andrew James (Andy) was born in Cedartown Georgia in 1976 and raised in this rural community throughout his childhood. In 1993, he was invited to study mathematics and literature at the Georgia Governors Honors Program. He graduated Salutorian from Cedartown High School in 1994 with degrees from the College Preparatory and Advanced Mechanical Drafting programs. He had 11 years of perfect attendance, having missed one day of school in first grade on account of chicken pox.

Andy James enrolled in the Georgia Institute of Technology in August 1994. He graduated in December 1999, earning high honors for bachelor degrees in Applied Psychology and Chemistry. He spent several months with his family–and shingling roofs–before enrolling in the University of Florida College of Medicine Interdisciplinary Program in Neuroscience. After graduating in December 2005, Andy will accept a postdoctoral position at Emory University and continue his neuroimaging investigations into cognition.